AD_____

Award Number: DAMD17-03-1-0287

TITLE: Development of km23-based Diagnostics and Therapeutics

PRINCIPAL INVESTIGATOR: Kathleen M. Mulder, Ph.D.

CONTRACTING ORGANIZATION: Pennsylvania State University
Hershey, PA 17033

REPORT DATE: May 2004

TYPE OF REPORT: Annual

PREPARED FOR: U.S. Army Medical Research and Materiel Command
Fort Detrick, Maryland 21702-5012

REPORT DOCUMENTATION PAGE

Form Approved
OMB No. 074-0188

1. AGENCY USE ONLY (Leave blank)	2. REPORT DATE	3. REPORT TYPE AND DATES COVERED
	May 2004	Annual (15 Apr 2003 - 14 Apr 2004)

4. TITLE AND SUBTITLE

Development of km23-based Diagnostics and Therapeutics

5. FUNDING NUMBERS

DAMD17-03-1-0287

6. AUTHOR(S)

Kathleen M. Mulder, Ph.D.

7. PERFORMING ORGANIZATION NAME(S) AND ADDRESS(ES)

Pennsylvania State University
Hershey, PA 17033

E-Mail: kmm15@psu.edu

8. PERFORMING ORGANIZATION REPORT NUMBER

9. SPONSORING / MONITORING AGENCY NAME(S) AND ADDRESS(ES)

U.S. Army Medical Research and Materiel Command
Fort Detrick, Maryland 21702-5012

10. SPONSORING / MONITORING AGENCY REPORT NUMBER

11. SUPPLEMENTARY NOTES

Original contains color plates: ALL DTIC reproductions will be in black and white

12a. DISTRIBUTION / AVAILABILITY STATEMENT

Approved for Public Release; Distribution Unlimited

12b. DISTRIBUTION CODE

13. ABSTRACT (Maximum 200 Words)

Similar to other solid tumors, ovarian cancers are resistant to the growth inhibitory effects of the natural epithelial growth inhibitor TGFβ, suggesting that alterations in TGFβ pathways contribute to ovarian cancer progression. The TGFβ resistance is frequent, perhaps exceeding 75% of cases, especially for recurrent ovarian cancers. Despite the high frequency of TGFβ resistance that occurs in ovarian cancers, thus far, no clinically useful agents, which target the signaling pathways of any of the TGFβ superfamily members, have been developed for this disease. Accordingly, there is a great need to develop TGFβ-based agents and indicators for the diagnosis, therapy, and prognosis of ovarian cancer. Further, TGFβ and some of its signaling components can function as tumor suppressors. We have identified a novel TGFβ signaling component (km23) that is altered in 42% of ovarian cancer patient tumors. km23 mediates growth inhibition and other TGFβ responses. A deletion mutant in the Drosophila homologue of km23, similar to the truncation of km23 we identified in ovarian cancer patient samples, resulted in an increase in mitotic index, suggesting that km23 may function as a tumor suppressor. We are in the process of developing anti-cancer diagnostics and therapeutics using km23 as the target.

14. SUBJECT TERMS

TGF-beta, signal transduction, growth factors, cytoskeleton, motor protein, dynein, tumor biology, ovarian cancer cells, tumor growth

15. NUMBER OF PAGES

135

16. PRICE CODE

17. SECURITY CLASSIFICATION OF REPORT	18. SECURITY CLASSIFICATION OF THIS PAGE	19. SECURITY CLASSIFICATION OF ABSTRACT	20. LIMITATION OF ABSTRACT
Unclassified	Unclassified	Unclassified	Unlimited

Table of Contents

INTRODUCTION

A novel TGFβ receptor-interacting protein, termed km23, has been cloned from a highly TGFβ-sensitive rat intestinal epithelial cell line (IEC4-1) using phosphorylated intracellular portions of TGFβ receptor I and receptor II (TβRI & TβRII) (Tang et al, 2002). This 11-kDa cytoplasmic protein is the mammalian homologue of the LC7 family of dynein light chains (DLCs). km23 is ubiquitously expressed in human tissues and highly conserved among different species (Jin et al, 2004). km23 interacts with the TGFβ receptor complex through TβRII, and it can be phosphorylated on serine residues after ligand binding. km23 interacts with Smad2 both *in vitro* and *in vivo* and is co-localized with Smad2 prior to the nuclear translocation of Smad2 (Jin et al, 2004). Forced expression of km23 induces specific TGFβ responses, including an activation of c-Jun N-terminal kinase (JNK), a phosphorylation of c-Jun, and an inhibition of cell growth. Moreover, TGFβ induces the recruitment of km23 to the intermediate chain of dynein (DIC) (Tang et al, 2002; Yue et al, 2004). The kinase activity of TβRII is required for both km23 phosphorylation and its interaction with DIC. Furthermore, we have identified alterations in TGFβ-resistant human ovarian cancer cell lines and in ovarian cancer patients (Ding and Mulder, 2004; Mulder, 2004). The alterations occur at precise locations in km23, which appear to modify km23 functions (Ding et al, 2004; Ilangovan, et al, 2004). Thus, km23 appears to be a novel TGFβ signaling target for the development of anti-cancer diagnostics and therapeutics.

BODY

With regard to **Task 1** in the Statement of Work (SOW), we have completed sub-tasks a-f and h, and are working on sub-task g. We are also currently addressing some aspects of **Task 2**, and have included an additional technology (siRNA approaches; Liu et al, 2004) to delineate the biological significance of km23 in TGFβ signaling, as described in Task 2. Thus, we have partially addressed sub-tasks b, c, and g from Task 2. Under sub-task 2g, we have so far examined the ARE and phTG5 TGFβ-specific reporters. The work from these Tasks can be summarized by the following abstracts.

Requirement of km23 for TGF β-mediated growth inhibition and induction of fibronectin expression. (Qunyan Jin, Wei Ding, Cory M. Staub, Guofeng Gao, Qian Tang, and Kathleen M. Mulder, Submitted, 2004).

We previously identified km23 as a novel TGFβ receptor-interacting protein. Here we show that km23 is ubiquitously expressed in human tissues and that cell-type specific differences in endogenous km23 protein expression exist. In addition, we demonstrate that the phosphorylation of km23 is TGFβ-dependent, in that EGF was unable to phosphorylate km23. Further, the kinase activity of both TGFβ receptors appears to play a role in the TGFβ-mediated phosphorylation of km23, although RII kinase activity is absolutely required for km23 phosphorylation. Forced expression of km23 induces specific TGFβ responses, including an activation of c-Jun N-terminal kinase (JNK), a phosphorylation of c-Jun, and an inhibition of cell growth. Moreover, TGFβ induces the recruitment of km23 to the intermediate chain of dynein (DIC). The kinase activity of TβRII is required for both km23 phosphorylation and its interaction with DIC. Blockade of km23 using small interfering RNA (siRNA) significantly decreased key

TGFβ responses, including induction of fibronectin expression and inhibition of cell growth. Thus, our results demonstrate that km23 is required for TGFβ induction of fibronectin expression and is necessary, but not sufficient, for TGFβ-mediated growth inhibition.

Requirement of km23 in a Smad2-dependent TGFβ signaling pathway. (Qunyan Jin, Wei Ding, and Kathleen M. Mulder, Submitted, 2004).

We have identified km23 as a novel TGFβ receptor-interacting protein that is also a light chain of the motor protein dynein. Here we show that km23 is co-localized with the TGFβ signaling component Smad2 at early time periods after TGFβ treatment of epithelial cells, prior to translocation of Smad2 to the nucleus. km23 interacts with Smad2, but not Smad3, in both immunoprecipitation/blot and GST pull-down assays. More significantly, km23 interacts with Smad2 once it has been phosphorylated by constitutively active RI *in vivo*. Further, blockade of km23 using siRNA significantly reduced several TGFβ signaling events important for growth inhibition, namely the levels of phosphorylated Smad2, nuclear translocation of Smad2, and TGFβ-dependent Smad2 transcriptional activation (ARE reporter activity). Our findings demonstrate that km23 is required for Smad2-dependent TGFβ signaling events.

No studies have yet been performed related to **Task 3**. However, progress has also been made on portions of **Tasks 4 and 5**. For example, we have addressed sub-tasks 4a-d, f, and h. We have found that we can use RT-PCR to analyze the tumor tissue samples, but that PCR analysis of DNA does not reveal the alterations. These results indicate that the alterations occur at the RNA level, suggesting that the defects occur as a result of RNA splicing or editing abnormalities. These types of alterations have been shown previously to contribute to cancer initiation or progression, but for cancer types other than ovarian. With regard to Task 5, we have addressed sub-tasks a-c, and have concluded that RNA, and not DNA, must be analyzed in the serum as well. The following abstract addresses aspects of these tasks.

A TGFβ receptor-interacting protein frequently mutated in epithelial ovarian cancer. (Wei Ding, Eileen M. Estes, Virginia Espina, Lance A. Liotta, and Kathleen M. Mulder, Submitted, 2004).

Ovarian carcinomas, particularly recurrent forms, are frequently resistant to transforming growth factor (TGF)-β-mediated growth inhibition. Mutations in the TGFβ receptor I and receptor II (TβR-I and TβR-II) genes were only reported in a minority of ovarian carcinomas, suggesting that other alterations in TGFβ signaling components may play an important role in the loss of TGFβ responsiveness. Using laser-capture microdissection (LCM) and a nested reverse-transcription polymerase chain reaction (RT-PCR), we found that km23, which interacts with the TGFβ receptor complex, is altered at a high frequency in human ovarian carcinoma cell lines and tissues. A novel form of km23, missing exon 3, was found in two out of six ovarian cancer cell lines, as well as in two out of nineteen tumor tissues from patients with ovarian cancer. In addition to this alteration, a stop codon mutation (TAA→CAC) was detected in two patients. This alteration results in an elongated protein, encoding 107 amino-acid residues, instead of the wild type 96-amino acid form of km23. Furthermore, five missense mutations (T38I, S55G, T56S, I89V, and V90A) were detected in four

patients, providing a total alteration rate of 42.1% (8 out of 19 cases) in ovarian cancer. No km23 alterations were detected in 15 normal tissues. Such a high alteration rate in ovarian cancer suggests that km23 may play an important role in either TGFβ resistance or tumor progression in this disease. Functional studies indicate that both the truncated and elongated forms of km23 had diminished binding with the dynein intermediate chain (DIC) *in vitro*, and that the latter alteration also dose-dependently inhibited Smad2-mediated activin responsive element (ARE) promoter reporter activity. Thus, the alterations we have found in human ovarian cancer result in aberrant TGFβ signaling.

KEY RESEARCH ACCOMPLISHMENTS:

- We have extensive functional data to demonstrate that km23 is an important component of TGFβ signaling pathways.
- We also have functional data to indicate that km23 is an important component of the cell's motor machinery, responsible for moving TGFβ signaling components to their appropriate destinations in the cell.
- km23 interacts with the TGFβ signaling component Smad2 in two different biochemical assays, and under *in vivo* conditions. km23 is also co-localized with Smad2 at very early time points (i.e., within 2 min) after TGFβ addition to cells, prior to the nuclear translocation of Smad2.
- km23 is required for Smad2-specific TGFβ signaling events such as ligand-dependent Smad2 phosphorylation, nuclear translocation, and transcriptional regulation.
- km23 alterations occur in human ovarian cancer at specific sites that are critical for the cellular functions of km23. The alterations appear to occur at a high frequency in human ovarian cancer.
- We have validated km23 as a critical anti-cancer therapeutic target using siRNA approaches, and are in the process of assessing its validity as a diagnostic reagent.

REPORTABLE OUTCOMES:

Publications:

Yue J, Sun B, Liu G, Mulder KM. Requirement of TGFβ receptor-dependent activation of c-Jun N-terminal kinases (JNKs)/Stress-activated protein kinases (Sapks) for TGFβ up-regulation of the urokinase-type plasminogen activator receptor. *J. Cell. Physiol.* 199: 284-292, 2004.

Ding, W. and **Mulder, K.M.** km23: A novel TGFβ signaling target altered in ovarian cancer. In Molecular Targeting and Signal Transduction. Molecular Therapeutics. Ed, Kumar, R. Kluwer Academic Publishers, Cancer Treatment and Research Book Series. Chap. 15, 315-327, 2004.

Abstracts:

Jin Q, MD, Ding W, MD, PhD, Staub CM, Gao G, MD, Mulder KM, PhD. A novel target for the development of anti-cancer diagnostics and therapeutics. Innoventure 2003, Hershey, PA, May 2, 2003.

Jin Q, Ding W, Staub CM, Gao G, Tang Q, Mulder KM. A TGF-β receptor-interacting protein frequently mutated in epithelial ovarian cancer. AACR Annual Meeting, Washington, DC, July 2003.

Liu G, Ding W, Zehner G, Jin, Q, **Mulder KM**. c-Fos plays a Critical Role in TGFβ1 Promoter AP-1 binding and transactivation in human carcinoma cells. AACR Annual Meeting, March, 2004.

Invited Speaker:

Seminar at the University of Texas, San Antonio, TX, 2003
Presentation at the AACR Annual Meeting, Washington, DC, 2003
Seminar for Penn State College of Medicine IBIOS Program, 2003
Seminar at Fox Chase Cancer Center, Philadelphia, PA, 2004
Seminar at H. Lee Moffitt Cancer Center and Research Institute, Tampa, FL, 2004

CONCLUSIONS

1. The phosphorylated, activated cytoplasmic domains of the TGFβ receptors were used as probes to screen an expression library that was prepared from a highly TGFβ-responsive intestinal epithelial cell line.

2. The TGFβ receptor-interacting protein km23 was isolated and identified to be a light chain of the motor protein dynein.

3. km23 interacts with endogenous TGFβ receptors and TGFβ stimulates this interaction.

4. TGFβ receptor activation results in phosphorylation of km23 on serine residues.

5. The kinase activity of TGFβ receptor RII is required for phosphorylation of km23.

6. Forced expression of km23 mediates TGFβ signaling and TGFβ responses: Activation of JNK, phosphorylation of c-Jun, and inhibition of cell growth.

7. Blockade of km23 expression using siRNA led to a reduction in the ability of TGFβ to inhibit DNA synthesis; km23 was necessary but not sufficient for mediating TGFβ growth inhibition.

8. The km23 members comprise a distinct family within the larger superfamily of robl-like/LC7/bxd-like members; the km23 family appears to function as TGFβ signaling components.

9. km23 is the human homologue of the Drosophila protein robl; defects in robl result in an increase in mitotic index and accumulation of cargoes inside cells.

10. TGFβ induces the interaction of km23 with the dynein intermediate chain (DIC) within 2 min of TGFβ addition.

11. The kinase activity of TGFβ receptor RII is required for km23 interaction with DIC.

12. km23 interacts with Smad2 in both GST pull-down and IP/blot analyses.

13. km23 is co-localized with Smad2 at early times after TGFβ addition to cells (before nuclear translocation of Smad2).

14. km23 displays a punctate staining pattern after TGFβ receptor activation, similar to TGFβ RII and Smad2, indicating it is associated with vesicular compartments.

15. Blockade of endogenous km23 using siRNA results in a decrease in TGFβ-dependent Smad2 phosphorylation, translocation, and regulation of transcription.

16. We have developed a highly sensitive and specific assay to detect genetic alterations in km23 in cancer patient tissues by combining two micro-scale technologies -- LCM and nested RT-PCR.

17. Various mutations in km23 were detected in tumors from 8 out of 19 ovarian cancer patients, providing a total km23 alteration rate of 42%. These mutations were not present in tumor-free tissue groups.

18. In GST pull-down assays, the truncated form of km23 displays a weaker interaction with the DIC than does wild-type km23, suggesting that mutations in km23 may block the intracellular transport of TGFβ signaling components, thereby altering TGFβ responses.

19. Altered forms of km23 in ovarian cancer patients also reduce TGFβ- and Smad2-dependent transcriptional activation events.

SO WHAT SECTION:

- Our results provide the first demonstration of a link between cytoplasmic dynein

and a natural, growth inhibitory cytokine.

- km23 appears to specify the signaling intermediates that are transported along microtubules by the dynein motor after TGFβ receptor activation.

- km23 appears to be a motor receptor important for transporting TGFβ signaling components to their cellular sites of action, thereby maximizing the efficiency of signal propagation and maintaining signal specificity.

- km23 represents a novel target for the development of ovarian cancer diagnostics and therapeutics.

- km23 appears to function as a tumor suppressor, blocking cancer cell growth under normal conditions. In contrast, km23 alterations in human ovarian cancer abrogate the tumor suppressive function of km23.

- Several therapeutic approaches have been employed to repair or replace the loss of tumor suppressor protein functions (i.e., gene therapy approaches, blockade of binding proteins, etc); these are also applicable to km23.

- Pharmacological screens are underway to identify novel agents that can restore the normal functions of km23, or replace the altered forms/functions of km23.

REFERENCES

Tang Q, Staub C, Gao G, Jin Q, Wang Z, Ding W, Aurigemma R, **Mulder KM.** A novel transforming growth factor-β receptor-interacting protein that is also a light chain of the motor protein dynein. Mol. Biol. Cell, 2002; 13: 4484-4496.

Yue J, Sun B, Liu G, **Mulder KM.** Requirement of TGFβ receptor-dependent activation of c-Jun N-terminal kinases (JNKs)/Stress-activated protein kinases (Sapks) for TGFβ up-regulation of the urokinase-type plasminogen activator receptor. J. Cell. Physiol. 2004; 199:284-292.

Jin Q, Ding W, Staub CM, Gao G, Tang Q, **Mulder KM.** Requirement of km23 for TGFβ-mediated growth inhibition and induction of fibronectin expression. Submitted, Cell. Signaling, 2004.

Jin Q, Staub CM, **Mulder KM.** Requirement of km23 in a Smad2-dependent TGFβ signaling pathway, Submitted, J Cell Biol, 2004.

Mulder KM. A new target for the development of anti-cancer diagnostics and therapeutics. Amer. Clin. Lab., In Preparation, 2004.

Ding W, Estes E, Espina V, Liotta LA, **Mulder KM.** A TGFβ receptor-interacting protein frequently mutated in epithelial ovarian cancer. Submitted, Cancer Res., 2004.

Liu G, Ding W, **Mulder KM.** c-Fos plays a Critical Role in TGFβ1 Promoter AP-1 binding and transactivation in human colon carcinoma cells. Submitted, J. Biol. Chem., 2004.

Ding W, **Mulder KM.** km23: A novel TGFβ signaling target altered in ovarian cancer. In Molecular Targeting and Signal Transduction. Molecular Therapeutics. Ed, Kumar, R. Kluwer Academic Publishers, Cancer Treatment and Research Book Series. Chap. 15, 315-327, 2004.

Ilangovan U, Ding W, Zuniga J, Wilson, CL, Hinck AP, **Mulder KM.** NMR high-resolution structure of the dynein light chain km23. In Preparation, 2004.

APPENDICES

1. **Publication** -- Ding W, **Mulder KM.** km23: A novel TGFβ signaling target altered in ovarian cancer. In Molecular Targeting and Signal Transduction. Molecular Therapeutics. Ed, Kumar, R. Kluwer Academic Publishers, Cancer Treatment and Research Book Series. Chap. 15, 315-327, 2004.

2. **Manuscript Submitted:** Jin Q. Ding W, Staub CM, Gao G, Tang Q, **Mulder KM.** Requirement of km23 for TGFβ-mediated growth inhibition and induction of fibronectin expression. Submitted, Cell. Signaling, 2004.

3. **Manuscript Submitted:** Jin Q, Staub CM, **Mulder KM.** Requirement for km23 in a Smad2-dependent TGFβ signaling pathway, Submitted, J Cell Biol, 2004.

4. **Manuscript Submitted:** Ding W, Estes E, Espina V, Liotta LA, **Mulder KM.** A TGFβ receptor-interacting protein frequently mutated in epithelial ovarian cancer. Submitted, Cancer Res., 2004.

5. **Curriculum Vitae** – Kathleen M. Mulder, Ph.D.

km23: A NOVEL TGFβ SIGNALING TARGET ALTERED IN OVARIAN CANCER

WEI DING AND KATHLEEN M. MULDER

1. INTRODUCTION

Transforming growth factor β superfamily members play a pivotal role in almost every aspect of cellular and tissue activities, including cell cycle control, regulation of early embryonic development, cell differentiation, cell motility, extracellular matrix formation, angiogenesis, and induction of apoptosis [1, 2].

TGFβ has been shown to initiate at least two prominent signaling cascades, the Smad and the Ras/ MAPK pathways, to regulate cellular and tissue activities [2]. In the Smad pathway, TGFβ binds to TβRII and recruits TβRI into a heterotetrameric complex, resulting in transphosphorylation of TβRI in the GS-domain by TβRII [3, 4]. Phosphorylated Smad2 and/or Smad3 by activated TβRI form(s) a heteromeric complex with Smad4 and enter(s) the nucleus to regulate gene transcription [1, 2, 5]. As we first demonstrated, TGFβ can activate the Ras/MAPK pathways in TGFβ-sensitive epithelial cells [6, 7, 8, 9]. Three members of this family, including the extracellular signal-regulated kinases (ERKs), c-Jun N-terminal kinases (JNKs)/stress-activated protein kinases (SAPKs), and p38, can be activated by TGFβ in a wide variety of cell types [2]. These pathways have been shown to be required for several of the major TGFβ responses, including growth inhibition, production of $TGF\beta_1$, and induction of fibronectin [1, 2, 10].

In addition to the Smad and Ras/MAPK pathways, various proteins have been identified based upon their interaction with the TβRs and/or Smads. Smad anchor for receptor activation (SARA) and hepatic growth factor-regulated tyrosine kinase substrate (Hgs/Hrs) have been shown to facilitate Smad2/3 recruitment to the activated TβRI/activin receptor I (ActRI) [11, 12]. Disabled-2 (Dab-2) is an adaptor protein that can bind TβRs and Smad2/Smad3 to bridge the TβR complex to the Smad pathway [13]. Serine-threonine kinase receptor-associated protein (STRAP) recruits Smad7 to activated TβRI and forms a complex. The complex stabilizes the association

between Smad7 and the activated receptor, thereby blocking Smad2/3-mediated transcriptional activation [14]. The immunophilin FK506 binding protein 12 (FKBP12) functions as an inhibitor of TβRI by binding to the ligand-free form. FKBP12 is released upon ligand-induced, TβRII-mediated phosphorylation of TβRI [15]. TGFβ-receptor interacting protein-1 (TRIP-1) associates with TβRII in a kinase-dependent manner, but does not interact with the type II activin receptor or TβRI. It does, however, associate with the heteromeric TGFβ receptor complex (16). Death-associated protein (Daxx) interacts with the cytoplasmic domain of TβRII and also associates with the Fas receptor, which mediates activation of JNK and programmed cell death [17]. TGFβ receptor I-associated protein-1 (TRAP-1) only interacts with TβRI that has been activated through mutation or ligand binding. In the absence of TGFβ, TRAP-1 will not interact with wild-type TβRI [18]. TRAP-1-like protein (TLP) has been identified to interact with both active and kinase-deficient TβRs and activin type II receptors, but interacts with the common-mediator Smad4 only in the presence of TGFβ□activin signaling [19].

Herein, we describe a novel TGFβ receptor-interacting protein, termed km23. This protein is the mammalian homologue of the LC7 family of DLCs [20]. TGFβ stimulates not only the phosphorylation of km23, but also the recruitment of km23 to the DIC. Kinase-active TβRs are required for km23 phosphorylation and interaction with DIC [20]. We also demonstrate that km23 interacts with Smad2 both *in vitro* and *in vivo*, and it co-localizes with Smad2 in the cytoplasm at very early time points after TβR activation. Moreover, km23 can mediate specific TGFβ responses, including JNK activation, c-Jun phosphorylation, and growth inhibition [20]. Furthermore, we have identified altered forms of km23 both in TGFβ-resistant human ovarian cancer cell lines and in cancer tissues from ovarian cancer patients. Our data suggest that these alterations in km23 may modify km23 functions in TGFβ signaling and tumorgenesis.

2. CLONING OF km23 IN A HIGHLY TGFβ-RESPONSIVE RAT EPITHELIAL CELL LINE

We have developed a novel method for the identification of TGFβ receptor-interacting proteins [20]. The intracellular portions both of TβRI and TβRII were expressed in E. coli, purified by affinity chromatography, and phosphorylated by in vitro kinase assays. These activated cytoplasmic domains of the TβRs were used as probes to screen an expression protein library prepared from a highly TGFβ-responsive rat intestinal epithelial IEC4-

1 cell line [21]. Several positive clones were isolated using this method. Among these clones, km23 was the most interesting because it is also a homologue of the regulatory region of the Drosophila's Ultrabithorax (Ubx) unit, through which transcription can be activated by one of the TGFβ superfamily members, Dpp. It was conceivable that km23 might be an important intermediate in a TGFβ signaling pathway.

3. GENE STRUCTURE AND HOMOLOGY OF HUMAN km23

Human km23 is a 96-amino acid protein encoded by a 291-base pair open reading frame. km23 is localized on human chromosome 20 (20 q11.21) and is composed of 4 exons. Northern blots have shown that km23 is ubiquitously expressed, with higher levels of message detected in brain, kidney, and placenta tissues. Western blots have indicated km23 is an 11-kDa cytoplasmic protein. The human and rat km23 amino acid sequences differ by only three amino acids and show 98% similarity. Additional alignments of human km23 with sequences in the National Center for Biotechnology Information database indicate that km23 is also the mammalian homologue of the Chlamydomonas LC7 class of DLCs. It is relatively conserved across different species, including Chlamydomonas (ch/LC7, 74% similarity), Drosophila (robl gene, 82% similarity), Caenorhabditis elegans (T24H10.6 gene, 76% similarity), and Danio Rerio (ZFIN gene, 93% similarity). Another mammalian form of km23 has been identified, termed km23-2. Human km23-2 localizes to chromosome 16 (16 q23.3), can be translated into a 96-amino acid protein, and displays 70% homology and 91% similarity with human km23. The rat and mouse forms of km23-2 display 71% homology and 91% similarity with human km23.

4. km23 DIRECTLY INTERACTS WITH TβII, BUT NOT WITH TβRI ALONE

Since km23 was isolated using activated intracellular regions of TβRI and TβRII, it was of interest to verify this interaction *in vivo*. ^{125}I-TGFβ cross-linking assays indicated that both TβRI and TβRII were present in km23 immunocomplexes. Also, TGFβ induced the interaction of TβRII with km23 in two epithelial cell lines at early times after TGFβ addition. The results of immunoprecipitation/blot (IP/blot) assays in either direction indicated that km23

can interact with TβRII and with the TGFβ receptor complex, but that TβRI may not be a direct binding partner of km23 [20].

5. km23 PHOSPHORYLATION

km23 can be phosphorylated when both TβRI and TβRII are expressed in 293T cells, but it is not constitutively phosphorylated when expressed alone. km23 could not be phosphorylated by kinase-deficient (KN) RII when it was co-expressed with wild-type (wt) RI, suggesting that the kinase activity of TβRII is required for km23 phosphorylation. In contrast, km23 could still be phosphorylated after co-expression of wt RII and KN-RI, suggesting that the RI kinase does not directly phosphorylate km23. In support of this finding, km23 was also not phosphorylated when a kinase active RI mutant (T204D) was expressed alone. Thus, the mechanism for the phosphorylation of km23 differs from that of the R-Smads [22]. Collectively, our results strongly suggest that although both RI and RII are present in the complex with km23, the RII kinase is the primary mediator of km23 phosphorylation. The kinase activity of RI does appear to play some role in km23 phosphorylation, however, since expression of KN-RI with wt RII reduced the level of phosphorylation relative to that observed after expression of RII alone.

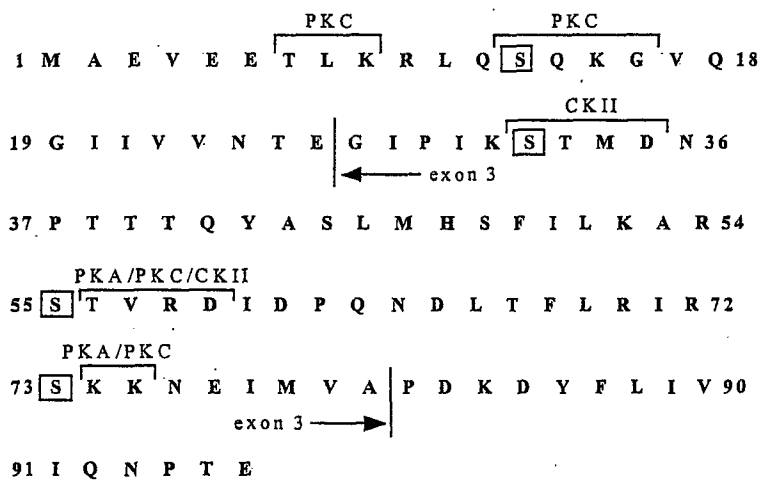

Figure 1. Human km23 sequence depicting expected phosphorylation sites. Potential phosphorylation sites for PKA, PKC, and CKII were predicted using PhosphoBase v. 2.0 and NetPhos 2.0 [24]. For these sites, prediction scores for serine and threonine were all over 0.91. Four serine residues that are conserved among the mammalian km23 forms are boxed. Exon 3 of km23 contains three potential phosphorylation sites for PKA, PKC, and/or CKII.

Phosphoamino acid analysis indicated that km23 is phosphorylated primarily on serine residues in response to TGFβ receptor activation [20]. This finding is in keeping with the known serine-threonine kinase specificity of the TβRs [1, 2, 22]. In contrast, epidermal growth factor (EGF), known to phosphorylate many downstream targets on tyrosine residues after receptor activation [23], could not phosphorylate km23.

km23 also contains several potential phosphorylation sites for a variety of other kinases, including protein kinase A (PKA), protein kinase C (PKC), and/or casein kinase II (CKII) predicted by PhosphoBase v. 2.0 and NetPhos 2.0 [24]. Among the serine residues, four are conserved between the human and rat forms (Fig. 1).

6. ACTIVATION OF JNK AND PHOSPHORYLATION OF c-Jun

Since our data indicate that km23 may function as a signaling intermediate for TGFβ, it was of interest to investigate whether km23 could mediate any of the known TGFβ signaling events. We have previously reported that TGFβ rapidly activates the Jun N-terminal kinase (JNK) family of MAPKs [9]. Further, JNK activation by TGFβ appears to play a role in TGFβ-mediated growth inhibition, either through the amplification of $TGF\beta_1$ production, via cross-talk with the Smads, and/or by regulation of cell cycle inhibitors [2, 25]. Thus, we examined whether stable expression of km23 could activate JNK as TGFβ does. We found that JNK was super-activated in the absence of TGFβ upon expression of km23 in Mv1Lu cells [20]. JNK activity was about 15 times greater in the km23-expressing cells than in the empty vector-expressing cells during an early period after TGFβ addition. Furthermore, phospho-c-Jun, a downstream effector of JNK, was also super-activated in the absence of TGFβ in the same Mv1Lu cells, compared with cells only stably expressing the empty vector [20]. These findings suggest that km23 may function as a signaling intermediate for TGFβ, in a pathway that involves JNK.

7. RECRUITMENT OF km23 TO DIC REQUIRESTGFβ RECEPTOR ACTIVATION

DLCs such as km23 are known to interact with the dynein motor complex through the DIC [20, 26]. For the DIC termed IC74-1A, the km23/roadblock-binding domain has been localized to a region spanning amino acids 243 to

282 [26]. In contrast, two other DLC families, Tctex-1 and DLC8, have been shown to bind to the same DIC through different binding domains. DLCs are also known to interact with a diverse array of cargo to exert their diverse functions. For example, Tctex-1 was found to interact with Doc2 [27] and the N-terminus of the $p59^{fyn}$ Src family tyrosine protein kinase [28] to exert diverse functions. Tctex-1 also can interact directly with the C-terminal tail of rhodopsin to mediate the transport of the visual pigment to the base of the connecting cilium within the photoreceptor [29]. Similarly, DLC8 binds to IC74 and a diverse set of other proteins, such as neuronal nitric-oxide synthase (nNOS) [30, 31], the proapoptotic Bcl-2 family member Bim [32], the Drosophila mRNA localization protein Swallow [33], and the rabies virus P protein [34]. The binding of DLC8 to these diverse proteins occurs at a conserved GIQVD motif or (K/R)XTQT motif [34, 35, 36].

With regard to the role of the DLC km23 in TGFβ signaling, we have shown that TGFβ could rapidly stimulate the recruitment of km23 to DIC, suggesting a connection between TGFβ signaling and DLC recruitment. Moreover, the association between km23 and DIC required the kinase activity of TβRII, since KN-RII blocked the recruitment of km23 to the DIC [20]. It is likely that the binding of km23 to the DIC after TGFβ receptor activation is important for specifying the nature of the cargo that will be transported along the MTs. Thus, km23 may behave similar to the Tctex-1 and DLC8.

8. CO-LOCALIZATION AND INTERACTION WITH Smad 2 IN VITRO AND IN VIVO

km23 associates with the TGFβ signal transducer Smad2 both *in vitro* and *in vivo*. In addition, immunofluorescence studies indicate that km23 and Smad2 are co-localized at very early times after TGFβ addition to cells. However, once Smad2 has translocated to the nucleus (within 15 min), the two proteins are no longer co-localized. Since km23 may function as a motor receptor to recruit TGFβ signaling components to the dynein motor for intracellular transport along microtubules (MTs) toward the nucleus, our results suggest that Smad2 may be one of the cargoes that km23 links to the dynein motor. It was reported that Smad2 must be translocated to the nucleus prior to its transcriptional regulation of target genes [37]. Thus, the interaction and co-localization of Smad2 with km23 may be an early step in Smad2 signaling of TGFβ responses. That is, km23 may transport Smad2 in the cytoplasm along MTs, prior to Smad2 nuclear translocation and transcriptional regulation.

9. km23 ALTERATION IN OVARIAN CANCER TISSUES

Ovarian carcinoma is often diagnosed at an advanced stage and is the leading cause of death from gynecological neoplasia, accounting for more than 14,000 deaths per year [38]. Overall, the molecular changes that underlie the initiation and development of this tumor are poorly understood. It has been reported that more than 75% of ovarian carcinomas are resistant to TGFβ, particularly recurrent ones [39, 40]. As such, the loss of TGFβ responsiveness may play an important role in the pathogenesis and/or progression of ovarian cancer.

It has been reported that TGFβ1, the TGFβ receptors, and several TGFβ signaling components (ie, Smad2, Smad4, and Dab-2) are altered in different types of cancers [1, 2, 13, 25]. Alterations in TβRII have been identified in 25% of ovarian carcinomas [41], while mutations in TβRI were reported in 33% of such cancers [42]. Loss of function mutations in TGFβ1, TβRI, and TβRII can lead to disruption of TGFβ signaling pathways and subsequent loss of cell cycle control [41, 42, 43, 44]. However, these alterations only account for a minority of TGFβ-resistant ovarian carcinomas, suggesting that other alterations in TGFβ signaling components may be involved in the pathogenesis of this type of cancer.

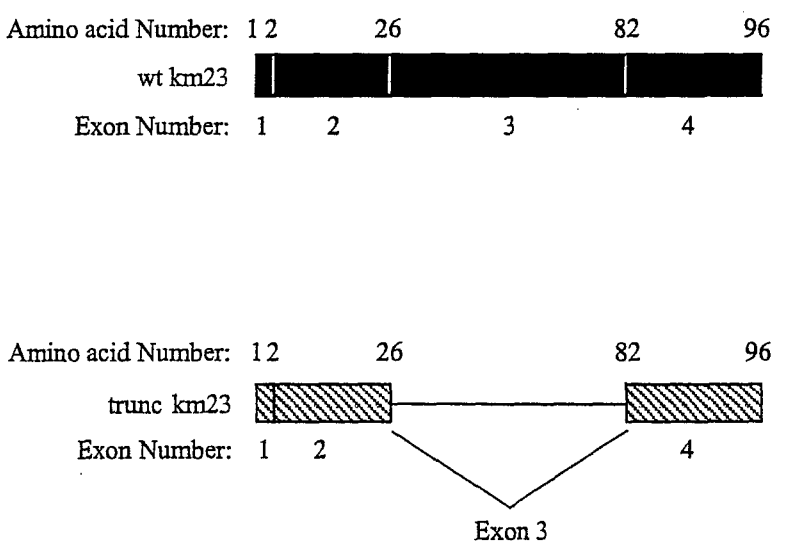

Figure 2. Amino acid sequence alignment of the truncated form of km23 with the wild-type form, indicating exon and amino acid sequence numbers. The 27th-81st amino acid residues have been deleted in the truncated form of km23. This form was detected both in ovarian tumor cell lines and ovarian cancer patients, resulting in a smaller 41-amino acid peptide.

In order to investigate whether this novel TGFβ receptor-interacting protein was altered in human ovarian cancer cells, we analyzed 19 ovarian carcinoma samples from patients, as well as six ovarian cancer cell lines, using laser capture micro-dissection (LCM) and nested reverse transcription-polymerase chain reaction (RT-PCR) strategies. Our data revealed a truncated form of km23, missing exon 3 of km23, in two ovarian cancer cell lines (SK-OV-3 and IGROV-1), both of which are resistant to TGFβ [45, 46]. The same truncated form of km23 was also detected in two out of nineteen ovarian cancer patients (Fig. 2). As mentioned above, km23 consists of 4 exons, and among them, the third exon is the longest, encoding amino acid residues 27-81 of km23. In addition, exon 3 contains three potential phosphorylation sites for PKA, PKC, and/or CKII (Fig. 1). The loss of these potential phosphorylation sites in the truncated protein may result in a disruption of signal transduction.

In *Drosophila*, a deletion mutant of km23/robl, which lacks portions of intron 2 and exon 3, displays mitotic defects [47]. This alteration is similar to the truncated form of km23 we identified in the ovarian tumor cell lines and cancer patients. The mitotic index of the mutant Drosophila hemizygotes was about five times that of the wt form [47]. In addition, the km23/robl mutant homozygotes cannot be fully rescued by the genomic or cDNA rescue constructs, suggesting that this mutation can act in a dominant fashion to inhibit the action of wt km23/robl [47]. Here we have shown that the wt form of km23 was still present in the tumor cell lines and in the tumor tissues from patients, despite the presence of the truncated form. Thus, the alterations in km23 we have identified here may also act in a dominant fashion in ovarian tumors. Increases in mitotic index and mitotic defects are commonly observed in the majority of cancers, including ovarian carcinomas. Thus, the truncated form of km23 may play an important role in the formation or progression of ovarian and other types of tumors.

In addition to the truncated form of km23 described above, several missense mutations were identified in the ovarian cancer patients. In two patients, the stop codon of km23 was altered from TAA to CAC. This alteration resulted in a larger protein, encoding 107 amino-acid residues, instead of the wt 96-amino acid form of km23. In addition to this missense mutation, five other missense mutations, including T38I, S55G, T56S, I89V and V90A, were detected in four other patients.

of the five missense mutations identified, T56S and S55G appeared to be the most interesting. As mentioned above, there are several potential PKA, PKC, and/or CKII phosphorylated sites in km23 (Fig. 1). Among them, the threonine at the 56th amino-acid residue spans a predicted phosphorylation site for PKA, PKC, and CKII. Mutation of this site may result in disruption

of signals transduced by these kinases. Further, we have reported that km23 is phosphorylated primarily on serines after activation of TGFβ receptors [20]. There are 4 serine residues in km23 that are conserved among the mammalian forms (boxed in Fig. 1). Among these, three are located in exon 3, including Ser55, which was found to be mutated in one of the ovarian carcinomas. Thus, this site and/or the other two in exon 3 may be potential phosphorylation sites modified by TGFβ.

10. CONCLUSIONS

km23 is a novel motor receptor found to be linked to a TGFβ signaling pathway. Based upon our observations, we have constructed the following model (Fig. 3). Upon phosphorylation of km23 by TβRs, DIC is recruited to form a motor complex. This complex transports membrane vesicles containing TGFβ signaling components such as Smad2 along the microtubules to a new vesicular compartment. After reaching the new compartment, the Smad complex may be translocated to the nucleus for transcriptional regulation of target genes. At this time point, km23 is no longer co-localized with Smad2. Future studies are still required to answer several questions about this novel TGFβ signaling intermediate. For example, we would like to identify other cargoes that km23 carries along the MTs. In addition, it would be of interest to know precisely which serine residues are phosphorylated by TGFβ, as well as what the consequences of dephosphorylation of these sites may be. Overall, we would like to develop km23-based cancer diagnostics and therapeutics, since km23 is altered at such a high rate in ovarian cancer. km23 most likely plays an important role in tumorgenesis or tumor progression in at least this type of cancer. Future studies will reveal whether this is the case for other tumor types as well.

Wei Ding and Kathleen M. Mulder
Department of Pharmacology, Penn State University College of Medicine, Hershey, Pennsylvania

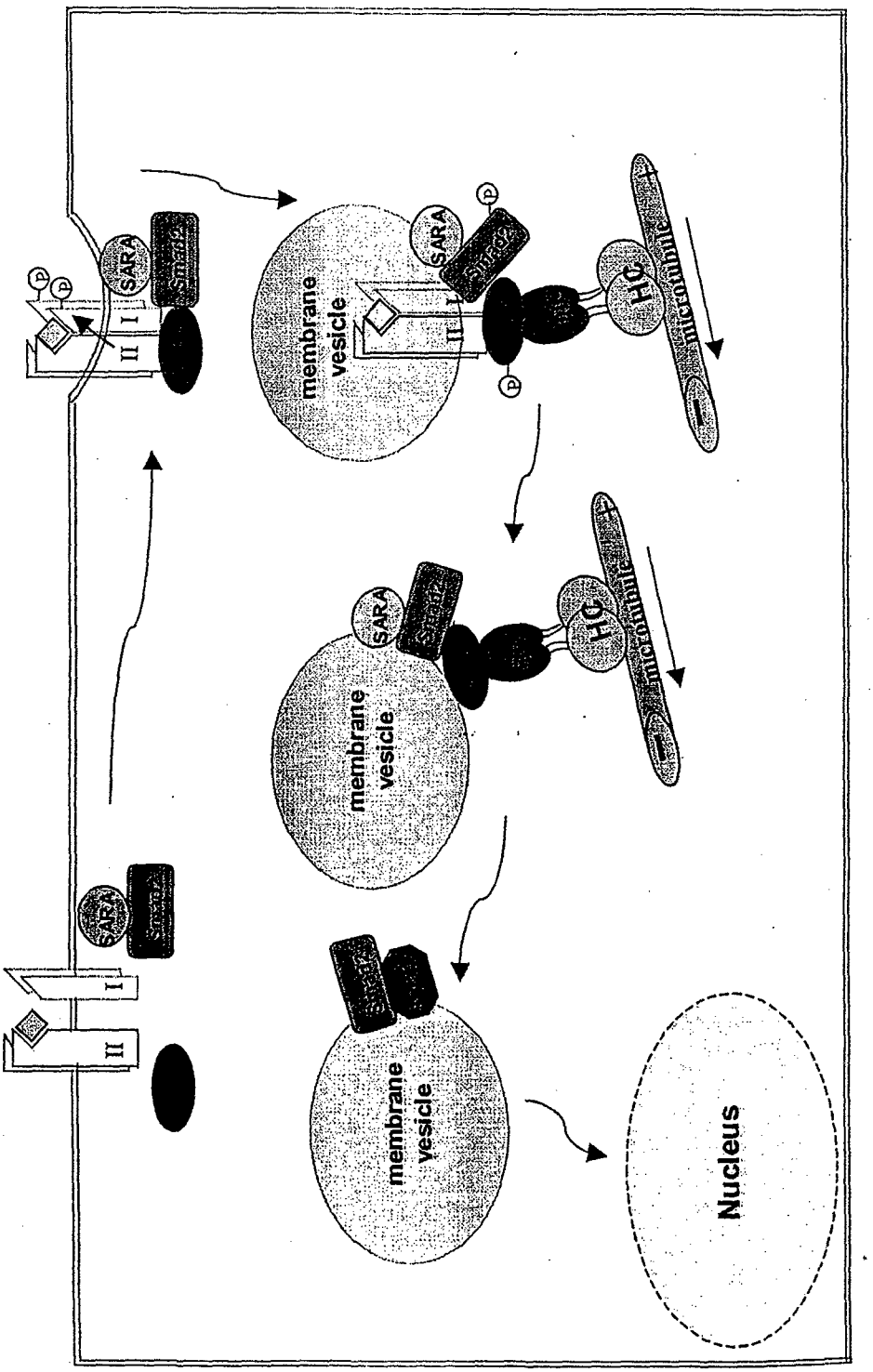
SARA
Smad2
I
II
P
membrane vesicle
HC
microtubule
Nucleus

Figure 3. km23 transports membrane vesicles containing TGFβ signaling components along the MTs toward the nucleus. Phosphorylated by ligand binding, the activated TβRII recruits and transphosphorylates TβRI. TβRII also phosphorylates km23, which then recruits DIC to form a motor complex. This complex transports the vesicles containing Smad2 along the microtubules toward the nucleus. Upon reaching the next compartment, the Smad complex may translocate from here to the nucleus for transcriptional regulation of target genes.

11. REFERENCES

1. Massague J., Blain S.W., and Lo R.S. TGFβ signaling in growth control, cancer, and heritable disorders. Cell 2000; 103: 295-309.
2. Yue J. and Mulder K.M. Transforming growth factor-β signaling transduction in epithelial cells. Pharmacol Ther 2001; 91: 1-34
3. Heldin C.H., Miyazono K., and ten Dijke P. TGF-β signalling from cell membrane to nucleus through SMAD proteins. Nature 1997; 390: 465-471.
4. Massague J. TGF-β signal transduction. Annu Rev Biochem 1998; 67: 753-791.
5. Abdollah S., Macias-Silva M., Tsukazaki T., Hayashi H., Attisano L., and Wrana J.L. TβRI phosphorylation of Smad2 on Ser465 and Ser467 is required for Smad2-Smad4 complex formation and signaling. J Biol Chem 1997; 272: 27678-27685.
6. Mulder K.M. and Morris S.L. Activation of p21ras by transforming growth factor β in epithelial cells. J Biol Chem 1992; 267: 5029-5031.
7. Hartsough M.T. and Mulder K.M. Transforming growth factor β activation of p44mapk in proliferating cultures of epithelial cells. J Biol Chem 1995; 270: 7117-7124.
8. Hartsough M.T., Frey R.S., Zipfel P.A., Buard A., Cook S.J., McCormick F., and Mulder K.M. Altered transforming growth factor signaling in epithelial cells when ras activation is blocked. J Biol Chem 1996; 271: 22368-22375.
9. Frey R.S. and Mulder K.M. Involvement of extracellular signal-regulated kinase 2 and stress-activated protein kinase/Jun N-terminal kinase activation by transforming growth factor β in the negative growth control of breast cancer cells. Cancer Res 1997; 57: 628-633.
10. Hocevar B.A., Brown T.L., and Howe P.H. TGF-β induces fibronectin synthesis through a c-Jun N-terminal kinase-dependent, Smad4-independent pathway. EMBO J 1999; 18: 1345-1356.
11. Tsukazaki T., Chiang T.A., Davison A.F., Attisano L., and Wrana J.L. SARA, a FYVE domain protein that recruits Smad2 to the TGFβ receptor. Cell 1998; 95: 779-791.
12. Miura S., Takeshita T., Asao H., Kimura Y., Murata K., Sasaki Y., Hanai J.I., Beppu H., Tsukazaki T., Wrana J.L., Miyazono K., and Sugamura K. Hgs (Hrs), a FYVE domain protein, is involved in Smad signaling through cooperation with SARA. Mol Cell Biol 2000; 20: 9346-9355.
13. Hocevar B.A., Smine A., Xu X.X., and Howe P.H. The adaptor molecule disabled-2 links the transforming growth factor β receptors to the Smad pathway. EMBO J 2001; 20: 2789-2801.
14. Datta P.K. and Moses H.L. STRAP and Smad7 synergize in the inhibition of transforming growth factor β signaling. Mol Cell Biol 2000; 20: 3157-3167.
15. Wang T., Li B.Y., Danielson P.D., Shah P.C., Rockwell S., Lechleider R.J., Martin J., Manganaro T., and Donahoe P.K. The immunophilin FKBP12 functions as a common inhibitor of the TGFβ family type I receptors. Cell 1996; 86: 435-444.
16. Chen R.H., Miettinen P.J., Maruoka E.M., Choy L., and Derynck R. A WD-domain

protein that is associated with and phosphorylated by the type II TGF-β receptor. Nature 1995; 377: 548-552.

17. Perlman R., Schiemann W.P., Brooks M.W., Lodish H.F., and Weinberg R.A. TGFβ-induced apoptosis is mediated by the adapter protein Daxx that facilitates JNK activation. Nat Cell Biol 2001; 3: 708-714.
18. Charng M.J., Zhang D., Kinnunen P., and Schneider M.D. A novel protein distinguishes between quiescent and activated forms of the type I transforming growth factor β receptor. J Biol Chem 1998; 273: 9365-9368.
19. Felici A., Wurthner J.U., Parks W.T., Giam L.R., Reiss M., Karpova T.S., McNally J.G., and Roberts A.B. TLP, a novel modulator of TGF-β signaling, has opposite effects on Smad2- and Smad3-dependent signaling. EMBO J 2003; 22 : 4465-4477.
20. Tang Q., Staub C.M., Gao G., Jin Q., Wang Z., Ding W., Aurigemma R.E., and Mulder K.M. A novel TGFβ receptor-interacting protein that is also a light chain of the motor protein dynein. Mol Biol Cell 2002; 13: 4484-4496.
21. Mulder K.M., Segarini P.R., Morris S.L., Ziman J.M., and Choi H.G. Role of receptor complexes in resistance or sensitivity to growth inhibition by TGFβ in intestinal epithelial cell clones. J Cell Physiol 1993; 54: 162-174.
22. Shi Y. and Massague J. Mechanisms of TGF-β signaling from cell membrane to the nucleus. Cell 2003; 113: 685-700.
23. Jorissen R.N., Walker F., Pouliot N., Garrett T.P., Ward C.W., and Burgess A.W. Epidermal growth factor receptor: mechanisms of activation and signalling. Exp Cell Res 2003; 284: 31-53.
24. Kreegipuu A., Blom N., and Brunak S. PhosphoBase, a database of phosphorylation sites: release 2.0. Nucleic Acids Res 1999; 27: 237-239.
25. Derynck R., Akhurst R.J., and Balmain A. TGF-β signaling in tumor suppression and cancer progression. Nat Genet 2001; 29: 117-129.
26. Susalka S.J., Nikulina K., Salata M.W., Vaughan P.S., King S.M., Vaughan K.T., and Pfister K.K. The roadblock light chain binds a novel region of the cytoplasmic dynein intermediate chain. J Biol Chem 2002; 277: 32939-32946.
27. Nagano F., Orita S., Sasaki T., Naito A., Sakaguchi G., Maeda M., Watanabe T., Kominami E., Uchiyama Y., and Takai Y. Interaction of Doc2 with tctex-1, a light chain of cytoplasmic dynein. J Biol Chem 1998; 273: 30065-30068.
28. Campbell K.S., Cooper S., Dessing M., Yates S., and Buder A. Interaction of p59fyn kinase with the dynein light chain, Tctex-1, and colocalization during cytokinesis. J Immunol 1998; 161: 1728-1737.
29. Tai A.W., Chuang J.Z., Bode C., Wolfrum U., and Sung C.H. Rhodopsin's carboxy-terminal cytoplasmic tail acts as a membrane receptor for cytoplasmic dynein by binding to the dynein light chain Tctex-1. Cell 1999; 97: 877-887.
30. Jaffrey S.R. and Snyder S.H. PIN: an associated protein inhibitor of neuronal nitric oxide synthase. Science. 1996; 274: 774-777.
31. Fan J.S., Zhang Q., Li M., Tochio H., Yamazaki T., Shimizu M., and Zhang M. Protein inhibitor of neuronal nitric-oxide synthase, PIN, binds to a 17-amino acid residue fragment of the enzyme. J Biol Chem 1998; 273: 33472-33481.
32. Puthalakath H., Huang D.C., O'Reilly L.A., King S.M., and Strasser A. The proapoptotic activity of the Bcl-2 family member Bim is regulated by interaction with the dynein motor complex. Mol Cell 1999; 3: 287-296.
33. Schnorrer F., Bohmann K., and Nusslein-Volhard C. The molecular motor dynein is involved in targeting swallow and bicoid RNA to the anterior pole of Drosophila oocytes. Nat Cell Biol 2000; 2:185-190.
34. Rodriguez-Crespo I., Yelamos B., Roncal F., Albar J.P., Ortiz de Montellano P.R., and Gavilanes F. Identification of novel cellular proteins that bind to the LC8 dynein light chain using a pepscan technique. FEBS Lett 2001; 503: 135-141.

35. Lo K.W., Naisbitt S., Fan J.S., Sheng M., and Zhang M. The 8-kDa dynein light chain binds to its targets via a conserved (K/R)XTQT motif. J Biol Chem 2001; 276: 14059-14066.
36. Martinez-Moreno M., Navarro-Lerida I., Roncal F., Albar J.P., Alonso C., Gavilanes F., and Rodriguez-Crespo I. Recognition of novel viral sequences that associate with the dynein light chain LC8 identified through a pepscan technique. FEBS Lett 2003; 544: 262-267.
37. Massague J. and Wotton D. Transcriptional control by the TGF-β/Smad signaling system. EMBO J 2000; 19: 1745-1754.
38. Landis S.H., Murray T., Bolden S., and Wingo P.A. Cancer statistics, 2001. CA Cancer J Clin 2001; 51: 15-36.
39. Yamada S.D., Baldwin R.L., and Karlan B.Y. Ovarian carcinoma cell cultures are resistant to TGF-β1-mediated growth inhibition despite expression of functional receptors. Gynecol Oncol 1999; 75: 72-77.
40. Hu W., Wu W., Nash M.A., Freedman R.S., Kavanagh J.J., and Verschraegen C.F. Anomalies of the TGF-β postreceptor signaling pathway in ovarian cancer cell lines. Anticancer Res 2000; 20: 729-733.
41. Lync M.A., Nakashima R., Song H.J., Degroff V.L., Wang D., Enomoto T., and Weghorst C.M. Mutational analysis of the transforming growth factor β receptor type II gene in human ovarian carcinoma. Cancer Res 1998; 58: 4227-4232.
42. Chen T., Triplett J., Dehner B., Hurst B., Colligan B., Pemberton J., Graff J.R., and Carter J.H. Transforming growth factor-β receptor type I gene is frequently mutated in ovarian carcinomas. Cancer Res 2001; 61: 4679-4682.
43. Cadillo M.R., Yap E., and Castagna G. Molecular genetic analysis of TGF-β1 in ovarian neoplasia. J Exp Clin Cancer Res 1997; 16: 49-56.
44. Wang D., Kanuma T., Muzunuma H., Takama F., Ibuki Y., Wake N., Mogi A., Shitara Y., and Takenoshita S. Analysis of specific gene mutations in the transforming growth factor-β signal transduction pathway in human ovarian cancer. Cancer Res 2000; 60: 4507-4512.
45. Zeinoun Z., Teugels E., De Bleser P.J., Neyns B., Geerts A., and De Greve J. Insufficient TGF-β1 production inactivates the autocrine growth suppressive circuit in human ovarian cancer cell lines. Anticancer Res 1999; 19: 413-420.
46. Jozan S., Guerrin M., Mazars P., Dutaur M., Monsarrat B., Cheutin F., Bugat R., Martel P., and Valette A. Transforming growth factor β1 (TGF-β1) inhibits growth of a human ovarian carcinoma cell line (OVCCR1) and is expressed in human ovarian tumors. Int J Cancer 1992; 52: 766-770.
47. Bowman A.B., Patel-King R.S., Benashski S.E., McCaffery J.M., Goldstein L.S., and King S.M. Drosophila roadblock and Chlamydomonas LC7: a conserved family of dynein-associated proteins involved in axonal transport, flagellar motility, and mitosis. J Cell Biol 1999; 146:165-180.

Requirement of km23 for TGF β-mediated growth inhibition and induction of fibronectin expression

Qunyan Jin*, Wei Ding*, Cory M. Staub*[ς], Guofeng Gao*[§], Qian Tang*[π] and Kathleen M. Mulder*[§ǂ]

*Department of Pharmacology, Pennsylvania State University College of Medicine, 500 University Dr., Hershey, PA 17033

[ς]Current address: Fox Chase Cancer Center, Philadephia, PA, 19111-2497

[π]Current address: Lexicon Genetics Inc., 8800 Technology Forest Place, The Woodlands, TX 77381-1160

[§]Intercollege Graduate Program in Genetics, Pennsylvania State University College of Medicine, 500 University Dr., Hershey, PA 17033

[ǂ]To whom correspondence should be addressed:

Department of Pharmacology—MC H078

Penn State College of Medicine

500 University Drive, Hershey, PA 17033

Telephone: 717-531-6789; FAX: 717-531-5013

E-mail kmm15@psu.edu

Running title: Blockade of km23 inhibits TGFβ responses

Key words: TGFβ, signal transduction, siRNA, growth, fibronectin, km23, EGF, dynein

ABSTRACT

We previously identified km23 as a novel receptor-interacting protein. Here we show that km23 is ubiquitously expressed in human tissues and that cell-type specific differences in endogenous km23 protein expression exist. In addition, we demonstrate that the phosphorylation of km23 is TGFβ-dependent, in that EGF was unable to phosphorylate km23. Further, the kinase activity of both TGFβ receptors appears to play a role in the TGFβ-mediated phosphorylation of km23, although RII kinase activity is absolutely required for km23 phosphorylation. Blockade of km23 using small interfering RNA significantly decreased key TGFβ responses, including induction of fibronectin expression and inhibition of cell growth. Thus, our results demonstrate that km23 is required for TGFβ induction of fibronectin expression and is necessary, but not sufficient, for TGFβ-mediated growth inhibition.

Abbreviations: TGFβ, transforming growth factor β; ECM, extracellular matrix; FN, fibronectin; JNK, c-Jun N-terminal kinases; siRNA, small interfering RNA; MDCK, Madin Darby canine kidney; Ab, antibody; DIC, dynein intermediate chain; EGF, Epidermal growth factor; hkm23, human km23

INTRODUCTION

Transforming growth factor β (TGFβ) is the prototype for a family of highly conserved ubiquitous peptides that show a remarkable diversity in the biological actions they mediate. These biological responses include effects on cell growth, cell death, cell differentiation, and the extracellular matrix (ECM) (1-3). TGFβ is growth inhibitory for normal cells of endothelial, hematopoietic, neuronal, and epithelial origin (1, 4-5) . However, cancers are often refractory to this growth inhibitory effect, due to genetic loss of TGFβ signaling components or, more commonly, perturbation of TGFβ signaling pathways (1, 4).

TGFβ initiates its signals by producing an active tetrameric receptor complex consisting of RI and RII serine/threonine kinase receptors. After TGFβ binds to RII, it transphosphorylates, and thereby activates RI. The active receptor complex then propagates signals to downstream cellular components and regulatory proteins (2-3, 6). Two primary signaling cascades downstream of the TGFβ receptors have been elucidated: the Smads and the Ras/mitogen-activated protein kinase (MAPK) pathways (1-2, 7). In addition, several TGFβ receptor-interacting factors (1) and Smad-interacting factors (8) have been reported. However, additional TGFβ signaling components and pathways are likely required to mediate the diverse biological responses of this polypeptide factor.

Fibronectin (FN), a major component of the ECM, plays important roles in cell adhesion, migration, growth and differentiation (9-10). TGFβ is one of the most potent stimulators of the ECM, and it has been shown to play a significant role in the

accumulation of specific ECM components such as FN and collagen (1, 11-12). Despite the suggestion that Smads play a critical role in TGFβ-mediated responses, the signaling mechanisms leading to TGFβ-mediated accumulation of ECM proteins are unclear. For example, Hocevar et al (13) have shown that TGFβ can induce FN synthesis through a c-Jun N-terminal kinase (JNK)-dependent pathway, but that Smad4 was not involved. In addition, Gooch et al (14) reported that calcineurin was involved in TGFβ -mediated regulation of ECM accumulation. It is likely that other novel TGFβ signaling intermediates are required for mediating the effects of TGFβ on ECM components such as FN.

We have previously identified a novel TGFβ receptor-interacting protein that is also a light chain of the motor protein dynein (15). This TGFβ signaling intermediate, termed km23, interacts with the receptor complex through TGFβ RII and is phosphorylated after activation of the TGFβ receptor complex. Here we show that km23 is a ubiquitously expressed cytoplasmic protein. Further, TGFβ mediated a rapid increase in km23 phosphorylation, and the kinase activity of both receptors appeared to play a role in this phosphorylation event. Blockade of km23 using small interfering RNA (siRNA) decreased the ability of TGFβ to both inhibit cell growth and induce FN expression in Madin Darby canine kidney (MDCK) epithelial cells. Our findings indicate that km23 is a mediator of the growth inhibitory effect of TGFβ and is also required for the induction of FN expression by TGFβ.

MATERIALS AND METHODS

Reagents--The anti-Flag M2 (F3165) antibody (Ab) and mouse IgG were from Sigma-Aldrich (St. Louis, MO). The anti-dynein intermediate chain (DIC) monoclonal Ab (MAB1618) and anti-Lamin A/C Ab (MAB3211) were from Chemicon (Temecula, CA). The rabbit IgG was from Santa Cruz Biotechnology, Inc. (Santa Cruz, CA). The anti-FN Ab (610078) was from BD Biosciences Transduction Laboratories (Palo Alto, CA). Protein A or G agarose were purchased from Invitrogen (Carlsbad, CA). ^{32}P-orthophosphate (NEX-053) was from PerkinElmer Life Sciences (Boston, MA). TGFβ_1 was purchased from R & D Systems (Minneapolis, MN). Epidermal growth factor (EGF) was purchased from Upstate Cell Signaling Solutions (Lake Placid, NY). Lipofectamine 2000 (11668-019) was from Invitrogen (Carlsbad, CA).

Antibody production--The rabbit km23 anti-serum was prepared against the following sequence: GIPIKSTMDNPTTTQYA (corresponding to amino acids 27-43) of human km23 (hkm23) (Strategic BioSolutions, Newark, DE, or Covance Reseach Products, Inc., Denver, PA). Each company also provided pre-immune serum.

Cell culture--Mv1Lu (CCL-64), 293 (CRL-1573), and COS-1 (CRL-1650) cells were purchased from American Type Culture Collection (Manassas, VA) and were grown in DMEM supplemented with 10% FBS. MDCK cells (CCL-34) and HepG2 cells (HB-8065) were also obtained from ATCC and were grown in MEM-α supplemented with 10% FBS. 293T cells were obtained from T-W. Wong (Bristol-Myers Squibb, Princeton, NJ) and were maintained as for 293 cells. OVCA 433 cells were obtained from R.C. Bast Jr. (M.D. Anderson Cancer Center, Houston, TX) and were maintained

in MEM supplemented with 10% FBS. FET cells were maintained as described previously (16). Cultures were routinely screened for mycoplasma using Hoechst 33258 staining.

Transient transfections, IP/blot, Westerns, and In vivo phosphorylation assays-- were performed essentially as described previously (13, 15, 17-19).

siRNA -- km23 siRNA used in [^{3}H]thymidine incorporation assays was purchased from Dharmacon Research (Lafayette, CO). The double-stranded km23 siRNA corresponded to nucleotides 77-97 of the hkm23 coding region (5'-AAGGCATTCCCATCAAGAGCA-3'). siRNA was transfected using Oligofectamine (12252-011; Invitrogen).

siRNA plasmid constructs-- Human km23 hairpin siRNA was cloned into the pSilencer U6-1.0 vector containing the RNA polymerase III U6 promotor (Ambion, Austin, TX, Cat# 7208) after linearization with Apa I and EcoR I. The sense strand of the hairpin km23 siRNA-1 corresponded to nucleotides 230-250 of the km23 coding region (5'-AAATTATGGTTGCACCAGATA-3'). The sense strand of hairpin km23 siRNA-2 corresponded to nucleotides 130-150 of the km23 coding region (5'-CCTCATGCACAACTTCATC-3'). km23 siRNA-1 and km23 siRNA-2 plasmids were transfected using Lipofectamine 2000 reagent for the FN experiments.

Cellular fractionation--The NE-PER Nuclear and Cytoplasmic Extraction Reagent kit (78833; Pierce, Rockford, IL) was used to fractionate Mv1Lu cells according to the manufacturer's protocol.

Growth assays--The TGFβ growth inhibitory responsiveness of the cells was assessed by [^{3}H]thymidine incorporation assays, performed as described (20).

Statistical analyses--A Student's t-test was used to determine the level of statistical significance of the decrease in [^{3}H]thymidine incorporation by TGFβ between km23 siRNA-transfected and control-transfected MDCK cells.

RESULTS

We have demonstrated previously that km23 is a novel TGFβ receptor-interacting protein that is also a light chain of the motor protein dynein (15). As indicated in Fig. 1, hkm23 is very similar to the *Danio Rerio* (Zebrafish) ZFIN (80% identity or 93% similarity), *Drosophila* robl (68% identity or 82% similarity), and *Chlamydomonas* LC7 (55% identity or 81% similarity) sequences. In addition, a counterpart of km23 in *Caenorhabditis elegans* (T24H10.6) displays 56% homology to hkm23, and the predicted protein would be 76% similar. In contrast, hkm23 displays 71% similarity to *Spermatozopsis* B15 (21), 54% similarity to *Drosophila* bithoraxoid (bxd), and only 33% homology (predicted protein would be 32% similar) to *Leishmania* LMAJFV1 (22). The single-celled flagellar parasite *Leishmania* is an animal-like, Protozoan form of Protista, the Kingdom that also includes plant-like forms of green algae, such as *Chlamydomonas* and *Spermatozopsis.* Thus, km23 displays a considerable degree of conservation across different Kingdoms and Phyla.

In order to determine the tissue distribution of hkm23, we performed Northern blot analysis using a human tissue blot obtained from BD Biosciences Clontech. km23 was ubiquitously expressed, with a calculated hkm23-1 mRNA size of approximately 0.7 kb (data not shown). Similarly, it was of interest to determine whether the km23 protein was expressed in different cell types. In order to proceed with these studies, we developed a polyclonal anti-serum against amino acids 27-43 of hkm23 and performed initial Western blot analyses in MDCK epithelial cells to determine whether the km23 anti-serum was specific. As indicated in Fig. 2A, the

rabbit km23 anti-serum specifically recognized a single band of 11 kDa by Western blot analysis (lane 1). No band was visible when pre-immune serum was used (lane 2). Thus, the km23 serum was specific.

In order to further demonstrate the specificity of the rabbit km23 anti-serum and to determine whether it could also detect transfected km23, we performed Western blot analysis after subcellular fractionation of the cells. As indicated in Fig. 2B, the anti-Flag Ab could only detect expressed km23-Flag in the cytoplasmic fraction (lane 3, top panel). In contrast, the rabbit km23 anti-serum could detect both endogenous and expressed km23 in the cytoplasmic fraction (lanes1-3, middle panel). This cytoplasmic localization of km23 is consistent with the fact that km23 does not contain a nuclear localization sequence based upon nuclear localization sequence motifs previously published (23). As expected, endogenous Lamins A and C were not detectable in the cytoplasmic fraction (lanes 1-3, bottom panel). Further, both endogenous and expressed km23 were absent in the nuclear fraction (lanes 4-6, top panel), whereas Lamins A and C were easily detectable in this compartment (lanes 4-6, bottom panel) (24). The results indicate that km23 is a cytoplasmic protein and that the rabbit anti-serum can specifically recognize both endogenous and expressed km23.

Since we had demonstrated the specificity of our Ab, we could now assess km23 protein expression levels across multiple species. Thus, we examined the relative expression levels of endogenous km23 in several mammalian cell types. As shown in Fig. 2C, our Ab can detect km23 at high levels in HepG2 human hepatoma cells (lane 4, top panel) and in MDCK cells (lane 6, top panel), whereas lower levels

were detectable in Mv1Lu mink lung epithelial cells (lane 5, top panel). We also found that km23 was barely detectable in the TGFβ–resistant, human ovarian cancer cell line OVCA 433 (lane 3, top panel), compared with all of the other cell lines. km23 levels were intermediate in 293 human embryonic kidney cells (lane 1, top panel) and in partially TGFβ–responsive FET human colon cancer cells (lane 2, top panel). Equal loading was confirmed by blotting with a DIC Ab (bottom panel), since we have previously determined that DIC levels are relatively constant among such cell lines. Thus, our Ab could detect endogenous km23 across multiple species, and in malignant cells as well.

Since TGFβ often modulates gene expression, it was of interest to determine whether km23 levels were regulated by TGFβ at various times after TGFβ addition to cells. Thus, we performed Western blot analysis using the rabbit km23 anti-serum. As shown in Fig.2D, equal amounts of km23 were detectable from 5 to 30 min after TGFβ treatment (lanes 1-4). Equal loading was confirmed by blotting with a DIC Ab (data not shown). Thus, TGFβ did not induce the expression of endogenous km23.

The serine/threonine kinase activity of the TGFβ receptors mediates phosphorylation of downstream molecules to affect TGFβ responses. We have previously shown that km23 was phosphorylated by the TGFβ receptor complex in human embryonic kidney 293T cells (15). Since TGFβ increased the phosphorylation levels of km23, it was of interest to determine whether another growth factor ligand could produce a similar effect. EGF is known to phosphorylate many downstream targets after activation of its receptor (25). For example, Shc, Src, STATs, PLC-γ and PPARγ (26-30) have all been shown to be phosphorylated within 30 minutes of EGF

treatment. In order to determine whether km23 could be phosphorylated by EGF, we performed in vivo phosphorylation assays after transient expression of km23-Flag, RI-HA, and RII-HA in the absence and presence of TGFβ or EGF. However, as indicated in Fig.3A (right side), EGF did not stimulate km23 phosphorylation during a treatment period of 0-30 minutes (lanes 7-9). EGF has been shown to phosphorylate other substrates during this time period in this cell line (30). As expected, km23 was phosphorylated upon co-expression of both types of TGFβ receptors (lane 3). A ligand-dependent increase in km23 phosphorylation was observed at 5 and 15 min after TGFβ treatment (lanes 4 and 5). As shown previously, km23 was not auto-phosphorylated (lane 2), nor was there phosphorylation in the EV (lane 1), or the IgG (lane 6) control lanes. Collectively, our results suggest that km23 phosphorylation may be mediated specifically by TGFβ.

We have also previously shown that the kinase activity of RII was required for the phosphorylation of km23 (15). However, it was unclear whether the kinase activity of RI was also required for this phosphorylation event. In order to address the role of the kinase activity of RI in the TGFβ-mediated phosphorylation of km23, the in vivo phosphorylation assays in Fig. 3B were performed using either a wild-type or kinase-deficient form of RI (KN RI) alone or in combination with RII. Co-expression of RII with KN RI (lanes 9 and 10) resulted in a reduction in km23 phosphorylation, relative to that observed after expression of both receptors (lanes 2 and 3), or after expression of RII alone (lanes 7 and 8). As expected, co-expression of RI and RII without km23 resulted in no detectable phosphorylation (lane 1). The IgG control (lane 4) was also negative. Thus, phosphorylation of km23 by TGFβ can occur in the absence of RI, but

the kinase activity of RI does enhance km23 phosphorylation by RII to some extent. The mechanism underling the role of RI in km23 phosphorylation is the subject of future investigations.

We have previously shown that TGFβ RII kinase activity was required for km23 phosphorylation and interaction with the rest of the dynein motor, and that forced expression of km23 resulted in activation of known TGFβ signaling components and responses (15). Thus, we suggested that TGFβ signaling components might be the cargo transported by km23. Accordingly, km23 may function as a TGFβ signaling intermediate by assisting with the transport of TGFβ signaling complexes to the appropriate cell locations to mediate TGFβ responses. In order to more definitively establish whether km23 was required for mediating specific TGFβ responses, we utilized siRNA approaches. We examined the effect of blocking km23 expression on two major TGFβ responses, namely growth inhibition and induction of extracellular matrix protein expression.

Since a prominent biological effect of TGFβ in epithelial cells is growth inhibition (1, 4-5), we initially examined the effect of siRNA blockade of km23 on TGFβ inhibition of [^{3}H]thymidine incorporation. In order to establish that the km23 siRNA could block endogenous km23 expression, we transfected MDCK cells with the siRNA using Oligofectamine as described in the "Materials and Methods." Western blot analysis was then performed as shown in Fig. 4A. Transfection with either 0.10 μM or 0.12 μM siRNA resulted in a marked decrease (compared to control cells) in km23 levels at both 24 h (lanes 1-3) and 48 h (lanes 4-6) after addition of the siRNA. The decrease in endogenous km23 was maximal at 24 h after transfection of siRNA

(lanes 2 and 3, top panel), with a reduction of km23 expression by approximately 65%. The silencing effect was apparent for at least an additional 24 h, and was similar when a slightly higher siRNA concentration was used (0.12 μM; lanes 2, 3, 5, and 6, top panel). After 72 h, there was no difference in endogenous km23 levels between the control and siRNA-transfected cells (lanes 7-9, top panel). The bottom panel of Fig. 4A depicts the results of desitometric scans of the top panel, with the percent of control values provided above the relevant bars.

Since 0.1 μM siRNA resulted in maximal silencing at 24 h after addition to MDCK cultures, we examined TGFβ effects on [^{3}H]thymidine incorpration in MDCK cells in the presence and absence of 0.1 μM siRNA at this time point. The results in Fig. 4B indicate that blockade of endogenous km23 caused a reduction in the ability of TGFβ to inhibit DNA synthesis. While TGFβ inhibited the control cells by 92%, cells transfected with km23 siRNA displayed only a 73% inhibition by TGFβ. This difference was statistically significant ($p<0.01$). Thus, km23 is partially required for the repression of DNA synthesis by TGFβ.

TGFβ has been shown to potently induce FN expression at both the mRNA and protein levels (31-32). In addition, Hocevar et al (13) have shown that the JNK pathway is required for the induction of FN by TGFβ. We have previously shown that over-expression of km23 could induce JNK activation and result in phosphorylation of the downstream target c-Jun (15), suggesting that km23 regulates the JNK pathway and may contribute to FN induction in some manner. Thus, it was of interest to determine whether blockade of km23 would also decrease TGFβ induction of FN expression. Therefore, we transiently transfected MDCK cells with km23 siRNA-1 or

km23 siRNA-2 as described in the "Materials and Methods" and performed Western blot analysis to examine FN induction by TGFβ. As shown in Fig. 5A, both km23 siRNA-1 and km23 siRNA-2 resulted in a marked decrease in endogenous km23 levels (lanes 2 and 3, top panel) compared to control (lane 1, top panel). Equal protein loading was confirmed by blotting with a DIC Ab (bottom panel). Fig.5B indicates that, as expected, TGFβ induced FN expression in the controls (lanes 1 and 2, top panel). In contrast, both km23 siRNAs resulted in a decrease in the ability of TGFβ to induce FN expression, both in the absence and presence of TGFβ (lanes 3-6, top panel). Blockade of endogenous km23 was confirmed by blotting with km23 anti-serum (bottom panel). Thus, km23 siRNA can block FN induction by both autocrine and exogenous TGFβ. These results suggest that km23 is required for TGFβ induction of FN expression.

DISCUSSION

We have isolated km23 via its ability to interact with the intracellular portions of the TGFβ receptors and have shown that this protein is also a light chain of the motor protein dynein (15). Further, we have demonstrated that this TGFβ receptor-interacting protein is associated with the TGFβ receptor complex through RII, and that its expression can mediate some of the biological responses of TGFβ. In the current report, we show that although the kinase activity of RII is absolutely required for km23 phosphorylation, the kinase activity of RI is also involved. Further, km23 phosphorylation appeared to be induced specifically by TGFβ, since EGF was unable to alter the phosphorylation status of km23. More importantly, we demonstrate for the first time, using siRNA approaches, that km23 is required for TGFβ induction of FN expression and that it is necessary, but not sufficient, for grow inhibition by TGFβ. Thus, our results support an important role for km23 in TGFβ signaling.

The partial requirement of km23 for TGFβ-mediated inhibition of DNA synthesis is not an unexpected finding, as other pathway components are known to be involved in mediating this complex biological response. For example, TGFβ activation of Ras is also partially required for TGFβ–mediated growth inhibition, and for some of the cell cycle effects that mediate this response (33-35). TGFβ activation of extracellular signal-regulated kinases (Erks) and of stress-activated protein kinases/Jun N-terminal kinases (SAPK/JNKs) was also found to be required for negative growth control by TGFβ (7, 18, 36). Further, over-expression of the p65 subunit of the NF-κB/Rel family in Hs578T cells abrogated the ability of TGFβ to inhibit cell growth (37),

suggesting that TGFβ regulation of NF-κB/Rel activity is also associated with TGFβ-mediated growth inhibition. Thus, several TGFβ-regulated components appear to be required for mediating the growth inhibitory response to TGFβ. km23 may represent a novel member of this group of signaling components.

As mentioned above, we have demonstrated herein that silencing of km23 resulted in a blockade of the ability of TGFβ to mediate another major TGFβ response, namely induction of FN expression. The induction of FN by TGFβ was previously shown to be mediated by an activation of JNK and was Smad4-independent (13). In addition, we have previously shown that stable expression of km23 resulted in a super-activation of JNK, as well as an increase in the phosphorylation of the downstream JNK target c-Jun, suggesting that km23 was involved in the activation of JNK by TGFβ (15). Thus, our novel finding here is in keeping with our previous results, and the results of others, and suggests that km23 may function as a signaling intermediate for the TGFβ induction of FN expression, possibly via the JNK pathway.

In summary, we have provided the following evidence to indicate that km23 is an important TGFβ signal transducer. First, we have shown that TGFβ, but not EGF, can induce phosphorylation of km23 in a ligand-dependent fashion. Second, our data indicate that the kinase activity of both TGFβ receptors plays a role in phosphorylation, although the RII kinase activity is obligatory. Third, siRNA blockade of km23 expression resulted in a partial loss of the ability of TGFβ to inhibit cell cycle progression, as assessed by a reduced S phase inhibition of DNA synthesis by TGFβ. Fourth, siRNA blockade of km23 expression blocked the ability of TGFβ to

induce the extracellular matrix protein FN. Our results also reveal that km23 is a highly conserved, ubiquitously-expressed, cytoplasmic protein, which can be detected in several species and cell types, in keeping with the ubiquitous and multifunctional nature of TGFβ. Future studies will unravel the precise signaling pathways and mechanisms involved in the km23-mediated TGFβ responses examined herein.

ACKNOWLEDGMENTS

We thank J. Massague (Memorial Sloan-Kettering Cancer Center, New York, NY) for KNRI-HA, KNRII-HA and pCMV5-HA-TGFRII; J. Wrana (Samuel Lunenfeld Research Institute, Toronto, Canada) for pCMV5-HA-TGFRI; H. Moses (Vanderbilt) for the T204D-HA. We also thank R.C. Bast Jr. (M.D. Anderson Cancer Center, Houston, TX) for the OVCA 433 cells and T-W. Wong (Bristol-Myers Squibb, Princeton, NJ) for the 293T cells. This work was supported by National Institutes of Health Grants CA90765, CA92889, and CA100239, and Dept of Defense IDEA AWAD # DAMD17-03-01-0287 (to K.M.M).

REFERENCES

1. Yue, J. and Mulder, K. M. (2001). *Pharmacol. Ther.* 91, 1-34

2. Derynck, R. and Zhang,Y. E. (2003) *Nature* 425, 577-584.

3. Shi, Y. G. and Massague, J. (2003) *Cell* 113, 685-700.

4. Akhurst, R. J. and Derynck, R. (2001) *Trends Cell Biol.* 11, S44-S51.

5. Roberts, A. B. and Wakefield, L. M. (2003) *Proc. Natl. Acad. Sci. U S A.* 100, 8621-8623.

6. Mehra, A. and Wrana, J. L. (2002) *Biochem. Cell Biol.* 80, 605-622.

7. Mulder, K. M. (2000) *Cytokine Growth Factor Rev.* 11, 23-35.

8. ten Dijke, P., Goumans, M. J., Itoh, F. and Itoh, S. (2002) *J. Cell Physiol.* 191,1-16.

9. Danen, E. H. J. and Yamada, K. M. (2001) *J. Cell Physiol.* 189, 1-13.

10. Pankov, R. and Yamada, K. M. (2002) *J. Cell Sci.* 115, 3861-3863.

11. Massague, J., Blain, S. W., Lo, R. S. (2000) Cell 103, 295-309.

12. Roberts, A. B., Russo, A., Felici, A. and Flanders, K. C. (2003) *Ann. N. Y. Acad. Sci.* 995, 1-10.

13. Hocevar, B. A., Brown, T. L. and Howe, P. H. (1999) *EMBO J.* 18, 1345-1356.

14. Gooch, J. L., Gorin, Y., Zhang, B. X. and Abboud, H. E. (2004) *J. Biol. Chem.* 279, 15561-15570.

15. Tang, Q., Staub, C. M., Gao, G., Jin, Q., Wang, Z., Ding, W., Aurigemma, R. E. and Mulder, K. M. (2002) *Mol. Biol. Cell* 13, 4484-4496.

16. Zipfel, P. A., Ziober, B. L., Morris, S. L. and Mulder, K. M. (1993) *Cell Growth Differ.* 4, 637-645.

17. Yue, J., Frey, R. S. and Mulder, K. M. (1999) *Oncogene* 18, 2033-2037.

18. Yue, J., Hartsough, M. T., Frey, R. S., Frielle, T. and Mulder, K. M. (1999) *J. Cell Physiol.* 178, 387-396.

19. Yue, J. and Mulder, K. M. (2000) *J. Biol. Chem.* 275, 30765-30773.

20. Hartsough, M. T. and Mulder, K. M. (1995) *J. Biol. Chem.* 270, 7117-7124.

21. Dole, V., Jakubzik, C. R., Brunjes, B. and Kreimer, G. (2000) *Biochim. Biophys. Acta.* 1490, 125-130.

22. Akopyants, N. S., Clifton, S. W., Martin, J., Pape, D., Wylie, T., Li, L., Kissinger, J.C., Roos, D. S. and Beverley, S. M. (2001) *Mol. Biochem. Parasitol.* 113, 337-340.

23. Mattaj, I. W. and Englmeier, L. (1998). Nucleocytoplasmic transport: the soluble phase. *Annu. Rev. Biochem.* 67, 265-306.

24. Georgatos, S. D., Meier, J. and Simos, G. (1994) *Curr. Opin. Cell Biol.* 6, 347-353.

25. Jorissen, R. N., Walker, F., Pouliot, N., Garrett, T. P. J., Ward, C. W. and Burgess, A. W. (2003) *Exp. Cell Res.* 284, 31-53.

26. Sakaguchi, K., Okabayashi, Y., Kido, Y., Kimura, S., Matsumura, Y., Inushima, K. and Kasuga, M. (1998) *Mol. Endo.* 12, 536-543.

27. Mao, W., Irby, R., Coppola, D., Fu, L., Wloch, M., Turner, J., Yu, H., Garcia, R., Jove, R. and Yeatman, T. J. (1997) *Oncogene* 15, 3083-3090.

28. David, M., Wong, L., Flavell, R., Thompson, S. A., Wells, A., Larner, A. C. and Johnson, G. R. (1996) *J. Biol. Chem.* 271, 9185-9188.

29. Wahl, M. I., Nishibe, S., Kim, J. W., Kim, H., Rhee, S. G. and Carpenter, G. (1990) *J. Biol. Chem.* 265, 3944-3948.

30. Camp, H. S. and Tafuri, S. R. (1997) *J. Biol. Chem.* 272, 10811-10816.

31. Ignotz, R. A. and Massague, J. (1986). *J Biol Chem.* 261, 4337-4345.

32. Wrana, J. L., Overall, C. M. and Sodek, J. (1991) *Eur. J. Biochem.* 197, 519-528.

33. Mulder, K. M. and Morris, S. L. (1992) *J. Biol. Chem.* 267, 5029-5031.

34. Hartsough, M. T., Frey, R. S., Zipfel, P. A., Buard, A., Cook, S. J., McCormick, F. and Mulder, K. M. (1996) *J. Biol. Chem.* 271, 22368-22375.

35. Yue, J., Buard, A. and Mulder, K. M. (1998) *Oncogene* 17, 47-55.

36. Frey, R. S. and Mulder, K. M. (1997) *Cancer Res.* 57, 628-633.

37. Sovak, M. A., Arsura, M., Zanieski, G., Kavanagh, K.T. and Sonenshein, G. E. (1999). *Cell Growth Differ.* 10, 537-544.

FIGURE LEGENDS

Fig. 1. Alignment of amino acid sequences comparing km23 family members. The coding region for the following km23 family members are aligned to illustrate the relative identities: hkm23-1 (accession # AY026513), ZFIN (accession # AAH46084; 74% homology to hkm23-1), robl (accession # AF141920; 67% homology to hkm23-1), LC7 (accession # AF140239; 59% homology to hkm23-1), T24H10.6 (accession #Z54216; 56% homology to hkm23-1), B15 (accession # AJ243446; 56% homology to hkm23-1), bxd (accession # M27999; 40% homology to hkm23-1), and LMAJFV1 (accession # AQ850960; 33% homology to hkm23-1).

Fig. 2. Development and specificity assessment of a rabbit polyclonal antiserum for detection of km23 protein expression. **A:** MDCK cell lysates were analyzed by SDS-PAGE (15%) and transferred to a PVDF membrane. The membrane was then incubated with rabbit km23 anti-serum (lane 1), pre-immune rabbit serum as a control (lane 2), respectively, followed by incubation with an anti-rabbit IgG secondary antibody (1:7500) to demonstrate the specificity of the km23 Ab. **B:** Mv1Lu cells were either mock transfected or transiently transfected with EV or km23-Flag. Twenty-four h later, cells were then fractionated as described in "Materials and Methods." Top panel, both cytoplasmic and nuclear fractions were subjected to SDS-PAGE (15%), transferred to a PVDF membrane, and blotted with anti-flag Ab. Middle panel, membrane was then reprobed with rabbit km23 anti-serum. Bottom panel, the membrane was then reprobed with anti-lamin A/C Ab as a nuclear marker. **C:** Top

panel, protein lysates (75 μg) were prepared from 293, FET, OVCA 433, HepG2, Mv1Lu, and MDCK cells, and analyzed as in Fig.3A. Equal loading was confirmed by blotting with a DIC Ab. **D:** MDCK cell lysates were incubated in serum-free MEM-α medium for 1 h in the absence (lane 1) or presence of (lanes 2-4) TGFβ (10 ng/ml). Lysates were analyzed by SDS-PAGE (15%) and transferred to a PVDF membrane. The membrane was then incubated with rabbit km23 polyclonal anti-serum, followed by incubation with an anti-rabbit IgG secondary antibody (1:7500). The results shown are representative of two similar experiments.

Fig. 3. The kinase activity of both RI and RII plays a role in the TGFβ–dependent phosphorylation of km23. **A:** Human embryonic kidney 293T cells were transiently transfected with either EV, km23-Flag, and/or RI-HA and RII-HA as indicated. Twenty-four h after transfection, cells were labeled for 3 h with [$^{32}P_i$] in the absence or presence of TGFβ (5 ng/ml) (lanes 1-6) or EGF (100 ng/ml) (lanes 7-9) for the indicated times. Thereafter, cells were lysed and immunoprecipitated with anti-Flag. In vivo phosphorylation of km23-flag was visualized by SDS-PAGE (15%) and autoradiography. **B:** COS-1 cells were transiently transfected with either EV, km23-Flag, and/or wild-type or mutant RI and RII as indicated and were analyzed as for A. The results shown are representative of three similar experiments.

Fig. 4. siRNA blockade of km23 expression reduces TGFβ-mediated inhibition of DNA synthesis in MDCK cells. **A:** Top panel, MDCK cells were transfected with 0.10 μM or 0.12 μM double-stranded siRNA as described in "Materials and Methods." After

incubation for 24-72 h, expression levels of endogenous km23 were analyzed via Western blot analysis using rabbit km23 anti-serum (1:500) as described for Fig. 2. Bottom panel, plot of densitometric results from top panel. The values in parentheses indicate a percent of control relative to the corresponding control values. **B:** MDCK cells were transfected with 0.1 μM siRNA as described in A. Twenty-four h after transfection, [^{3}H]thymidine incorporation analyses were performed as described in "Materials and Methods." The asterisk indicates a statistically significant difference (Student's t-test, $p<0.01$) in the inhibition of DNA synthesis by TGFβ between km23 siRNA-transfected and control-transfected MDCK cells. The results shown are representative of two similar experiments.

Fig.5. siRNA blockade of km23 expression reduces TGFβ induction of FN expression. **A:** MDCK cells were transiently transfected with siRNA plasmids as indicated: control (lane1), km23 siRNA (lanes 2 and 3). Top panel, blockade of endogenous km23 was analyzed via Western blotting with rabbit km23 anti-serum (1:500). Bottom panel, equal loading was confirmed by blotting with an anti-DIC Ab. **B:** MDCK cells were transiently transfected with siRNA plasmids: control (lanes 1-2), km23 siRNA plasmids (lanes 3-6). Twenty-four h after transfection, MDCK cells were incubated in serum-free medium for 60 min before addition of TGFβ (5 ng/ml) for the indicated times. Top panel, FN expression was detected by Western blot analysis using a mouse monoclonal anti-FN Ab. Bottom panel, blockade of km23 was confirmed by blotting with rabbit km23 anti-serum. The results shown are representative of two similar experiments.

Fig. 1

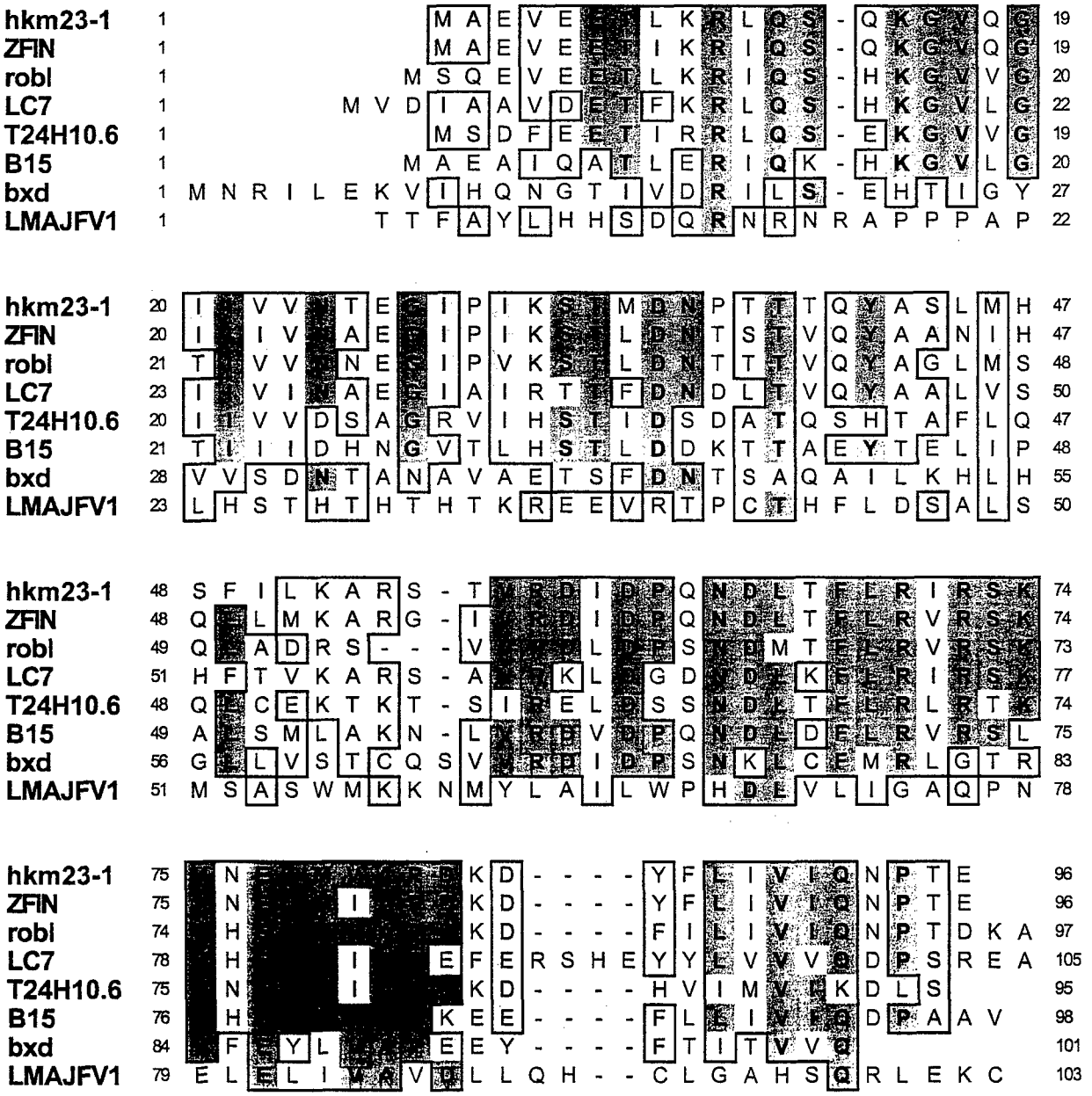
hkm23-1 1 MAEVEELKRLQS-QKGVQG 19
ZFIN 1 MAEVEEIKRIQS-QKGVQG 19
robl 1 MSQEVEETLKRIQS-HKGVVG 20
LC7 1 MVDIAAVDETFKRLQS-HKGVLG 22
T24H10.6 1 MSDFEETIRRLQS-EKGVVG 19
B15 1 MAEAIQATLERIQK-HKGVLG 20
bxd 1 MNRILEKVIHQNGTIVDRILS-EHTIGY 27
LMAJFV1 1 TTFAYLHHSDQRNRNRAPPPAP 22
hkm23-1 20 IIVVTEIPIKSTMDNPTTTQYASLMH 47
ZFIN 20 IIVAEIPIKLDNTSTVQYAANIH 47
robl 21 TVVNEIPVKSTLDNTTTVQYAGLMS 48
LC7 23 IVIAEIAIRTTFDNDLTVQYAALVS 50
T24H10.6 20 ITVVDSAGRVIHSTIDSDATQSHTAFLQ 47
B15 21 TIIIDHNGVTLHSTLDDKTTAEYTELIP 48
bxd 28 VVSDNTANAVAETSFDNTSAQAILKHLH 55
LMAJFV1 23 LHSTHTHTHTKREEVRTPCTHFLDSALS 50
hkm23-1 48 SFILKARS-TMRDIDPQNDLTFLRIRSK 74
ZFIN 48 QLLMKARG-IIRDIDPQNDLTFLRVRSK 74
robl 49 QADRS---VIRDLDPSNDMTFLRVRSL 73
LC7 51 HFTVKARS-ATRKLDGDVDLKFLRIRSA 77
T24H10.6 48 QLCEKTKT-SIRELDSSNDLTFLRLRTK 74
B15 49 ALSMLAKN-LVRDVDPQNDLDELRVRSL 75
bxd 56 GLLVSTCQSVIRDIDPSNKLCEMRLGTR 83
LMAJFV1 51 MSASWMKKNMYLAILWPHDLVLIGAQPN 78
hkm23-1 75 NKD----YFLIVLQNPTE 96
ZFIN 75 NIKD----YFLIVLQNPTE 96
robl 74 HKD----FILIVLQNPTDKA 97
LC7 78 HIEFERSHEYYLVVVQDPSREA 105
T24H10.6 75 NIKD----HVIMVHKDLS 95
B15 76 HKEE----FLLIVLQDPAAV 98
bxd 84 FYLE----EEY----FTITVVQ 101
LMAJFV1 79 ELELIVRVDLLQH--CLGAHSQRLEKC 103

Fig. 2

A

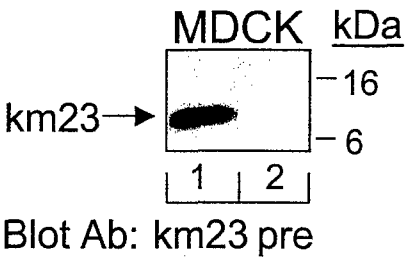
MDCK
kDa
km23
16
6
1
2
Blot Ab: km23 pre

B

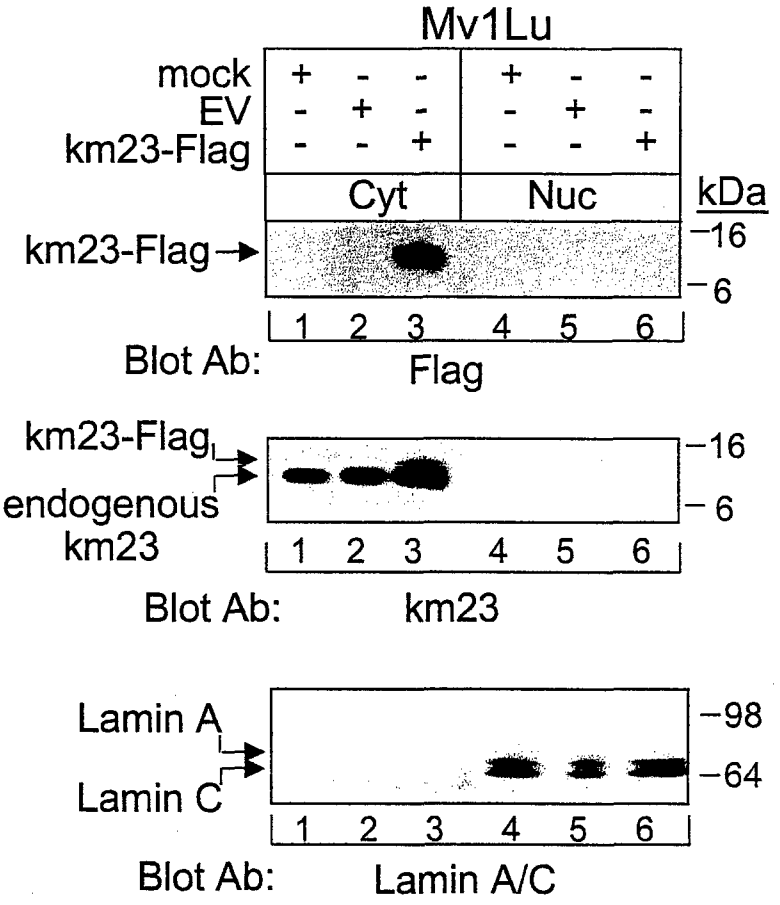
Mv1Lu
mock
EV
km23-Flag
Cyt
Nuc
kDa
km23-Flag
16
6
1 2 3 4 5 6
Blot Ab: Flag
km23-Flag
endogenous km23
16
6
1 2 3 4 5 6
Blot Ab: km23
Lamin A
Lamin C
98
64
1 2 3 4 5 6
Blot Ab: Lamin A/C

Fig. 2

C

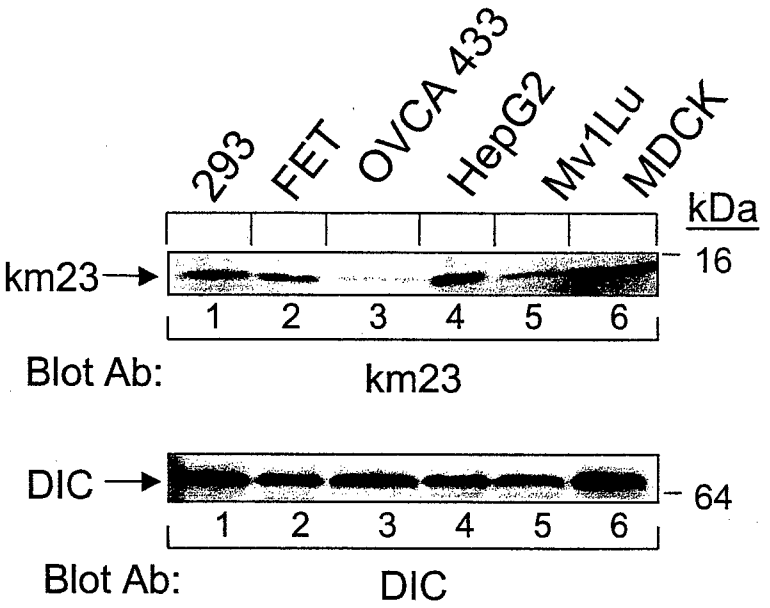
293
FET
OVCA 433
HepG2
Mv1Lu
MDCK
kDa
km23
16
1 2 3 4 5 6
Blot Ab:
km23
DIC
64
1 2 3 4 5 6
Blot Ab:
DIC

D

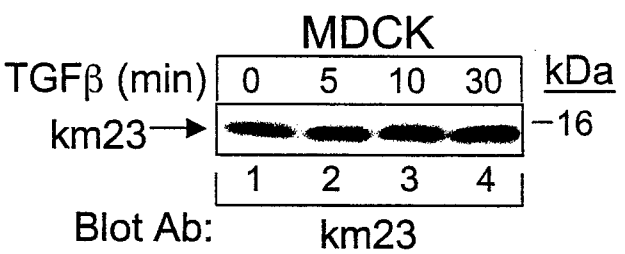
MDCK
TGFβ (min)
0 5 10 30
kDa
km23
16
1 2 3 4
Blot Ab:
km23

Fig. 3

A

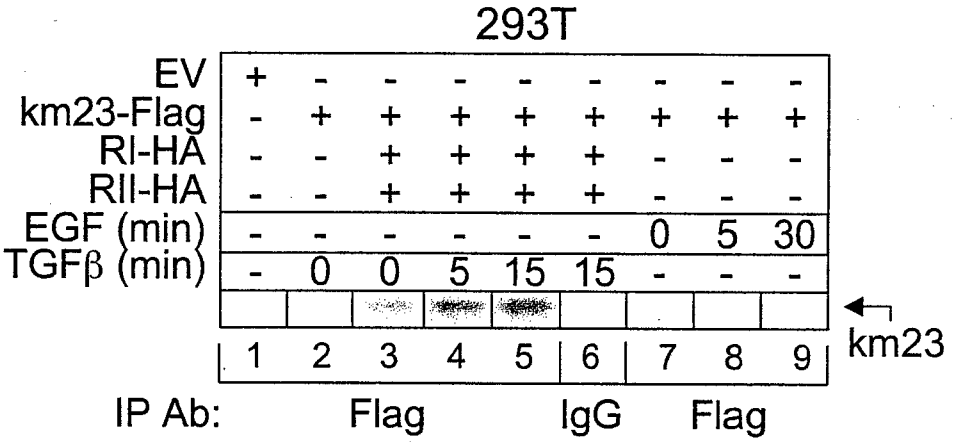
293T
EV + - - - - - - - -
km23-Flag - + + + + + + + +
RI-HA - - + + + + - - -
RII-HA - - + + + + - - -
EGF (min) - - - - - - 0 5 30
TGFβ (min) - 0 0 5 15 15 - - -
km23
1 2 3 4 5 6 7 8 9
IP Ab: Flag IgG Flag

B

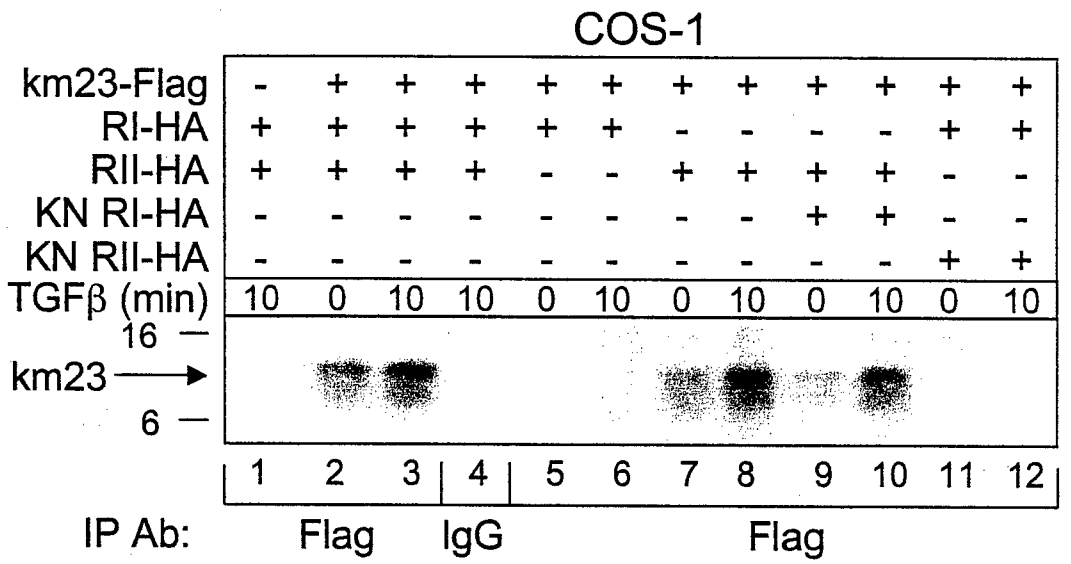
COS-1
km23-Flag - + + + + + + + + + + +
RI-HA + + + + + + - - - - + +
RII-HA + + + + - - + + + + - -
KN RI-HA - - - - - - - - + + - -
KN RII-HA - - - - - - - - - - + +
TGFβ (min) 10 0 10 10 0 10 0 10 0 10 0 10
16
km23
6
1 2 3 4 5 6 7 8 9 10 11 12
IP Ab: Flag IgG Flag

Fig. 4

A

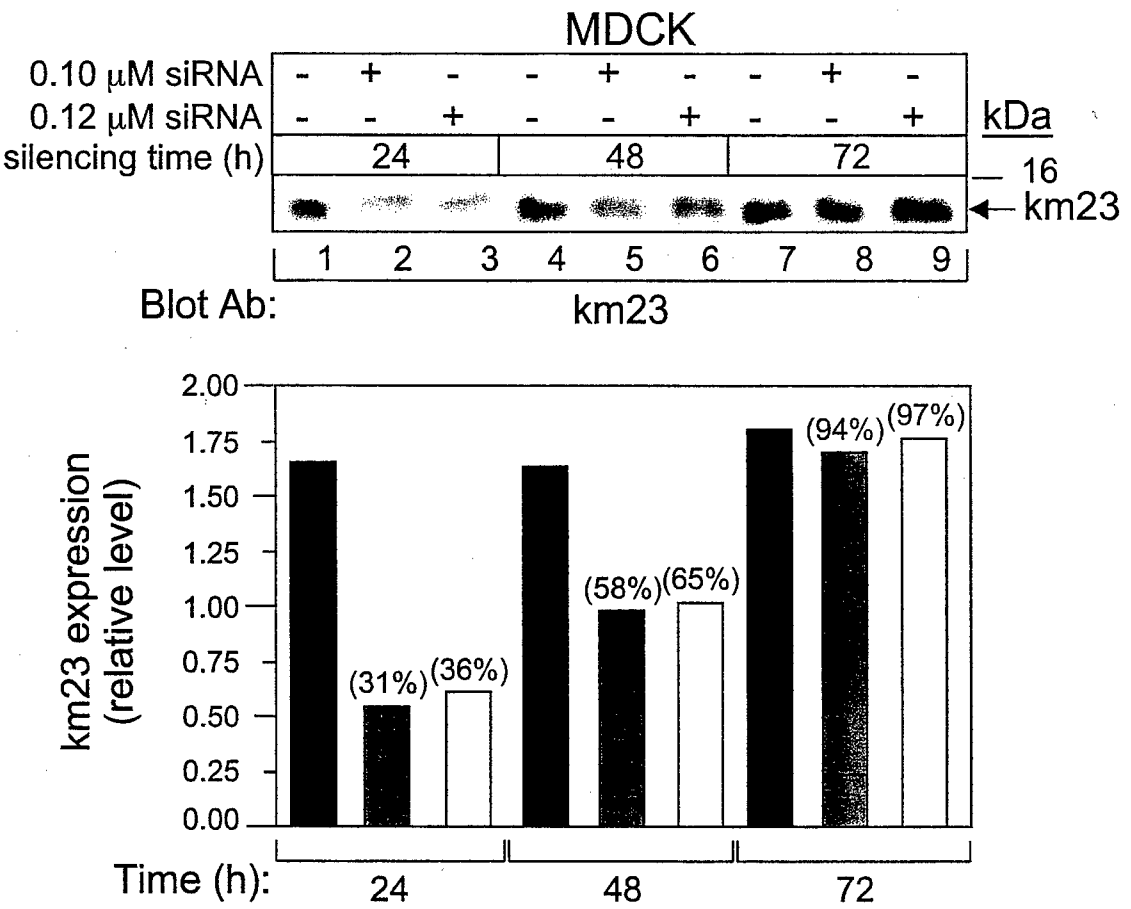
MDCK
0.10 μM siRNA
0.12 μM siRNA
silencing time (h)
kDa
16
km23
1 2 3 4 5 6 7 8 9
Blot Ab:
km23
km23 expression (relative level)
2.00
1.75
1.50
1.25
1.00
0.75
0.50
0.25
0.00
(31%)
(36%)
(58%)
(65%)
(94%)
(97%)
Time (h):
24
48
72

B

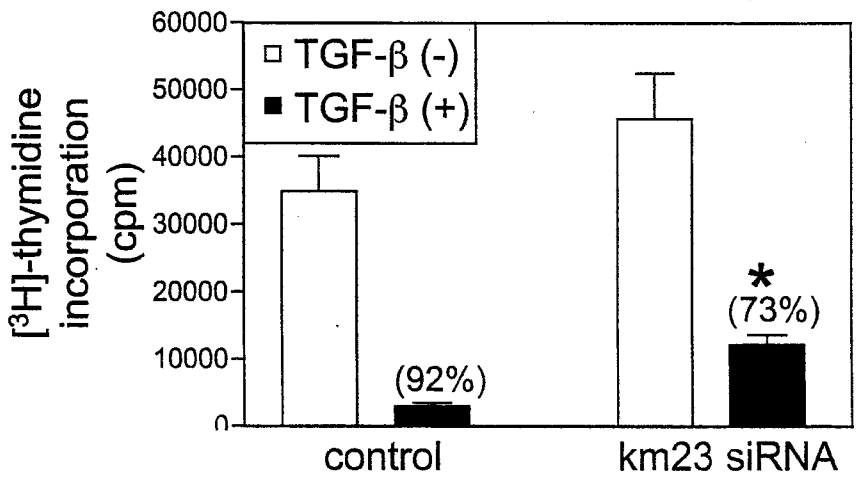
[3H]-thymidine incorporation (cpm)
60000
50000
40000
30000
20000
10000
0
TGF-β (-)
TGF-β (+)
(92%)
*
(73%)
control
km23 siRNA

Fig. 5

A

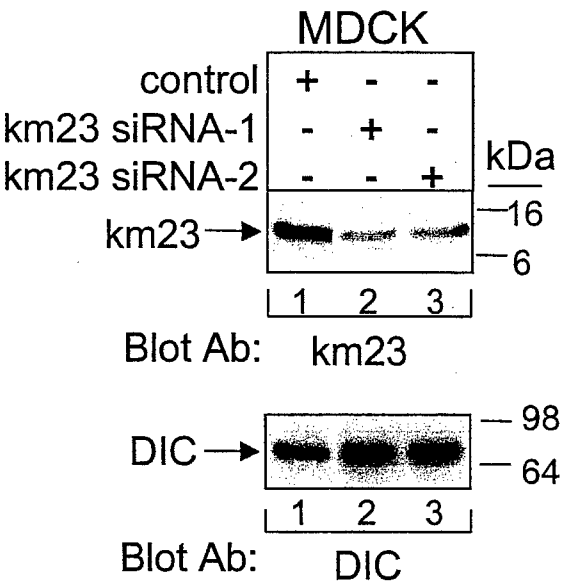
MDCK
control + - -
km23 siRNA-1 - + -
km23 siRNA-2 - - +
kDa
km23
16
6
1 2 3
Blot Ab: km23
DIC
98
64
1 2 3
Blot Ab: DIC

B

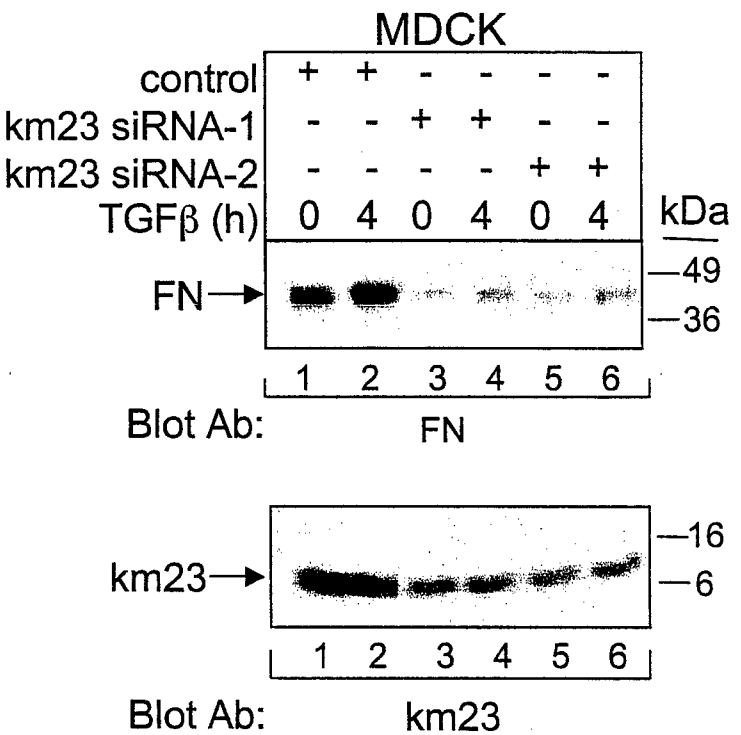
MDCK
control + + - - - -
km23 siRNA-1 - - + + - -
km23 siRNA-2 - - - - + +
TGFβ (h) 0 4 0 4 0 4
kDa
FN
49
36
1 2 3 4 5 6
Blot Ab: FN
km23
16
6
1 2 3 4 5 6
Blot Ab: km23

Requirement for km23 in a Smad2-dependent TGFβ signaling pathway

Qunyan Jin*, Wei Ding*, and Kathleen M. Mulder*⇑

*Department of Pharmacology, Pennsylvania State University

College of Medicine, 500 University Dr., Hershey, PA 17033

⇑To whom correspondence should be addressed:

Department of Pharmacology—MC H078

Penn State College of Medicine

500 University Drive, Hershey, PA 17033

Telephone 717-531-6789; FAX 717-531-5013

E-mail kmm15@psu.edu

Running title: Blockade of km23 inhibits Smad2 signaling

Key words: TGFβ, signal transduction, siRNA, Smad2, km23

SUMMARY

We have identified km23 as a novel TGFβ receptor-interacting protein that is also a light chain of the motor protein dynein. Here we show that km23 is co-localized with the TGFβ signaling component Smad2 at early time periods after TGFβ treatment of Madin Darby canine kidney epithelial cells, prior to translocation of Smad2 to the nucleus. Further, km23 interacted with Smad2, but not Smad3, in both immunoprecipitation/blot and GST pull-down assays. More significantly, km23 interacted with Smad2 once it has been phosphorylated by constitutively active RI in vivo. Further, blockade of km23 using small interfering RNA significantly reduced the levels of phosphorylated Smad2, nuclear translocation of Smad2, and TGFβ-dependent Smad2 transcriptional activation. Our findings demonstrate that km23 is required in a Smad2-dependent TGFβ signaling pathway.

INTRODUCTION

Transforming growth factor β (TGFβ) is the prototype of a large family of structurally related growth and differentiation factors that show remarkable diversity in the biological actions they mediate (Yue and Mulder, 2001; Derynck and Zhang, 2003; Shi and Massague 2003). These biological responses include effects on cell growth, cell death, cell differentiation, and the extracellular matrix (ECM). The effects are often cell type and context dependent (Yue and Mulder, 2001; Derynck and Zhang, 2003; Shi and Massague 2003).

TGFβ initiates its signals by producing an active tetrameric receptor complex consisting of RI and RII serine/threonine kinase receptors. After TGFβ binds to RII, it transphosphorylates, and thereby activates RI. The activated form of RI can phosphorylate Smad2 and Smad3, and these receptor-activated Smads (RSmads) then form a complex with Smad4. The TGFβ-activated, heteromeric Smad complexes then translocate into the nucleus, where they induce or repress transcription of defined genes, either directly by binding to congnate DNA consensus sites, or indirectly by interaction with other transcription factors, such as FAST1, FAST2, c-jun, and c-fos (Roberts et al, 2003; Derynck and Zhang, 2003; Shi and Massague, 2003).

Several receptor-interacting proteins have been shown to play a role in vesicular trafficking, as well as TGFβ receptor internalization, events involving Smad recruitment to the receptors (Derynck and Zhang, 2003). For example, SARA and Dab2 bind both TGFβ receptors and RSmads, and promote RSmad

phosphorylation and TGFβ signaling (Hocevar, 2001; Di Guglielmo et al., 2003). In addition, cytoskeletal proteins play a role in the localization and signaling of Smads (Denryck and Zhang, 2003). For example, unphosphorylated Smads2/3/4 bind microtubules (MTs), and TGFβ treatment induces their dissociation from these cytoskeletal components (Dong et al., 2000). Filamin, an actin crosslinking factor and scaffolding protein, also associates with Smads and positively regulates transduction of Smad signals (Sasaki et al., 2001). Collectively, these findings indicate that the interactions among TGFβ receptors, Smads, and adaptor/scaffolding proteins represent important regulatory mechanisms in TGFβ signaling.

km23 was identified as a novel TGFβ receptor-interacting protein that is also a light chain of the motor protein dynein (Tang et al., 2002). We have previously shown that TGFβ RII is absolutely required for km23 phosphorylation and interaction with the dynein intermediated chain (DIC). Collectively, our results suggest that TGFβ pathway components (such as Smads) may use km23 as an adaptor or motor receptor for their recruitment and transport along MTs.

We demonstrate here that km23 is co-localized with the TGFβ signaling component Smad2 at early time periods after TGFβ treatment, prior to translocation of Smad2 to the nucleus. km23 interacted with Smad2, once this RSmad had been phosphorylated by constitutively active RI in vivo. We also demonstrate a direct interaction between km23 and Smad2 in vitro. Further, blockade of km23 reduced the levels of phosphorylated Smad2, nuclear translocation of Smad2, and TGFβ-dependent Smad2 transcriptional activation.

Thus, km23 appears to be a signaling intermediate in a Smad2-dependent TGFβ pathway.

MATERIALS AND METHODS

Reagents--The anti-Flag M2 (F3165) antibody (Ab) and mouse IgG were from Sigma-Aldrich (St. Louis, MO). The anti-DIC monoclonal Ab (MAB1618) was from Chemicon (Temecula, CA). The rabbit IgG was from Santa Cruz Biotechnology, Inc. (Santa Cruz, CA). TGFβ_1 was purchased from R & D Systems (Minneapolis, MN). The phospho-Smad2 Ab (3101) was from Cell Signaling Technology (Beverly, MA). The rabbit Smad2 Ab (51-1300) was from Zymed (South San Francisco, CA). The mouse anti-Smad2/3 (610843) was from BD Biosciences Transduction Laboratories (Palo Alto, CA). The Fugene 6 transfection reagent was from Roche Applied Science (Indanapolis, IN).

Antibody production-- The rabbit polyclonal km23 anti-serum used for the immunofluorescence studies was prepared against the following sequence: MAEVEETLKRIQS (corresponding to amino acids 1-13 of human km23) (Strategic BioSolutions, Newark, DE). The company also provided preimmune serum.

Cell culture--Mv1Lu (CCL-64) cells were purchased from American Type Culture Collection (Manassas, VA) and were grown in DMEM supplemented with 10% FBS. MDCK cells (CCL-34) was also obtained from ATCC and were grown in MEM-α supplemented with 10% FBS. Cultures were routinely screened for mycoplasma using Hoechst 33258 staining.

Transient transfections, Immunpreciptation(IP)/blot, Westerns-- were performed essentially as described previously (Hocevar et al., 1999; Yue et al., 1999a; b; Yue and Mulder, 2000; Tang et al., 2002)

Small interfering RNA (siRNA)—a km23 siRNA pSIREN construct to target the human km23 (251st~271st nucleotide, 5'-AAGACTATTTCCTGATTGTGA-3') was prepared. This km23 siRNA also can knock down rat and mouse km23, since this targeting sequence is identical among human, rat, and mouse. In addition, we have made a negative control siRNA (NC siRNA) plasmid, the sequence of which does not match any genes by alignment with the NCBI database using BLAST. All of these constructs contain a human RNA polymerase III U6 promoter and can form a hairpin structure in vivo that is quite similar to chemically synthesized double-stranded siRNA. The pSIREN empty vector (EV) was purchased from BD Clontech (Cat# 631529).

Immunofluorescence -- For km23 and Smad2 co-localization experiments, MDCK cells were fixed with 4% paraformaldehyde in phosphate-buffered saline for 20 min at room temperature, and permeabilized with 0.5% Triton X-100 in phosphate-buffered saline for 5 min. Subsequently, these cells were incubated with km23 rabbit anti-serum (1:200) and 5 μg/ml anti-Smad2/3 monoclonal Ab for 1 h, respectively. The bound primary antibodies were visualized with 2 μg/ml Alexa 594 goat anti-rabbit IgG or Alexa 488 goat anti-mouse IgG, respectively. Immunofluorescence images were captured using a Nikon Diaphot microscope with a Retiga 1300 CCD camera (BioVision Technologies, Inc., Exton, PA), running IPLab v3.6.3 software (Scanalytics, Inc., Fairfax, VA). For

immunofluorescence analysis to study the effects of siRNA's on nuclear translocation of Smad2 by TGFβ, the cells were analyzed as for the co-localization studies, except that the cells were incubated only with 5μg/ml anti-Smad2/3 monoclonal Ab, and then the bound Ab was visualized with 2 μg/ml Alexa 594 goat anti-mouse IgG. One hundred GFP positive cells were counted for cultures with both km23 siRNA-transfected and NC siRNA-trasnsfected cells. DAPI staining designates individual cells.

Luciferase reporter assay-- Mv1Lu cells were plated at 1×10^4 cells/cm^2 in 12-well plates. Twenty-four hours after plating, the cells were transfected with the indicated amounts of either km23 siRNA or NC siRNA, together with activin-responsive element (ARE)-luc and forkhead activin signal transducer-1 (FAST-1)(Chen et al., 1996). Renilla was used to normalize transfection efficiencies, and pcDNA3.1 was used to normalize the amount of total DNA transfected. Twenty-four hours after transfection, the medium was replaced with DMEM serum-free medium. One hour after incubation, Mv1Lu cells were cultured in the absence or presence of TGF-β (5ng/ml) for another 18 h. The luciferase activity was measured using Promega's Dual-luciferase Reporter Assay System (Cat# E1960) following the manufacturer's instructions. All assays were performed in triplicate. Data are expressed as mean±SEM.

RESULTS

Our previous data suggested that km23 might function as a "motor receptor" to recruit TGFβ signaling complexes to the dynein motor complex for intracellular transport along MTs toward the nucleus (Tang et al., 2002). For example, we have demonstrated that TGFβ RII kinase activity was required for km23 phosphorylation and TGFβ-dependent binding of km23 to the rest of the dynein motor complex. Since Smad2 is a critical intracellular mediator of TGFβ responses (Attisano and Wrana, 1998, Massague 1998), co-localized with RII in specific endosomal compartments after receptor endocytosis (Hayes et al., 2002), it was conceivable that Smad2 might function as one of the cargo that km23 could recruit for intracellular transport. If this were the case, we would expect Smad2 to be co-localized with km23. Thus, we performed immunofluorescence studies in TGFβ-responsive MDCK cells, using km23-specific rabbit antiserum prepared against amino acids 1-13. As indicated in Fig. 1A, in the absence of TGFβ treatment, endogenous km23 was present in perinuclear puncta, whereas Smad2 displayed a different pattern of punctate staining. TGFβ treatment resulted in a greater co-localization of Smad2 with km23 at both 2 min (Fig. 1B) and 5 min (Fig. 1C) after TGFβ addition to MDCK cells. In contrast, once Smad2 had translocated to the nucleus by 15 min after TGFβ treatment (Fig. 1D), km23 was still localized in the cytoplasm and was no longer co-localized with Smad2. For all studies, the preimmune serum or relevant IgG controls were negative, confirming the spcecificity of the km23 Ab.

Thus, our results clearly indicate that km23 and Smad2 are co-localized intracellularly at 2 and 5 min after TGFβ treatment, prior to the entry of Smad2 into the nucleus.

Since km23 and Smad2 appeared to be co-localized, it was of interest to determine whether km23 and Smad2 interacted in vivo. We performed IP/blot analyses after transfection of km23-Flag and Smad3-Flag or Smad2-Flag, with or without constitutively activated TβRI (T204D-HA). As shown in Fig. 2A, in the presence of T204D-HA, immunoprecipitation (IP) of the Smad2 protein, using an anti-Smad2 Ab, resulted in co-IP of km23-Flag and Smad2 (lane 7). This km23-Smad2 interaction did not occur in the absence of activated TβRI (T204D-HA) (lane 6). Further, Smad3 did not interact with km23 under similar condition (lanes 2-3), indicating same specificity for Smad2. As expected, no band was visible for the IgG control (lanes 1, 5). The data suggest that Smad2 phosphorylation by constitutively active RI is required for Smad2 interaction with km23.

In order to determine whether km23 could directly interact with Smad2, we performed GST pull-down assays after transfection of either EV or Smad2-Flag into 293T cells. Cell lysates were incubated with sepharose-bound, bacterial-expressed GST alone or GST-km23. An anti-Flag Ab was used as the blotting Ab to detect Smad2-Flag in the GST-km23 complex. As shown in Fig. 2B, Smad2 was visible in the GST-km23 immunoprecipitates (lane 4), but not in the immunoprecipitates from GST only (lane 3). EV control lanes were also negative (lanes 1, 2). The results indicate that km23 interacts with Smad2 in

vitro.

In order to explore the possibility that km23 regulates Smad2 phosphorylation by TGFβ, it was of interest to determine whether blockade of endogenous km23 would block Smad2 phosphorylation and translocation. In order to demonstrate the ability of km23 siRNA to block endogenous km23 expression, we either mock-transfected or transiently transfected Mv1Lu cells with km23-Flag and km23 siRNA or km23-Flag and NC siRNA. As shown in Fig.3A, km23 siRNA specifically knocked down transfected km23 in vivo. To further confirm this, we transiently transfected Mv1Lu cells with km23 siRNA or NC siRNA and GFP-km23, and evaluated the level of km23 siRNA and NC siRNA blockade of GFP-km23 expression as described in "Materials and Methods". As shown in Fig.3B, there are approximately 20% GFP-positive cells in the NC siRNA -transfected cultures (top panels, right). In contrast, there are only a few positive cells in the km23siRNA-transfected cells (bottom panels, right), suggesting a significant level of knock-down of km23 expression. A similar result was observed at 48 h post-transfection (data not shown). Collectively, the results in Fig.3 indicate that the km23 siRNA can specifically block expression of the km23 protein.

Since km23 siRNA resulted in maximal silencing at 24 h or 48 h after addition to Mv1Lu cells, we performed Western blot analysis to examine whether blockade of km23 would block TGFβ induction of Smad2 phosphorylation during this time period. As shown in Fig.4 (left, top panel), TGFβ treatment of NC siRNA-transfected cells induced Smad2 phosphorylation as early as 5 min after

TGFβ treatment, and levels of phosphorylated Smad2 continued to increase to values 9-fold above basal levels by 15 min after TGFβ. In contrast, in the km23 siRNA-transfected cells (right, top panel), TGFβ induction of Smad2 phosphorylation was reduced to values 2-4 fold above baseline levels after similar time points. The results in Fig.4 indicate that km23 is partially required for the TGFβ-mediated increase in phospho-Smad2 levels that occurs at very early times after TGFβ treatment (5-15 min).

We also performed immunofluorescence studies to determine whether blockade of km23 could block nuclear translocation of Smad2 by TGFβ in individual cells. Mv1Lu cells were transiently transfected with either NC siRNA or km23 siRNA and GFP. As shown in Fig.5A, in the absence of TGFβ, the NC siRNA-transfected cells and the km23 siRNA-transfected cells displayed the same pattern of punctate staining. However, while the NC siRNA-transfected, GFP-positive cells still displayed Smad2 translocation in response to TGFβ (Fig. 5B), the km23 siRNA-transfected, GFP-positive cells displayed barely detectable levels of nuclear Smad2 expression (Fig. 5C). As expected, the non-transfected cells in Figs 5B and C responded to TGFβ with significant Smad2 translocation.

In order to quantify the levels of nuclear translocation of Smad2 by TGFβ, we counted one hundred GFP positive cells in cultures of either km23 siRNA-transfected and NC siRNA-trasnsfected cells treated with TGFβ (5ng/ml), and quantified the levels of nuclear translocation of Smad2. As shown in Table1, in NC siRNA-transfected cells, 93.2% of the GFP-positive cells displayed Smad2 nuclear translocation in response to TGFβ. As expected, 100% of the GFP-

negative cells responded to TGFβ with Smad2 translocation, whether NC or km23 siRNA had been transfected. In contrast, in the km23 siRNA-transfected cells, 89% of the GFP-positive cells displayed barely detectable levels of nuclear Smad2 expression. Thus, only 11% of the km23 siRNA, GFP-positive cells still displayed nuclear translocation of Smad2. Our results demonstrate that km23 is required for the nuclear translocation of Smad2 by TGFβ.

The transcriptional activity of Smad2 is dependent upon its prior phosphorylation (Macias-Silva et al., 1996). Since blockade of km23 could reduce both the levels of phosphorylated Smad2 and the nuclear translocation of Smad2, it was of interest to determine whether blockade of km23 could also influence the transcriptional activity of the Smad2 protein. To assess this, we transiently transfected Mv1Lu cells with either km23 siRNA or NC siRNA and ARE-luc/FAST-1 for analysis of ARE luciferase reporter activity. As shown in Fig.6, strong (up to 28-fold) activation the ARE-luc reporter by TGFβ was achieved in both mock-transfected and NC siRNA-transfected cells. However, the cells transfected with km23 siRNA displayed a significant decrease in TGFβ-stimulated ARE-luc induction to levels of only 10-fold. The results in Fig. 6 indicate that km23 is required for TGFβ induction of Smad2-dependent transcriptional activity.

DISCUSSION

We have previously reported that km23 is both a TGFβ receptor-interacting protein and a light chain of the motor protein dynein. Kinase-active TGFβ receptors are required for km23 phosphorylation and recruitment of km23 to the dynein motor complex, suggesting that subsequent to receptor activation, TGFβ signaling components may be transported along MTs through the interaction of km23 with DIC (Tang et al., 2002). Here, we show that km23 partially co-localizes with Smad2 in a TGFβ-dependent manner. Furthermore, km23 interacts with the TGFβ signaling intermediate Smad2 both in vitro and in vivo. More importantly, using siRNA approaches, we demonstrate for the first time, that km23 is required for TGFβ-stimulation of Smad2 phosphorylation, nuclear translocation, and transcriptional activation of Smad2.

Previous work has indicated that Smad2/3 activation by TGFβ is dependent upon receptor internalization (Penheiter et al., 2002). Further, activated TGFβ receptors are known to be internalized into EEA1/SARA-enriched endosomes where Smad2 is recruited by SARA (Hayes et al., 2002; Di Guglielmo et al., 2003). Smad2/3 can then be phosphorylated by the TGFβ receptors to promote TGFβ signaling, prior to receptor degradation. From our studies, it appears that km23 is being phosphorylated by the activated TGFβ receptors and is recruited to the dynein motor complex in approximately the same time frame as RSmad activation (Tang et al., 2002). Our results herein

indicate that km23 specifically interacts with Smad2 once it has been phosphorylated by constitutively active RI. Thus, km23 may function at a point after Smad2 has been localized to specific endosomal compartment to affect the next step in the intracellular transport process. In this way, km23 may provide a key link in the signaling of Smad2-specific TGFβ responses.

Although Smad2 and Smad3 are highly homologous and share some overlapping activities, they have distinct functions and are regulated differentially (Liu, 2003, Roberts et al, 2003). For example, Smad2 and Smad3 have opposite activities on the goosecoid (gsc) promotor; in that Smad2 activates it, while Smad3 represses it (Labbe et al., 1998). TRAP-1-like protein (TLP), a novel modulator of TGFβ signaling has opposite effects on Smad2- and Smad3-dependent signaling (Felici et al., 2003). In addition, there is no evidence that Smad2 and Smad3 are phosphorylated in the same endocytic locale. Here we show that while activated Smad2 can bind km23, this is not true for Smad3. We also show that blockade of km23 reduces TGFβ- and Smad2-dependent ARE-luc transcriptional activity. However, km23 knock-down is without effect on TGFβ- and Smad3-dependent effects on Smad binding element (SBE)-luc activity (data not shown). Thus, it appears that km23's critical function in mediating the phosphorylation, nuclear translocation, and transcriptional activation of Smad2 is specific to this RSmad. Perhaps a km23-like protein regulates Smad3 in a similar fashion. However, whether this is the case requires further investigation.

It is note worthy that when comparing Fig. 5B and 5C, there was no corresponding increase in cytoplasm Smad2, when nuclear Smad2 expression

was blocked by the km23 siRNA. This finding is consistent with degradation of Smad2 occurring when km23 function is blocked. Ubiquitin-proteaseome-mediated degradation is known to control the levels of Smads post-translationally (Derynck and Zhang, 2003; Izzi and Attisano, 2003). Accordingly, the ubiquitin pathway can regulate basal levels of Smads (Izzi and Attisano, 2003). Since our data demonstrate that blockade of km23 decreased Smad2 expression levels in the cytoplasm, as well as in the nucleus, it is possible that blockade of km23 stimulates a Smad2 ubiquitin–mediated degradation pathway. For example, such as one involving Smuf2, which could directly target Smad2 for degradation could play a role (lin et al., 2000). However, we cannot rule out a mechanism for Smad2 degradation that may specific km23 functions. Future studies will explore this issue more completely.

Blockade of km23 reduced the levels of Smad2 phosphorylation, nuclear translocation of Smad2, and Smad2-dependent transcriptional activity, suggesting a critical role for km23 in mediating Smad2-dependent responses. However, Smad2 phosphorylation and activation can also be regulated by TGFβ-dependent activation of the Erk, JNK, and p38 pathways (Derynck and Zhang, 2003; Fu et al., 2003). For example, activation of MEKK1, which is upstream of the JNK pathway, has been shown to enhance Smad2 phosphorylation, association with Smad4, nuclear accumulation, and transcriptional activity (Brown et al., 1999). Since we have previously shown that forced expression of km23 enhances JNK activation, it may be that km23 serves as a bridge to link

the Smad2 and JNK signaling pathways. Thus, Smad2 may not be the only TGFβ signaling component regulated by km23.

ACKNOWLEDGMENTS

We thank H. Moses (Vanderbilt) for the T204D-HA. This work was supported by National Institutes of Health Grants CA90765, CA92889, and CA100239, and Dept of Defense IDEA AWARD # DAMD17-03-01-0287 (to K.M.M).

REFERENCES

Arora, K. and Warrior, R. (2001). A new Smurf in the village. *Dev. Cell* **1**, 441-442.

Attisano, L. and Wrana, J. L. (1998). Mads and Smads in TGFβ signaling. *Curr. Opin. in Cell Biol.* **10**, 188-194.

Chen, X, Rubock, M. J., Whitman, M. (1996). A transcriptional partner for MAD proteins in TGF-beta signalling. *Nature* **384**, 648

Dennler, S., Itoh, S., Vivien, D., ten Dijke, P., Huet, S. and Gauthier, J. M. (1998). Direct binding of Smad3 and Smad4 to critical TGFβ-inducible elements in the promoter of human plasminogen activator inhibitor-type 1 gene. *EMBO J.* **17**, 3091-3100.

Derynck, R. and Zhang, Y. E. (2003). Smad-dependent and Smad-independent pathways in TGFβ- family signalling. *Nature* **425**, 577-584.

Di Guglielmo, G. M., Le Roy, C., Goodfellow, A. F. and Wrana, J. L. (2003). Distinct endocytic pathways regulate TGF-β receptor signalling and turnover. *Nat. Cell Biol.* **5**, 382-384.

Dong, C., Li, Z., Alvarez, Jr., R., Feng, X. H. and Goldschmidtch-Clermont, P. J. (2000). Microtubule binding to Smads may regulate TGF-β activity. *Mol. Cell* **5**, 27-34.

Felici, A., Wurthner, J. U., Parks, W. T., Giam, L. R., Reiss, M., Karpova, T. S., McNally, J. G., Roberts, A. B. (2003). TLP, a novel modulator of TGF-β signaling, has opposite effects on Smad2- and Smad3-dependent signaling. *EMBO J.* **22**, 4465-4477.

Feng, X. H. and Derynck, R. (1997). A kinase subdomain of transforming growth factor-beta (TGF-β) type I receptor determines the TGF-β intracellular signaling specificity. *EMBO J.* **16**, 3912-3923.

Feng, X. H., Zhang, Y., Wu, R. Y., Derynck, R. (1998). The tumor suppressor Smad4/DPC4 and transcriptional adaptor CBP/p300 are coactivators for smad3 in TGF-β -induced transcriptional activation. *Genes Dev.* **12**, 2153-2163

Fu, Y., O'Connor, L. M., Shepherd, T. G. and Nachtigal, M. W. (2003) The p38 MAPK inhibitor, PD169316, inhibits transforming growth factor-β induced Smad signaling in human ovarian cancer cells. *Biochem. Biophys. Res. Commun.* **310**, 391-397.

Hartsough, M. T. and Mulder, K. M. (1997). Transforming growth factor-β signaling in epithelial cells. *Pharmacol. Ther.* **75**, 21-41.

Hayes, S., Chawla, A. and Corvera, S. (2002). TGFβ receptor internalization into EEA1-enriched early endosomes: role in signaling to Smad2. *J Cell Biol.* **158**, 1239-1249.

Heldin, C.-H., Miyazono, K. and ten Dijke, P. (1997). TGF-β signalling from cell membrane to nucleus through SMAD proteins. *Nature* **390**, 465-471.

Labbe, E., Silvestri, C., Hoodless, P. A., Wrana, J. L., Attisano, L. (1998) Smad2 and Smad3 positively and negatively regulate TGFβ -dependent transcription through the forkhead DNA-binding protein FAST2. *Mol. Cell* **2**, 109-120.

Liu, F. (2003). Receptor-regulated Smads in TGF-β signaling. *Front Biosci.* **8**, 1280-1303.

Macias-Silva, M., Abdollah, S., Hoodless, P. A., Pirone, R., Attisano, L., Wrana, J.L. (1996). MADR2 is a substrate of the TGFβ receptor and its phosphorylation is required for nuclear accumulation and signaling. *Cell* **87**,1215-1224.

Massague, J. and Wotton, D. (2000). Transcriptional control by the TGF-β /Smad signaling system. *EMBO J.* **19**,1745-1754.

Miyazono, K. (2000). TGF-β signaling by Smad proteins. *Cytokine Growth Factor Rev.* **11**, 15-22.

Mulder, K. M. (2000). Role of Ras and Mapks in TGFβ signaling. *Cytokine Growth Factor Rev.* **11**, 23-35.

Penheiter, S. G., Mitchell, H., Garamszegi, N., Edens, M., Dore, J. J. Jr., and Leof, E. B. (2002). Internalization-dependent and -independent requirements for transforming growth factor β receptor signaling via the Smad pathway. *Mol. Cell Biol.* **22**, 4750-4759.

Pouponnot, C., Jayaraman, L., Massague, J. (1998). Physical and functional interaction of SMADs and p300/CBP. *J Biol Chem.* **273**, 22865-22868.

Shi, Y. G. and Massague, J. (2003). Mechanism of TGF-β signaling from cell membrane to the nucleus. *Cell* **113**, 685-700.

Tang, Q., Staub, C. M., Gao, G., Jin, Q., Wang, Z., Ding, W., Aurigemma, R. E., and Mulder, K. M. (2002). A novel transforming growth factor-β receptor

interacting protein that is also a light chain of the motor protein dynein. *Mol. Biol. Cell* **13**, 4484-4496.

ten Dijke, P., Miyazono, K. and Heldin, C.-H. (2000). Signaling inputs converge on nuclear effectors in TGF-β signaling. *Trends Biochem. Sci.* **25**, 64-70.

Yue, J., Frey, R. S. and Mulder, K. M. (1999a). Cross-talk between the Smad1 and Ras/MEK signaling pathways for TGFβ. *Oncogene* **18**, 2033-2037.

Yue, J., Hartsough, M. T., Frey, R. S., Frielle, T. and Mulder, K. M. (1999b). Cloning and expression of a rat Smad1: regulation by TGFβ and modulation by the Ras/MEK pathway. *J. Cell Physiol.* **178**, 387-96.

Yue, J. and Mulder, K.M. (2001). Transforming growth factor-β signal transduction in epithelial cells. *Pharmacol. Ther.* **91**, 1-34.

LEGENDS

Fig. 1. km23 colocalizes with Smad2 in a TGFβ-dependent manner. A:MDCK cells were cultured in the absence of TGFβ, and then were fixed and permeabilized. Endogenous km23 was detected using rabbit km23 anti-serum, followed by Alexa 594 goat anti-rabbit IgG (left, top row). Smad2 was detected using a mouse monoclonal Smad2/3 Ab and Alexa 488 goat anti-mouse IgG (left, middle row). The merge photos show potential co-localization of km23 and Smad2 as yellow punctate staining (left, bottom row) and an enlarged inset (right, bottom row). No signal was detected in the controls (right, top and middle rows). **B:** MDCK cells were incubated in serum-free medium for 1h before addition of TGFβ (5 ng/ml) for 2 min, and then analyzed as in A. **C:** MDCK cells were incubated in serum-free medium for 1h before addition of TGFβ (5 ng/ml) for 2 min, and then analyzed as in A. **D:** MDCK cells were incubated in serum-free medium for 1h before addition of TGFβ (5 ng/ml) for 15 min, and then analyzed as in A. The results shown are representative of three similar experiments.

Fig. 2. km23 interacts with Smad2 in IP/blot and GST pull-down assays. **A:** 293T cells were transfected with km23-flag and Smad3-flag or Smad2-flag, and/or T204D-HA as indicated. Twenty-four hours after transfection, 293T cell lysates were analyzed by IP/blot to determine whether there was an interaction between Smad2 or Smad3 and km23 in vivo. **B:** Top panel, 293T cells were transfected with either EV or Smad2-Flag, and lysates were incubated with sepharose

bound, bacterially-expressed GST alone or GST-rkm23. GST- bound proteins were analyzed by SDS-PAGE and were immunoblotted with an anti-Flag Ab. Smad2 interacts with GST-km23 (lane 4), but not with GST alone (lane 3). EV control lanes (lanes 1, 2) were also negative. Bottom panel, Western blot analysis of total cell lysates to confirm expression of Smad2 in the relevant samples prior to assay (lanes 3, 4). The results shown are representative of two similar experiments.

Fig.3. Demonstration of the specificity of km23 siRNA for blocking endogenous km23. **A:** Mv1Lu cells were either mock-transfected (lane 1), or transiently transfected with km23-Flag alone (lane 4), km23-Flag and km23 siRNA (lane 3), or km23-Flag and NC siRNA (lane 2). Forty-eight hours after transfection, cells were lysed and analyzed by Western blot analysis with an anti-flag Ab. Bottom, equal expression of DIC was confirmed by Western blot analysis. **B:** Mv1Lu cells were transiently transfected with either km23 siRNA and GFP-km23 (top panels) or NC siRNA and GFP-km23 (bottom panels). Twenty-four hours after transfection, cells were fixed and analyzed by immunofluorescence as described in " Material and Methods." DAPI staining is shown to visualize individual cells. The results shown are representative of two similar experiments for each.

Fig.4. siRNA blockade of endogenous km23 reduces the TGFβ–dependent increase in phosphorylated Smad2. Mv1Lu cells were transiently transfected with either km23 siRNA or NC siRNA. Twenty-four hours after transfection, cells were incubated in serum-free medium for 1h before addition of TGFβ (5 ng/ml)

for the indicated times. Top, cells were lysed and then analyzed by Western blot analysis with anti-phospho-Smad2. Middle, total Smad2 levels were confirmed by Western blotting. Bottom, plot of densitometric scan of results in top panel. The results shown are representative of two similar experiments.

Fig.5. SiRNA blockade of endogenous km23 reduces nuclear translocation of Smad2 by TGFβ. **A:** Mv1Lu cells were transiently co-transfected with either GFP and NC siRNA, or GFP and km23 siRNA. Twenty-four hours after transfection, cells were fixed and endogenous Smad2 was detected using a mouse monoclonal Smad2/3 Ab and Alexa 594 goat anti-mouse IgG (red). DAPI staining permits visualization of individual cells (blue). GFP is used as a marker to designate cells transfected with siRNA (green). **B:** Mv1Lu cells were transiently co-transfected with GFP and NC siRNA. Twenty-four hours after transfection, cells were incubated in serum-free medium before addition of TGFβ (5 ng/ml) for 15 min, and then analyzed as in A. **C:** Mv1Lu cells were transiently co-transfected with GFP and km23 siRNA. Twenty-four hours after transfection, cells were incubated in serum-free medium before addition of TGFβ (5 ng/ml) for 15 min, and then analyzed as in A. The results shown are representative of two similar experiments.

Fig.6. siRNA blockade of endogenous km23 dose-dependently inhibits Smad2-dependent transcription in TGF-β/activin reporter assays. Mv1Lu cells were transfected with increasing amounts of either km23 siRNA or NC siRNA (0.125μg

and 0.5μg respectively) along with 0.2 μg ARE-luc and 0.2 μg FAST1. To normalize the transfection efficiency, 0.2 μg renilla was co-transfected as an internal control. Twenty-four hours after transfection, the medium was replaced with serum-free medium for 1 h, followed by incubation of cells in the absence (open bar) and presence (black bar) of TGFβ (5ng/ml) for an additional 18 h. Luciferase activity was measured using the Dual Luciferase Reporter Assay System. All reporter assays were performed in triplicate. The fold of luciferase activity after TGFβ addition is indicated in parentheses on top of the relevant bars. The results shown are representative of two similar experiments.

Table1 Quantitation of siRNA effects on TGFβ-mediated nuclear translocation of Smad2

	GFP+NC siRNA	GFP+km23 siRNA
Transfection efficiency[1]	9.4%±0.4	11%±2
Cells with nuclear translocation of Smad2[2]/GFP positive cells	93%±2	11%±2
Cells with nuclear translocation of Smad2 /GFP negative cells[3]	100%±0	99.7%±0.3

1. GFP-positive cells divided by DAPI-positive cells in the relevant fields.
2. Smad2 translocates to the nucleus after addition of TGFβ (5ng/ml) for15min.
3. GFP negative cells: DAPI-positive cells minus 100 GFP-positive cells in the relevant fields.

Fig. 1A

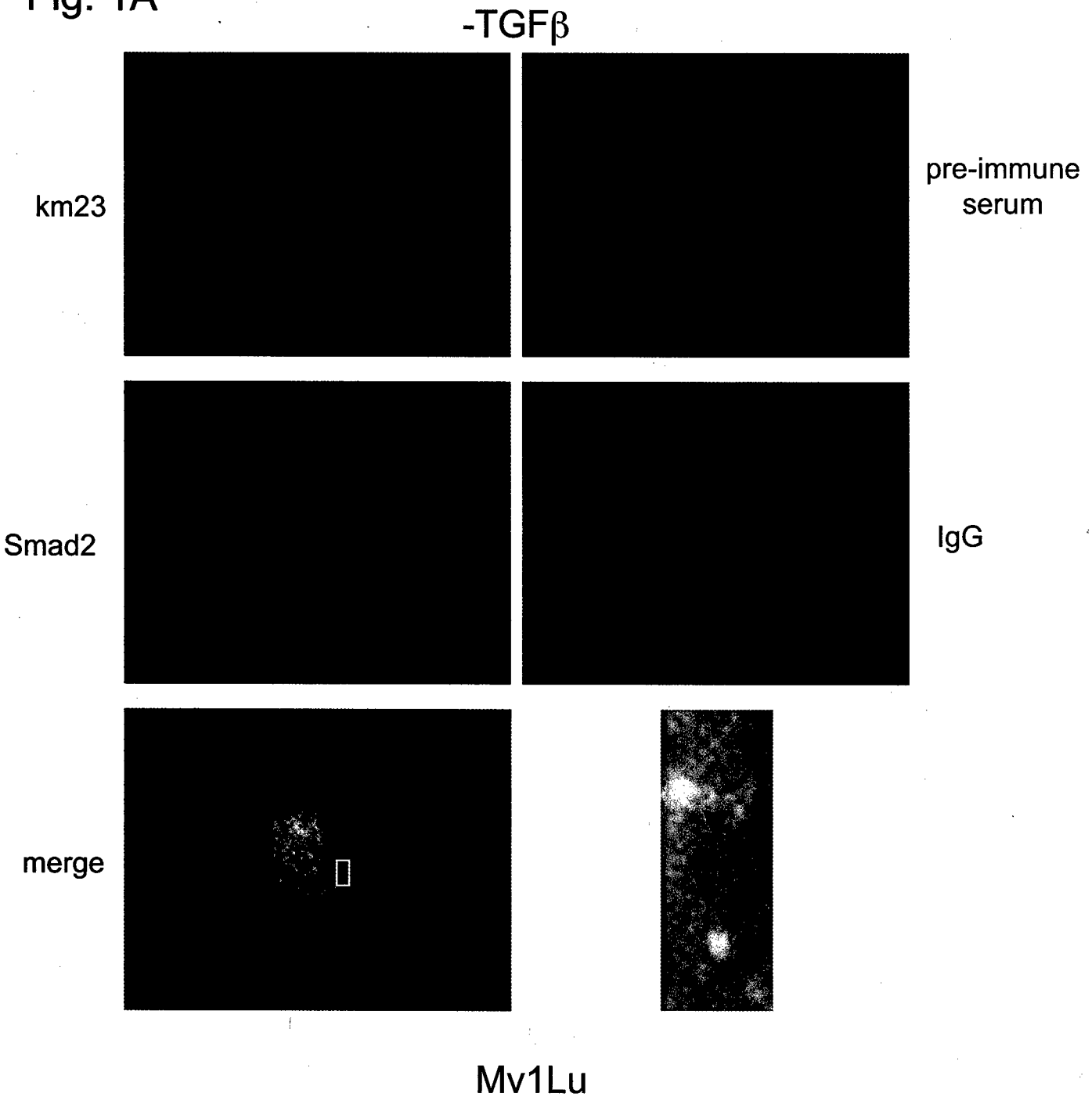

Fig. 1B

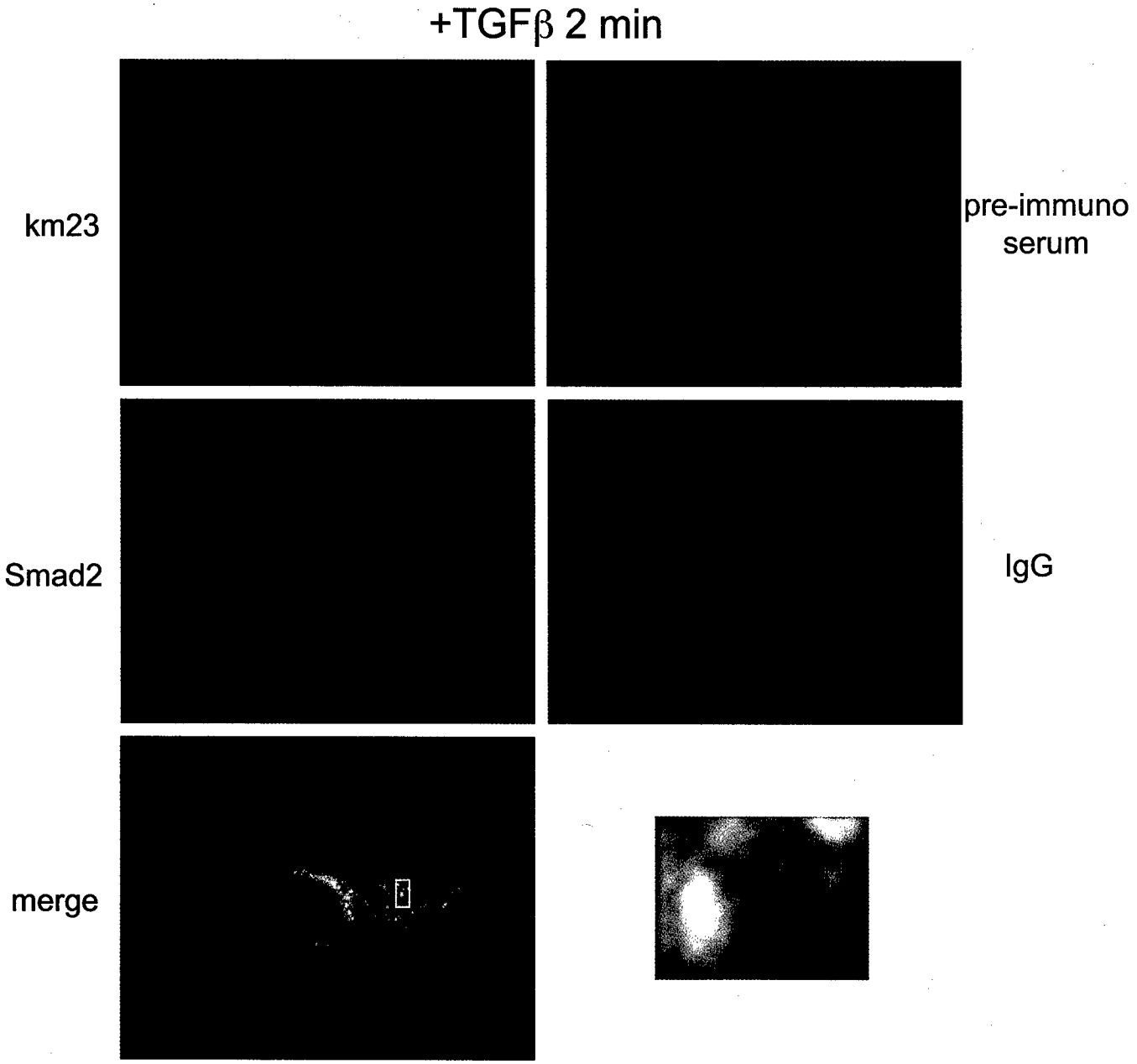

Fig. 1C

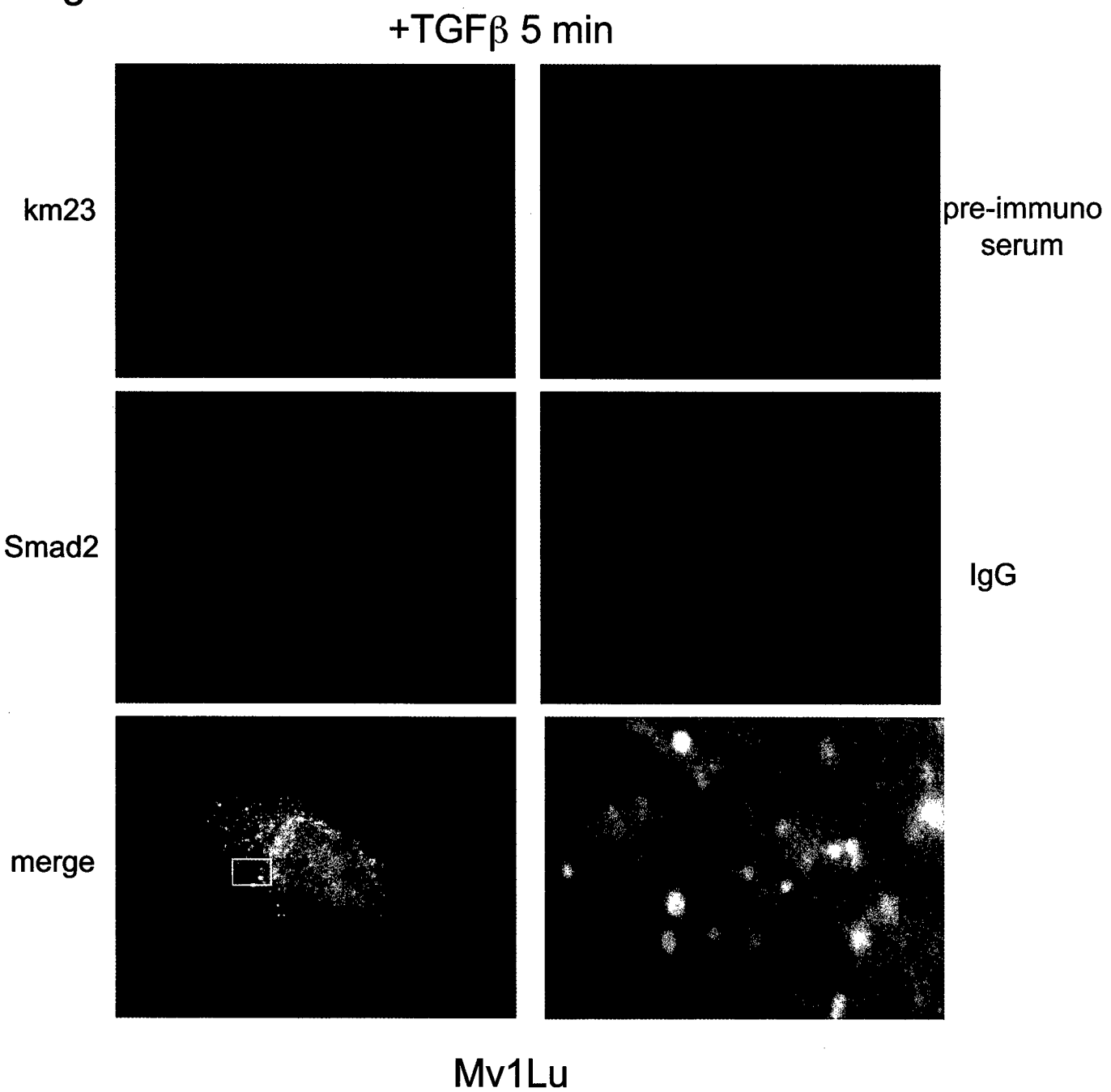

Fig. 1D

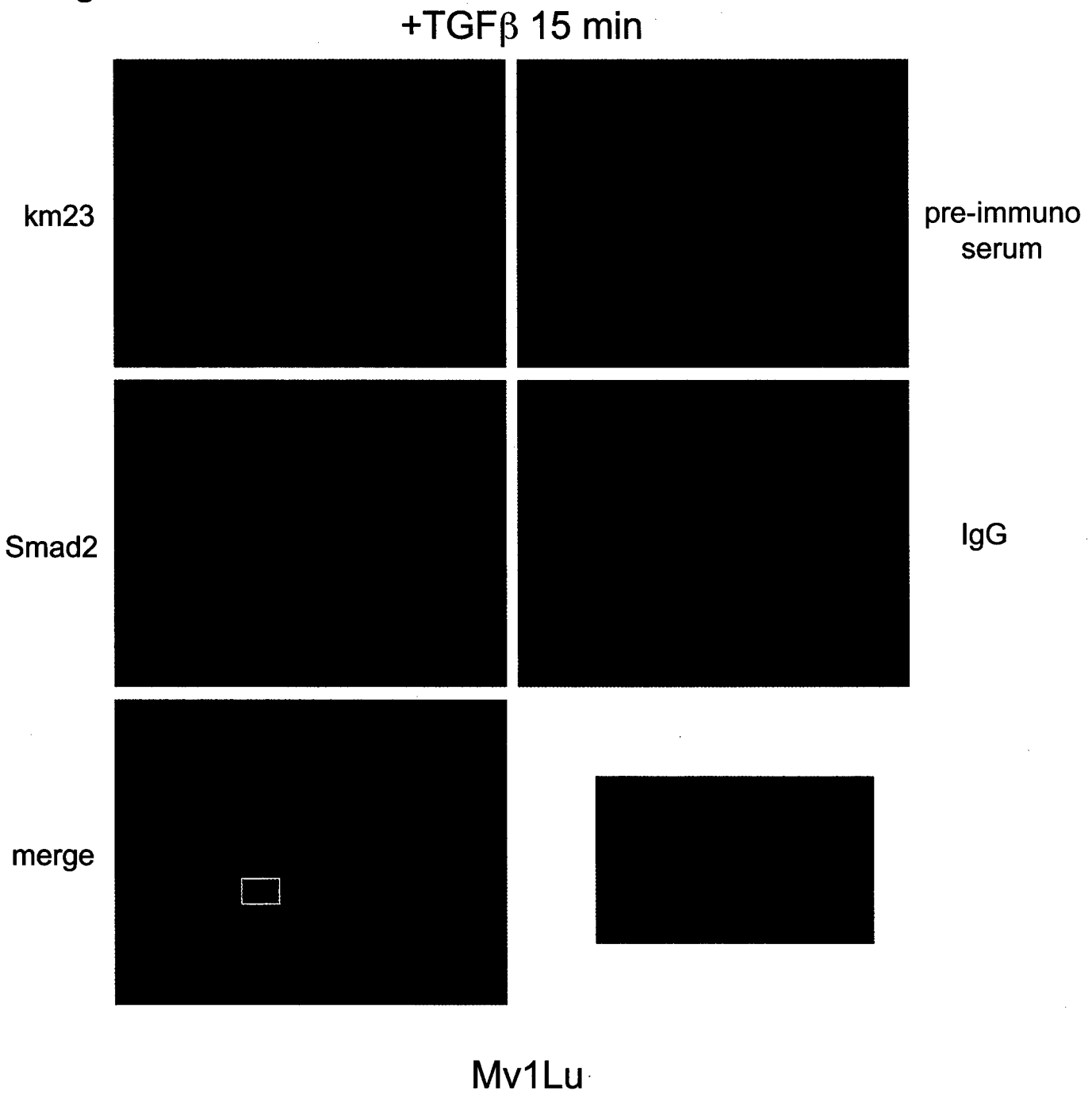

Fig. 2A

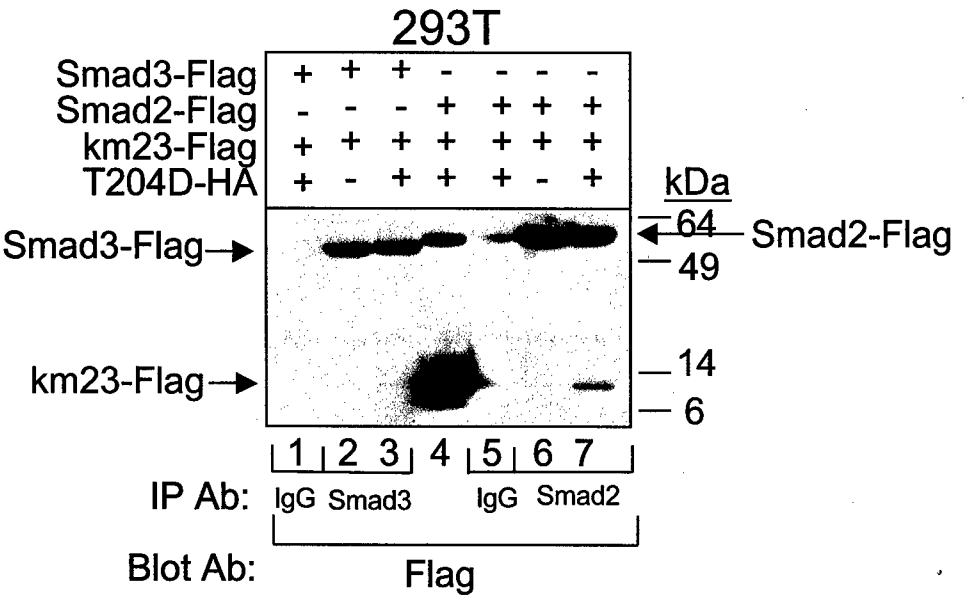
293T
Smad3-Flag + + + - - - -
Smad2-Flag - - - + + + +
km23-Flag + + + + + + +
T204D-HA + - + + + - +
kDa
64
49
14
6
Smad3-Flag
Smad2-Flag
km23-Flag
1 2 3 4 5 6 7
IP Ab: IgG Smad3 IgG Smad2
Blot Ab: Flag

Fig. 2B

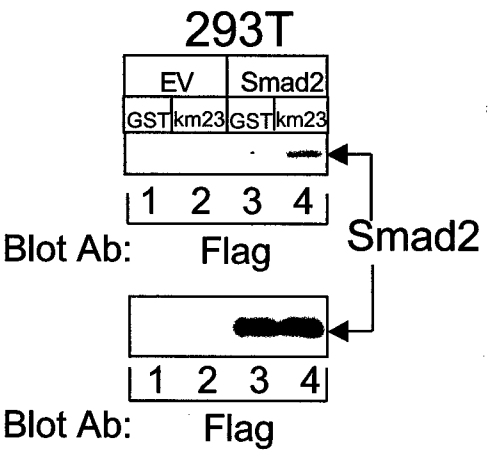
293T
EV Smad2
GST km23 GST km23
1 2 3 4
Blot Ab: Flag
Smad2
1 2 3 4
Blot Ab: Flag

Fig.3A

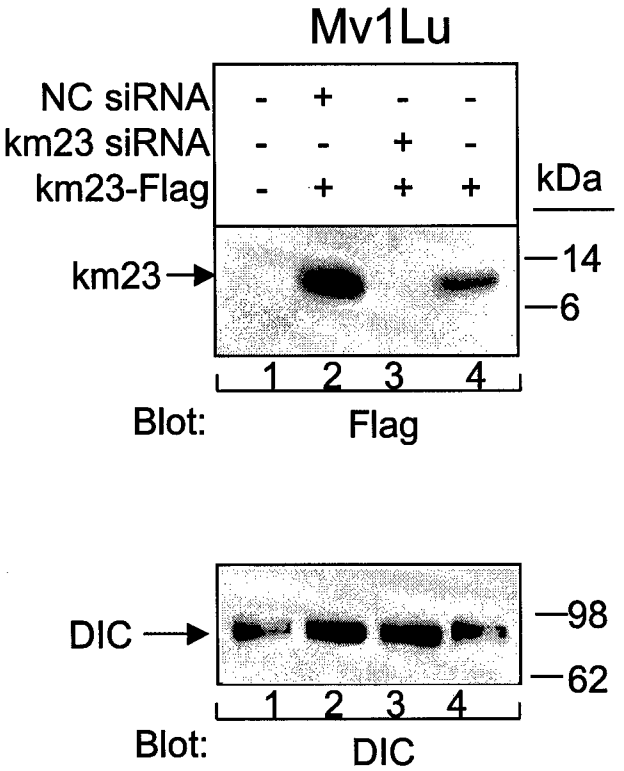
Mv1Lu
NC siRNA - + - -
km23 siRNA - - + -
km23-Flag - + + +
kDa
km23
14
6
1 2 3 4
Blot: Flag
DIC
98
62
1 2 3 4
Blot: DIC

Fig.3B

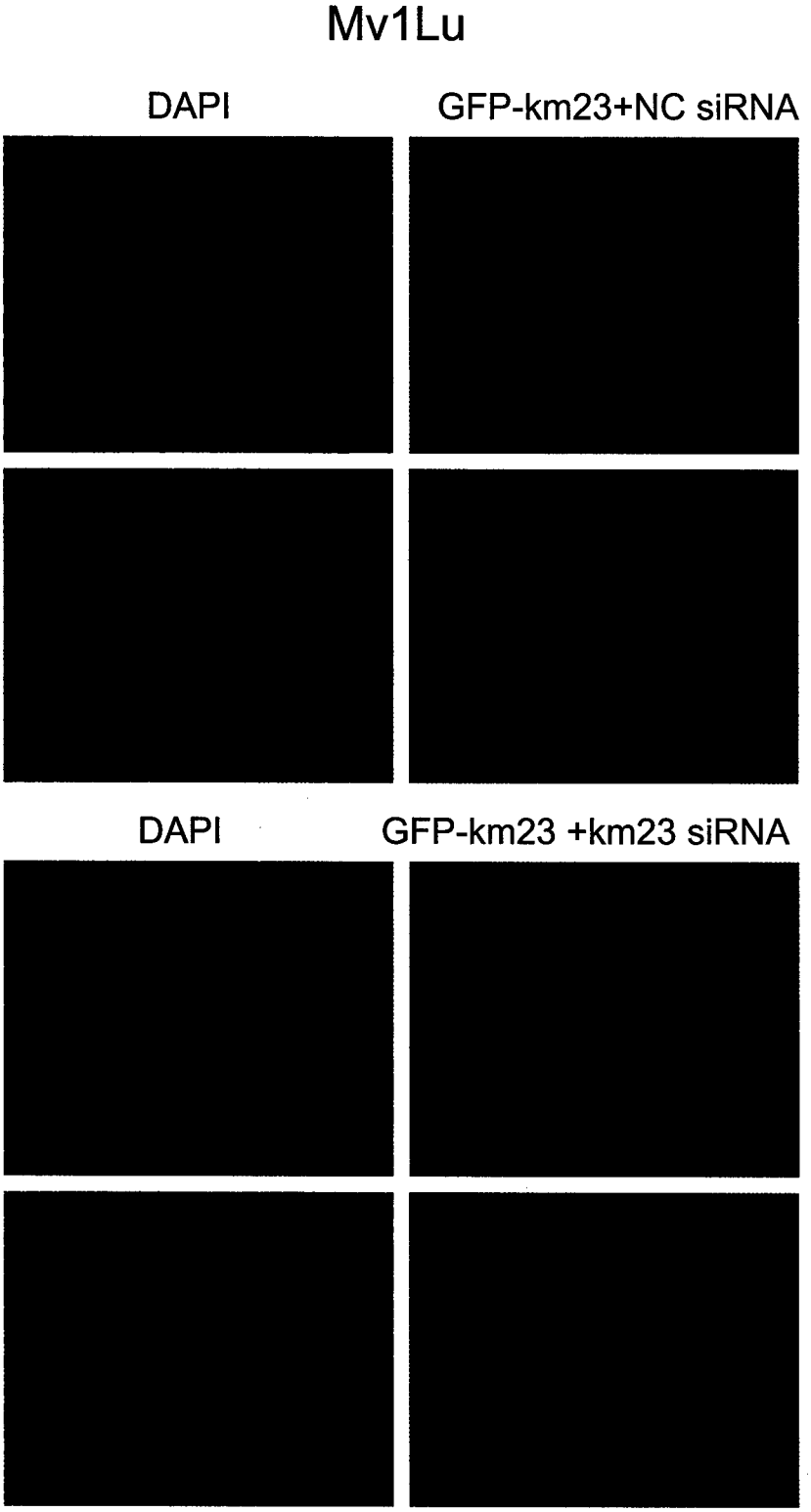

Fig.4

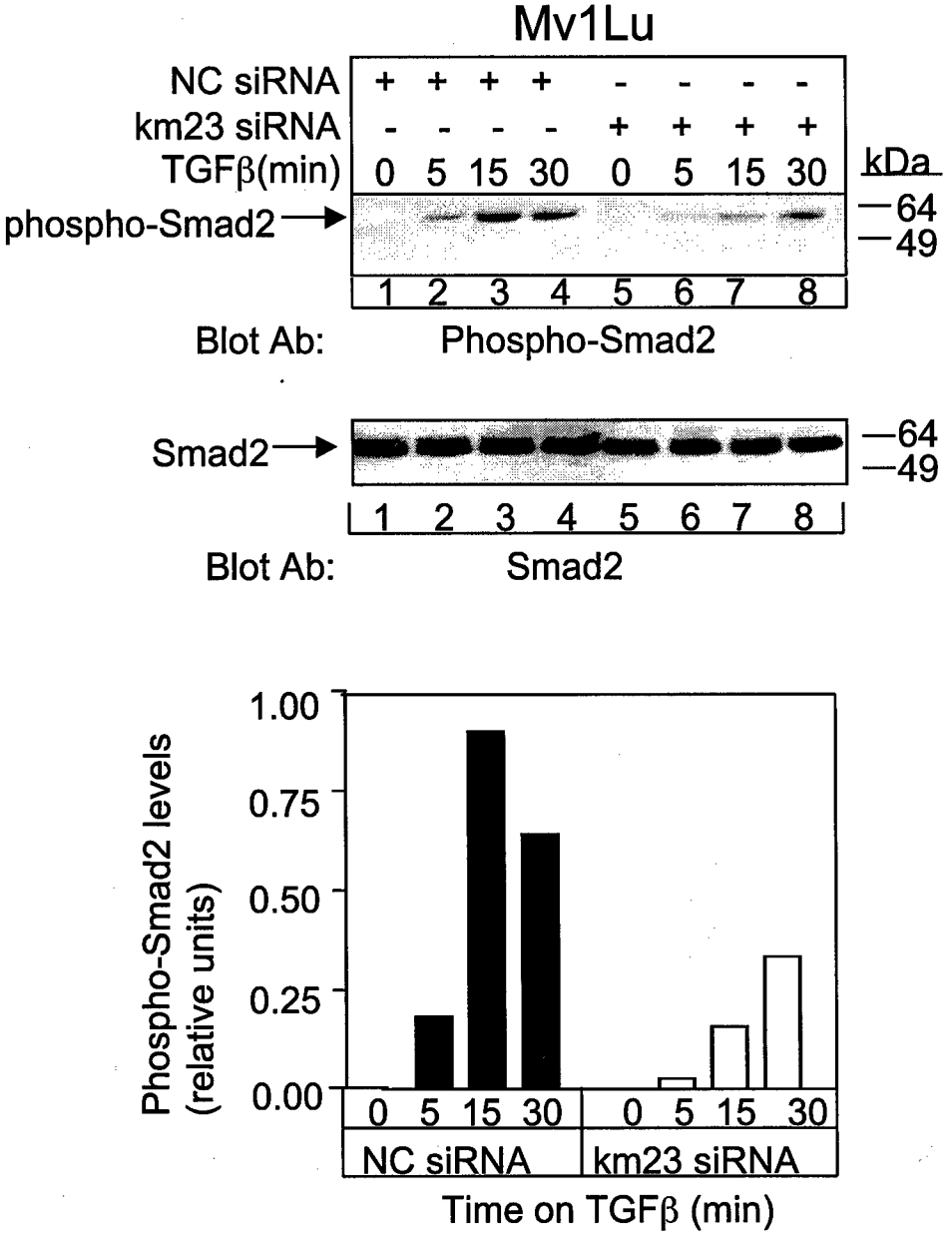
Mv1Lu
NC siRNA + + + + - - - -
km23 siRNA - - - - + + + +
TGFβ(min) 0 5 15 30 0 5 15 30
kDa
phospho-Smad2
64
49
1 2 3 4 5 6 7 8
Blot Ab: Phospho-Smad2
Smad2
64
49
1 2 3 4 5 6 7 8
Blot Ab: Smad2
Phospho-Smad2 levels (relative units)
1.00
0.75
0.50
0.25
0.00
0 5 15 30 0 5 15 30
NC siRNA
km23 siRNA
Time on TGFβ (min)

Fig.5A

-TGFβ

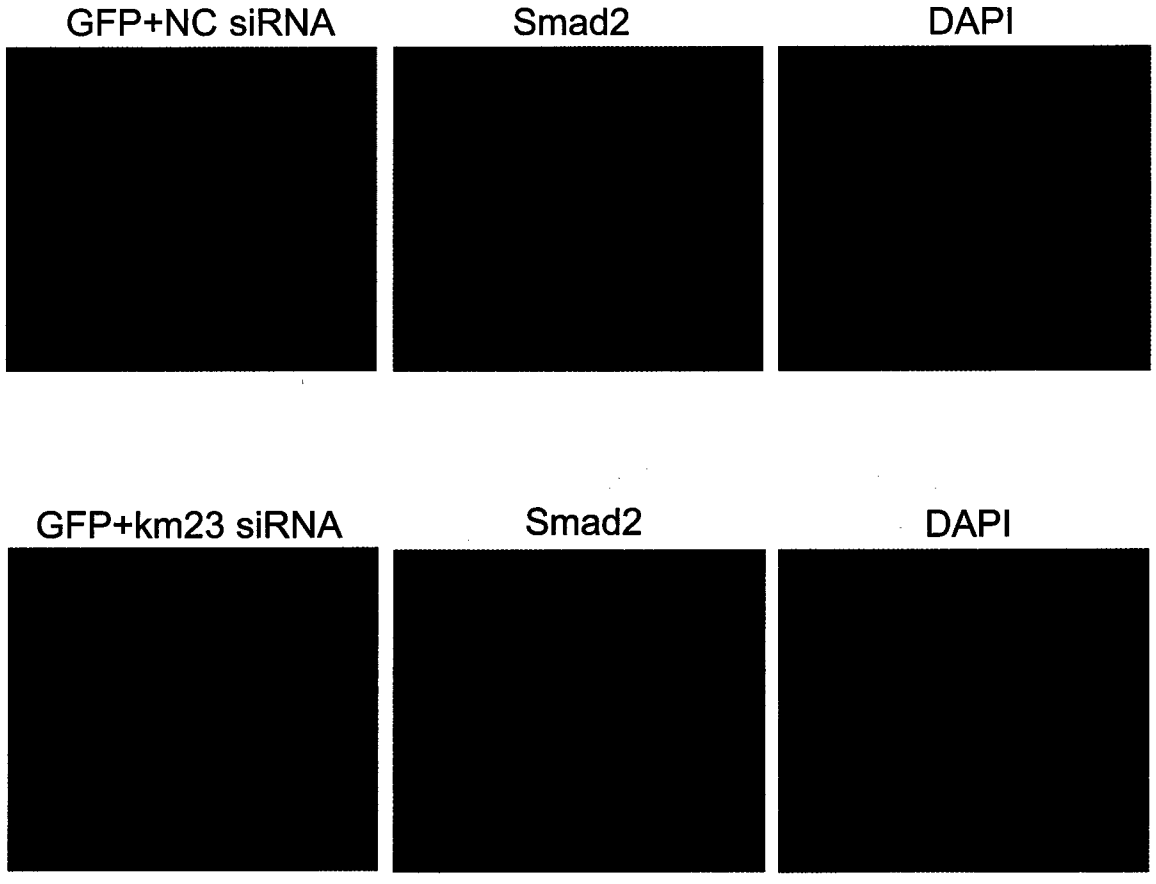

Mv1Lu

Fig.5B

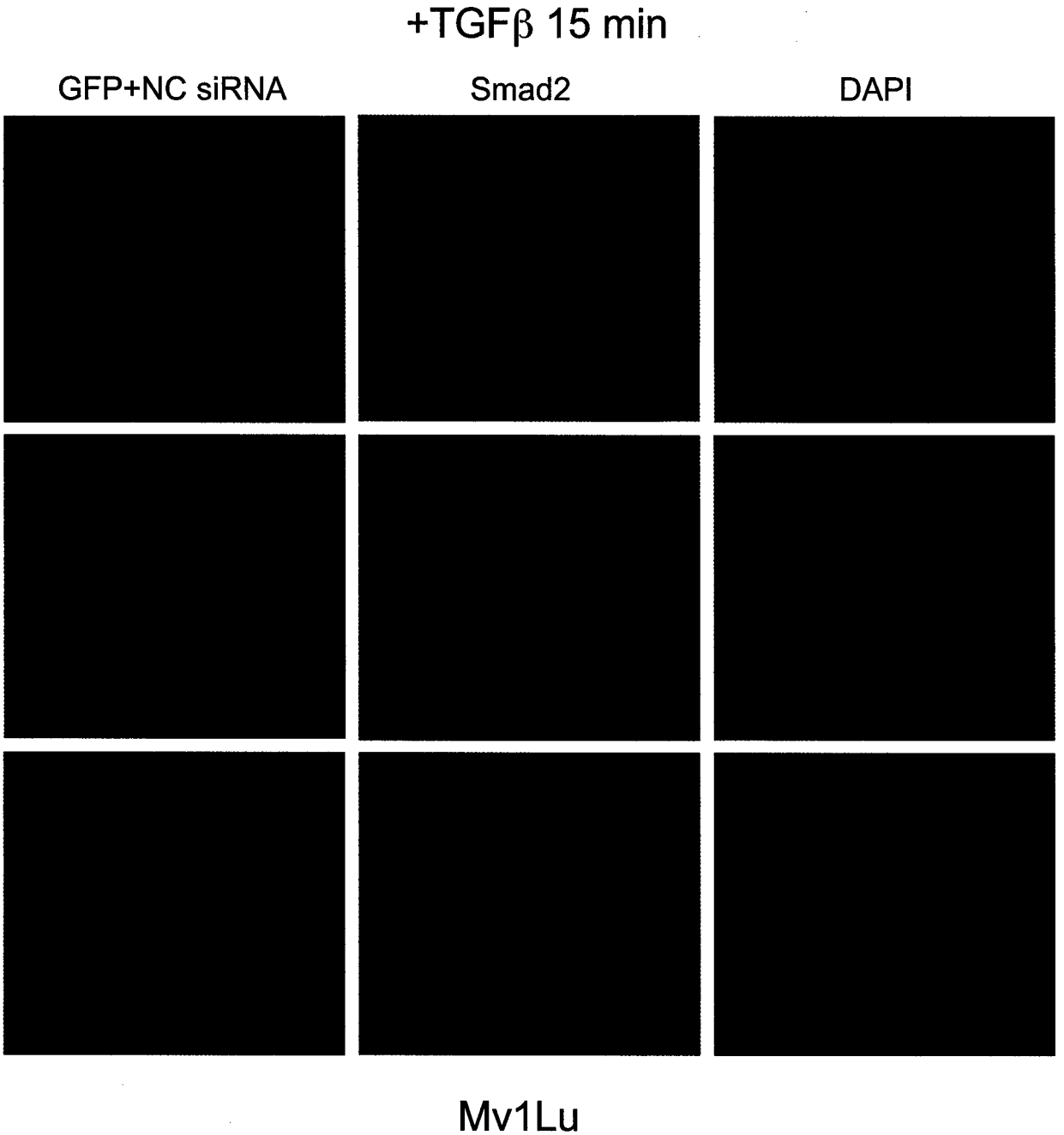

Fig.5C

+TGFβ 15 min

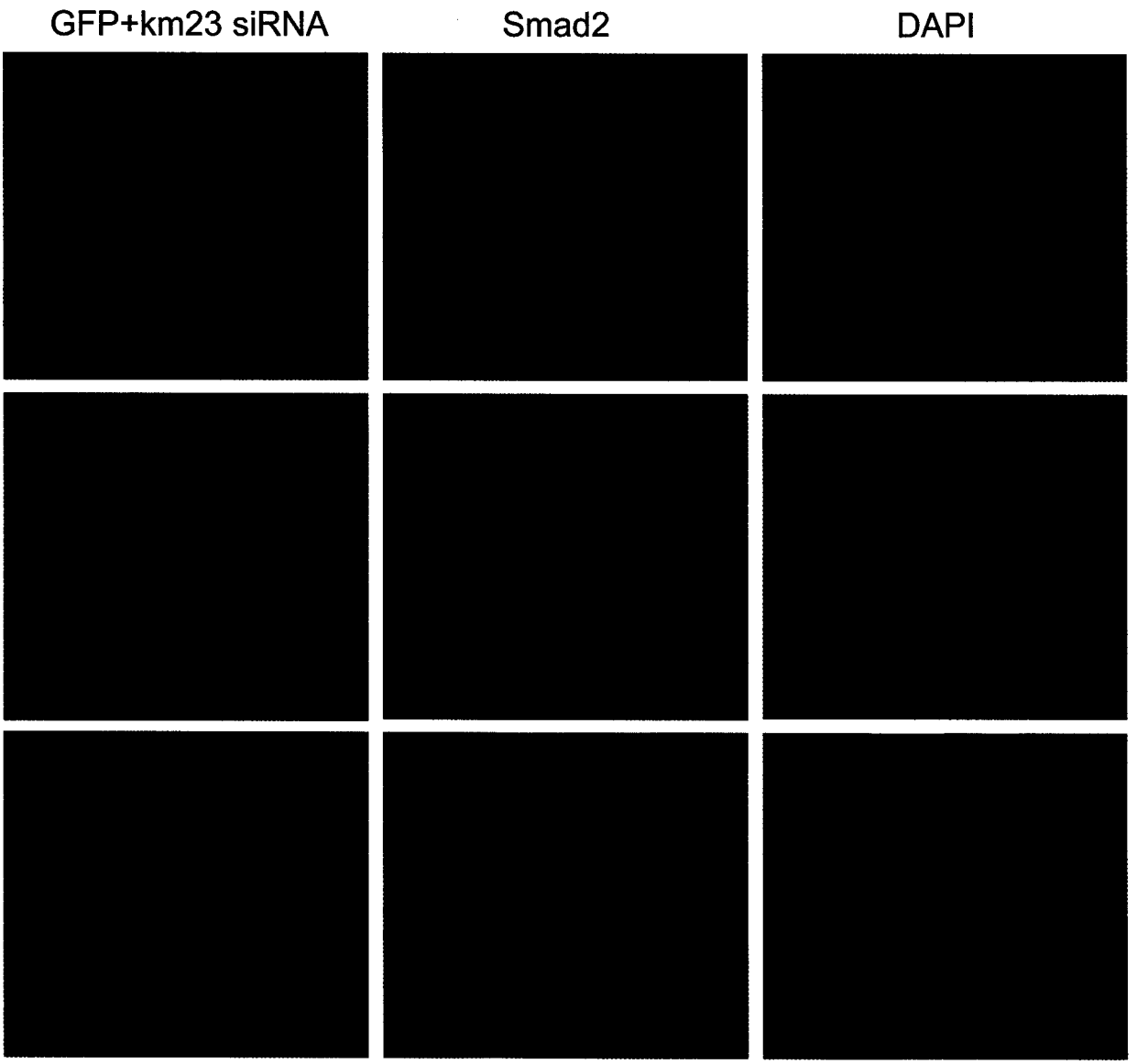

Mv1Lu

Fig.6

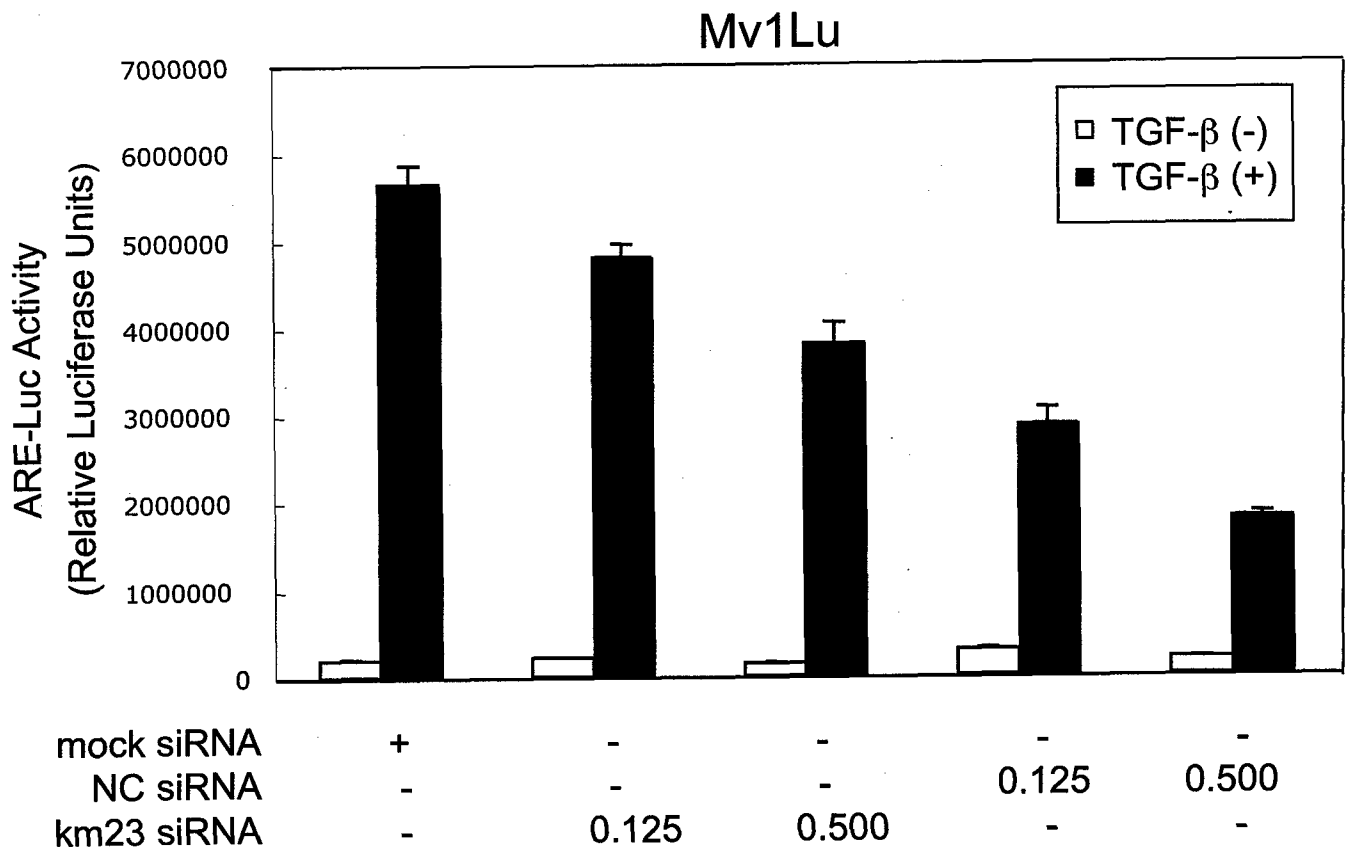
Mv1Lu
ARE-Luc Activity
(Relative Luciferase Units)
7000000
6000000
5000000
4000000
3000000
2000000
1000000
0
TGF-β (-)
TGF-β (+)
mock siRNA + - - - -
NC siRNA - - - 0.125 0.500
km23 siRNA - 0.125 0.500 - -

A TGFβ receptor-interacting protein frequently mutated in epithelial ovarian cancer

Wei Ding[1], Eileen M. Estes[1], Virginia Espina[2], Lance A. Liotta[2], and Kathleen M. Mulder[1*]

[1]Department of Pharmacology, Pennsylvania State University College of Medicine, Hershey, Pennsylvania 17033, USA

[2]FDA-NCI Clinical Proteomics Program, Laboratory of Pathology, Center for Cancer Research, National Cancer Institute, Bethesda, MD 20892, USA

[*]To whom correspondence should be addressed:

Department of Pharmacology-MC H078

Penn State College of Medicine

500 University Drive, Hershey, PA 17033

Telephone 717-531-6789; FAX 717-531-5013

E-mail kmm15@psu.edu

Running title: dynein light chain altered in ovarian cancer

Key words: ovarian carcinoma, mutation, robl, km23, LC7, bithoraxoid, dynein, TGFβ, Smad2

ABSTRACT

Ovarian carcinomas, particularly recurrent forms, are frequently resistant to transforming growth factor (TGF)-β-mediated growth inhibition. However, mutations in the TGFβ receptor I and receptor II (TβR-I and TβR-II) genes have only been reported in a minority of ovarian carcinomas, suggesting that alterations in TGFβ signaling components may play an important role in the loss of TGFβ responsiveness. Using laser-capture microdissection (LCM) and nested reverse-transcription polymerase chain reaction (RT-PCR), we found that km23, which interacts with the TGFβ receptor complex, is altered at a high frequency in human ovarian carcinoma cell lines and tissues. A novel form of km23, missing exon 3, was found in two out of six ovarian cancer cell lines, as well as in two out of nineteen tumor tissues from patients with ovarian cancer. In addition to this alteration, a stop codon mutation (TAA→CAC) was detected in two patients. This alteration results in an elongated protein, encoding 107 amino-acid residues, instead of the wild type 96-amino acid form of km23. Furthermore, five missense mutations (T38I, S55G, T56S, I89V, and V90A) were detected in four patients, providing a total alteration rate of 42.1% (8 out of 19 cases) in ovarian cancer. No km23 alterations were detected in 15 normal tissues. Such a high alteration rate in ovarian cancer suggests that km23 may play an important role in either TGFβ resistance or tumor progression in this disease. In keeping with this, the functional studies described herein indicate that both the truncated and elongated forms of km23 have diminished binding to the dynein intermediate chain (DIC) in vitro, and that the latter also dose-dependently inhibits TGFβ- and Smad2-dependent activin responsive element (ARE) reporter activity.

INTRODUCTION

Ovarian carcinoma is often diagnosed at an advanced stage and is the leading cause of death from gynecological neoplasia, accounting for more than 14,000 deaths per year (1). Overall, the molecular changes that underlie the initiation and development of this tumor are poorly understood. It has been reported that more than 75% of ovarian carcinomas are resistant to TGFβ, particularly recurrent ones (2, 3). As such, the loss of TGFβ responsiveness may play an important role in the pathogenesis and/or progression of ovarian cancer.

It has been reported that the $TGF\beta_1$, the TGFβ receptors, the TGFβ signaling components Smad2 and Smad4, and the adaptor molecule Dab2 were altered in different types of cancers (4-6). Alterations in TβR-II have been identified in 25% of ovarian carcinomas (7), while mutations in TβR-I were reported in 33% of such cancers (8). Loss of function mutations of $TGF\beta_1$, TβR-I, and TβR-II can lead to disruption of TGFβ signaling pathways and subsequent loss of cell cycle control (7-10). However, these alterations only account for a minority of TGFβ-resistant ovarian carcinomas, suggesting that other alterations in TGFβ signaling components may be involved in the pathogenesis of this type of cancer.

Recently, we have identified km23 as a TGFβ receptor-interacting protein that is also a light chain of the motor protein dynein (11). km23 can be phosphorylated on serine residues after ligand binding. Forced expression of km23 induced specific TGFβ responses, including Jun N-terminal kinase (JNK) activation, c-Jun phosphorylation, and cell growth inhibition (11). Further, TGFβ induced the recruitment of km23 to the dynein intermediate chain (DIC). A kinase-deficient form of TGF-β RII prevented both km23 phosphorylation and interaction with

DIC (11). This report was the first demonstration of a link between the cytoplasmic motor protein dynein and a natural, growth inhibitory cytokine. Our more recent studies have also demonstrated that km23 is co-localized with Smad2 after ligand binding. km23 interacted with Smad2 both *in vitro* and *in vivo*. Blockade of endogenous km23 inhibited Smad2 nuclear translocation and Smad2-mediated ARE-luc transcriptional activation (12). Thus, km23 appears to be an important component of a Smad2-dependent TGFβ signaling pathway.

Cytoplasmic dynein is a large multisubunit motor complex that moves various cargoes toward the minus end of microtubules in eukaryotic cells. It is composed of heavy, intermediate, light-intermediate, and light chain subunits (13). Two dynein heavy chains are responsible for microtubule binding and ATP hydrolysis, events that are essential for the movement of the motor complex along microtubules (13). The intermediate chains, light-intermediate chains, and light chains form the base of the dynein complex and are important for cargo binding (13). Several dynein light chains (DLCs) have been identified, and among them, LC8, Tctex-1/rp3, and Tctex-2 have been the most widely studied (13).

The *Drosophila* homologue of km23, termed robl, is essential for both flagellar and cytoplasmic dynein functions and is involved in mitosis and axonal transport (14). Mutants of this *Drosophila* homologue display defects in intracellular transport, an accumulation of cargoes, and an increase in mitotic index (14). In mammals, there appear to be two classes of km23 proteins (km23-1 and km23-2), based upon homology comparisons. Both of them contain open-reading frames of equal length, encoding 96-amino-acid peptides and displaying 77% identity. Expression of the rat km23-1/robl/LC7 is down-regulated in response to light within the visual cortex (15). In human hepatocellular carcinoma tissues, compared with adjacent tumor-free tissues, the expression level of km23-1/DNLC2A is up-regulated, while the km23-2/DNLC2B is down-regulated (16).

In this communication, we report the analysis of sequence alterations in human km23-1

in epithelial ovarian cancer cell lines and tissues using laser-capture microdissection (LCM) and nested RT-PCR approaches. We found a high incidence (42.1%) of km23 mutations in human ovarian carcinomas, while normal tissues did not contain such alterations ($p<0.005$). This is the first report of alterations in a cytoplasmic DLC in epithelial ovarian cancer. Further, we found two mutants, encoding truncated and elongated forms of km23, which both display diminished interactions with DIC. In addition, the elongated form of km23 inhibited TGFβ- and Smad2-dependent ARE-luc transactivation. Our results demonstrate that alterations in km23 found in ovarian cancer patients can result in altered dynein motor interactions and altered Smad2 signaling induced by TGFβ.

MATERIALS AND METHODS

Cell culture. Human ovarian cancer cell lines SK-OV-3 and OVCAR-3 were purchased from American Type Culture Collection (ATCC, Rockville, MD). OVCA420 and OVCA429 cells were provided by Dr. Bast (Texas M.D. Anderson Cancer Center, Houston, TX). CaOV-3 cells were obtained from Dr. Ruch (Medical College of Ohio, Toledo, OH), and IGROV-1 cells were obtained from Dr. MacLaughlin (Massachusetts General Hospital, Boston, MA). SK-OV-3 cells were cultured in McCoy's 5a medium and OVCAR-3 cells were cultured in RPMI1640 medium according to ATCC's recommendation. IGROV-1 cells were cultured in Dulbecco's Modified Eagle's Medium with glutamine. OVCA420, OVCA429, and CaOV-3 cells were cultured in Minimum Essential Medium. All media were supplemented with 10% heat-inactivated FBS. Cells were maintained in 5% CO_2 at 37°C. Cultures were routinely screened for mycoplasm using Hoechst staining.

Ovarian tissues. 19 ovarian carcinoma tissues and 12 normal ovarian tissues were provided by Cooperative Human Tissue Network (CHTN). Tissues were sent on dry ice and stored at -80°C prior to use. Institutional Review Board approval for this study was received from the Penn State College of Medicine (Hershey, PA).

H&E staining. Sections of frozen tissues (10μm) were mounted on slides (SL Microtest, Germany). H&E staining was performed as described by Goldsworthy et al (17). All reagents for H&E staining were prepared with diethyl-pyrocarbonate (DEPC)-treated distilled water.

LCM. LCM was performed using a μCut Laser Microdissection system (SL Microtest, Germany) according to the manufacturer's instructions. After microdissection of each specimen, the thermoplastic film-coated cap containing the captured tissue was placed in a

0.5 ml microtube.

RNA isolation. Total RNA was isolated from the cell lines and ovarian tissues using TRIzol reagent according to manufacturer's protocol (Invitrogen, life technologies, Carlsbad, CA, Cat# 15596-026). Total RNA was isolated from LCM'd tissue using a Total RNA Microprep Kit (Stratagene, La Jolla, CA, Cat# 400752) according to manufacturer's recommendations.

Nested RT-PCR and DNA sequencing. cDNA synthesis was performed using Sensicript Reverse Transcriptase (QIAGEN, Germany, Cat# 205211), according to the manufacturer's suggestion. Nested PCR was performed using two pairs of primers spanning the whole open reading frame of km23. The forward primer for the first round of PCR was 5'-GTTTTGACAGAAACCTTTGCG-3' and the reverse primer was 5'-TTGGTGCACACAGG GGTTC-3'. The conditions used for the first round of PCR were: 94°C, 50 sec; 54°C, 50 sec; 72°C, 1 min; 30 cycles. The second round of PCR was performed using the first round of PCR products as a reaction template (forward primer, 5'-ACTCGCTAAGTGTTCGCTACG-3'; reverse primer, 5'-TGCCATGTGCTAGTCCACTGA-3'), with the following conditions: 94°C, 50 sec; 62°C, 50 sec; 72°C, 1min; 33 cycles. All PCR assays were performed using recombinant Pfu polymerase with 3'-5' exonuclease activity (Stratagene, La Jolla, CA. Cat# 600154-81). The PCR products were electrophoresed on 2% agarose gels, visualized with ethidium bromide staining, and purified using a QIAquick Gel Extraction Kit (QIAGEN, Germany, Cat# 28704). DNA sequencing was performed in both directions using the primers for the second round of PCR.

Statistics. The statistical difference in alteration rate between the ovarian carcinoma tissues and the tumor-free ovarian tissue groups was calculated using *Fisher's exact test*.

Phosphorylation site prediction and secondary structure prediction. Phosphorylation site prediction for km23 was performed using PhosphoBase v. 2.0 and NetPhos 2.0 (http://www.cbs.dtu.dk/databases/PhosphoBase) (18). The secondary structure for km23

was predicted using the Jnet method (http://www.compbio.dundee.ac.uk/~www-jpred/jnet/) (19).

GST pull-down assays. GST-km23 and GST-elongated km23 mutant constructs were prepared using the pGEX-4T-1 vector (Amersham Biosciences, Piscataway, NJ) as previously described (11). The bacterially expressed GST fusion proteins were isolated according to the manufacturer's instructions (Pierce) and used in GST pull-downs by standard methods (Current Protocols in Molecular Biology). The products were analyzed by SDS-PAGE or immunoblotting/Coomassie blue staining.

Luciferase reporter assays. Mv1Lu cells were plated at a density of 1×10^4 cells/cm^2 in 24-well plates 24 h prior to transfection. The cells were co-transfected with ARE-luc, forkhead activin signal transducer-1 (FAST-1) (20), and the indicated amount of either wt km23 or elongated km23. pcDNA3.1 was used to normalize the amount of total DNA. 24 h after transfection, the medium was replaced with DMEM serum-free medium. 1 h later, the cells were incubated in the absence or presence of TGF-β (2.5ng/ml) for 18 h. Luciferase activity was measured using Promega's Dual-Luciferase Reporter Assay System (Cat# E1960) according to the manufacturer's instructions, using renilla as an internal control to normalize transfection efficiencies. All assays were performed in triplicate.

RESULTS

A truncated form of km23, missing exon 3, was detected in two out of six ovarian cancer cell lines, as well as in two out of nineteen ovarian carcinoma tissues. Using a highly sensitive and specific nested RT-PCR strategy, we amplified a PCR fragment of 424 base pairs using forward and reverse primers located in the 5'-UTR and 3'-UTR regions respectively. This fragment spans the entire coding region of human km23. In two (SK-OV-3 and IGROV-1) out of six ovarian cancer cells, a smaller band of 254 bp was detected in addition to the 424 bp product (Fig.1A). DNA sequencing indicated that this short fragment is a truncated form of km23, which is missing exon 3 and contains only 123 nucleotides, as opposed to the 291 found in wild-type (wt) km23. No sequence alterations were detected in the 424 bp product in all six cell lines.

In order to investigate whether this novel TGFβ receptor interactor was also altered in human epithelial ovarian cancer tissues, we analyzed 19 ovarian carcinoma samples from patients. In order to prevent RNA degradation, snap-frozen tissues were analyzed under RNAse-free conditions by RT-PCR. LCM was performed to separate epithelial tumor cells from adjacent tumor-free normal cells. Combining two micro-scale analysis technologies, LCM and nested RT-PCR, we amplified the entire coding region of km23 in all samples. In two of nineteen tumor tissues (cases 3 and 8), an additional band of 254 bp was detected (Fig.1B). DNA sequencing confirmed that this band was identical to the truncated form of km23 (missing exon 3), which was identified in the tumor cell lines. In case 8, we also analyzed the km23 sequence in tumor-free stroma cells. No truncated form of km23 was detectable. The predicted size of the truncated form of km23 is 41-amino-acids (Fig. 1C).

Five Missense mutations in km23 were detected in 21% of epithelial ovarian

carcinoma tissues. In addition to the above-mentioned findings, we obtained five missense mutations in km23 in four patients. In case 1, diagnosed with serous cystadenocarcinoma, the 163rd nucleotide of the coding region was changed from an adenine to a guanine (A→G). This alteration corresponds to an amino acid change from a serine to a glycine (S55G). Also in this patient, the 265th nucleotide of the coding region was altered from an adenine to a guanine (A→G), corresponding to an amino acid change in residue 89 of km23 from an isoleucine to a valine (I89V). In addition to these alterations, three other missense mutations, including T38I, T56S, and V90A, were detected in three other patients (cases 7, 15, and 18) (Table 1).

A stop codon mutation in km23 was detected in 10% of epithelial ovarian carcinoma tissues. In two cases (cases 4 and 14), the stop codon of km23 was altered from TAA to CAC. This alteration results in a larger protein, encoding 107 amino-acid residues, instead of the wt 96-amino acid form of km23 (Table 1). The expression of this altered form of km23 has been confirmed in 293T cells (data not shown).

No similar alterations in km23 were detectable in normal tissues. We also analyzed 12 normal ovarian samples, as well as 3 tumor-free stroma samples (procured from cases 8, 9, and 11 by LCM), using the nested PCR strategy. In all 15 normal samples, the km23 sequence was not changed. Our findings demonstrate a statistically significant difference in the km23 alteration rate between cancer and non-cancer groups (42.1% vs 0%; $p < 0.005$, *Fisher's exact test,* Table 2).

The truncated and elongated forms of km23 displayed a reduced interaction between km23 and DIC. In order to examine whether the altered forms of km23 could still interact with DIC, we performed GST-pull-down assays using bacterially expressed GST fusion proteins of the km23 mutant forms. Total lysates from MDCK cells were incubated with the purified GST-fusion proteins, and DIC was detected by SDS-PAGE and

immunoblotting after the pull-down assays. As shown in Fig. 2A, the binding capability of GST-truncated km23 to the DIC was significantly reduced compared with the GST-wt km23. The km23 interaction with DIC was also diminished when the elongated form of km23 was used in the same assay (Fig. 2B).

Elongated km23 dose-dependently inhibits Smad2-dependent transcription in TGF-β/activin reporter assays. Since our recent studies showed that blockade of endogenous km23 by small interfering RNA blocked the nuclear translocation of Smad2, and also inhibited Smad2-dependent ARE promoter transcriptional activation (our unpublished data), it was of interest to address the effect of km23 alterations on this promoter. To examine induction of the ARE from the Xenopus Mix.2 gene (20), Mv1Lu cells were transfected with increasing amounts of either wt km23 or elongated km23, along with the ARE-luc reporter and FAST1. As shown in Fig.3, compared with wt km23, the elongated form of km23 inhibited both basal and TGFβ-stimulated ARE-luc reporter activity in a dose-dependent manner.

Discussion

Our data reveal a truncated form of km23, missing exon 3 of km23, in two ovarian cancer cell lines (SK-OV-3 and IGROV-1), both of which are resistant to TGFβ (21, 22). The same truncated form of km23 was detected in two out of nineteen ovarian cancer patients. Among the four exons of km23, the third exon is the longest, encoding amino acid residues 27-81 of km23. As predicted by PhosphoBase v. 2.0 and NetPhos 2.0 (18), this region contains potential phosphorylation sites for protein kinase A (PKA), protein kinase C (PKC) and/or casein kinase II (CKII) (Fig.4). The loss of potential phosphorylation sites when exon 3 is missing may result in a disruption of signal transduction. Furthermore, secondary structure predictions using Jnet (19) indicated that km23 contains two α-helices, one located at the N-terminus (residues 2-13) and another in the central portion of the protein (residues 37-56) (Fig.4, black bars). The second α-helix and four β-strands (Fig.4, gray bars) were removed in the truncated form of km23, indicating that exon 3 may be essential for km23's functions.

In *Drosophila*, a deletion mutant of km23/robl, which lacks portions of intron 2 and exon 3, displays mitotic defects (14). This alteration is similar to the truncated form of km23 we identified in ovarian tumor cell lines and cancer patients. The mitotic index of the mutant *Drosophila* hemizygotes is about five times that of the wild type (14). In addition, the km23/robl mutant homozygotes cannot be fully rescued by the genomic or cDNA rescue constructs, suggesting that this mutation can act in a dominant fashion to inhibit the action of wild-type km23/robl (14). Here we have shown that the truncated form of km23 resulted in a reduced interaction with DIC. Since it is believed that DLC binding to the DIC is required for appropriate movement of cargo along MTs intracellularly (23), this defect would be expected

to result in altered intracellular trafficking and accumulations of cargos in an aberrant manner. This is precisely what was observed with this mutant in Drosophila, consistent with our data for this truncated form of human km23. Thus, we expect that the truncated form of km23 may play an important role in the formation or progression of ovarian and other types of tumors.

Two mutations in km23 that may be important are those at positions 55 and 56 (S55G, T56S). As mentioned above, there are potential PKA, PKC, and/or CKII phosphorylated sites in km23 (Fig.4). Among them, the threonine at the 56th amino-acid residue spans a predicted phosphorylation site for PKA, PKC and CKII. Mutation of this site may result in disruption of signals transduced by these kinases. Further, we have reported that km23 is phosphorylated primarily on serines after activation of TGFβ receptors (11). There are 4 serine residues in km23 that are conserved among the mammalian forms (boxed in Fig.4). Among these, three are located in exon 3, including Ser55, which was found to be mutated in one of the ovarian carcinomas. Thus, this site and/or the other two in exon 3 may be potential phosphorylation sites modified by TGFβ.

Of the five missense mutations identified, the stop codon mutation appeared to be the most interesting. Not only has this same mutation been detected in two patients, but it also results in decreased binding DIC, with a resulting inhibition of Smad2-dependent ARE transcriptional activation induced by TGFβ. These findings are in keeping with our current model for km23 function. According to our model, km23 is phosphorylated by the active TGFβ receptor complex, thereby resulting in DIC recruitment to the rest of the motor complex. This complex transports membrane vesicles containing TGFβ signaling components, such as Smad2, along the microtubules to a new vesicular compartment. After reaching the new compartment, the signaling components such as Smad2 can be translocated to the nucleus for transcriptional regulation of target genes. Thus, it would be

expected that altered intracellular transport of Smad2 would result in reduced Smad2-dependent transcriptional activity.

As a tumor suppressor, Smad2 has been found to be altered in several types of cancer, including ovarian cancer (10). In addition, one report demonstrated that loss of Smad2 did not initiate tumorigenesis by itself, but that this event accelerated the malignant progression of tumors to invasive cancer in later stages of carcinogenesis (24). As a Smad2 transporter, km23 would also be expected to function as a mediator of tumor progression when it is mutated. Future studies will investigate this possibility.

ACKNOWLEDGEMENT

We appreciate CHTN for providing the ovarian tissues. We also thank R. C. Bast (Texas M.D. Adderson Cancer Center, Houston, TX), R. J. Ruch (Medical College of Ohio, Toledo, OH), and D. T. Maclaughlin (Massachusetts General Hospital, Boston, MA) for the ovarian cancer cell lines. We also appreciate W. Stewart (Department of Histology, Penn State College of Medicine) for assistance with tissue sectioning. We also thank S. Gestl (Jake Gittlen Cancer Research Institute, Penn State College of Medicine) and D. Shearer (Department of Obstetrics/ Gynecology, Penn State College of Medicine) for assistance with the LCM. We thank D. Mauger (Department of Health Evaluation Sciences, Penn State College of Medicine) for the statistics. This work was supported by National Institutes of Health grants CA-51452, CA-100239, CA-90765, CA-92889, and Dept of Defense award DAMD 17-03-1-0287 to K.M.M.

REFERENCES

1. Landis, S. H., Murray, T., Bolden, S., and Wingo, P. A. Cancer statistics, 2001. CA Cancer J. Clin., *51*: 15-36, 2001.
2. Hu, W., Wu, W., Nash, M. A., Freedman, R. S., Kavanagh, J. J., and Verschraegen, C. F. Anomalies of the TGF-β postreceptor signaling pathway in ovarian cancer cell lines. Anticancer Res., *20*: 729-733, 2000.
3. Yamada, S. D., Baldwin, R. L., and Karlan, B. Y. Ovarian carcinoma cell cultures are resistant to TGF-β1-mediated growth inhibition despite expression of functional receptors. Gynecol. Oncol., *75:* 72-77, 1999.
4. Yue, J., and Mulder, K. M. Transforming growth factor-β signaling transduction in epithelial cells. Pharmacol. Ther., *91*: 1-34, 2001.
5. Massague, J., Blain, S. W., and Lo, R. S. TGFβ signaling in growth control, cancer, and heritable disorders. Cell, *103*: 295-309, 2000.
6. Hocevar, B. A., Smine, A., Xu, X. X., and Howe, P. H. The adaptor molecule disabled-2 links the transforming growth factor β receptors to the Smad pathway. EMBO. J., *20*: 2789-2801, 2001.
7. Lynch, M. A., Nakashima, R., Song, H. J., Degroff, V. L., Wang, D., Enomoto, T., and Weghorst, C. M. Mutational analysis of the transforming growth factor β receptor type II gene in human ovarian carcinoma. Cancer Res., *58*: 4227-4232, 1998.
8. Chen, T., Triplett, J., Dehner, B., Hurst, B., Colligan, B., Pemberton, J., Graff, J. R., and Carter, J. H. Transforming growth factor-β receptor type I gene is frequently mutated in ovarian carcinomas. Cancer Res., *61*: 4679-4682, 2001.
9. Cadillo, M. R., Yap, E., and Castagna, G. Molecular genetic analysis of TGF-β1 in ovarian

neoplasia. J. Exp. Clin. Cancer Res., *16*: 49-56, 1997.

10. Wang, D., Kanuma, T., Muzunuma, H., Takama, F., Ibuki, Y., Wake, N., Mogi, A., Shitara, Y., and Takenoshita. Analysis of specific gene mutations in the transforming growth factor-beta signal transduction pathway in human ovarian cancer. Cancer Res., *60*: 4507-4512, 2000.
11. Tang, Q., Staub, C. M., Gao, G., Jin, Q., Wang, Z., Ding, W., Aurigemma, R. E., and Mulder, K. M. A novel TGFβ receptor-interacting protein that is also a light chain of the motor protein dynein. Mol. Biol. Cell., *13*: 4484-4496, 2002.
12. Jin, Q., Ding. W., and Mulder K. M. Requirement for km23 in a Smad2-dependent TGFβ signaling pathway. Submitted, 2004.
13. King, S. M. The dynein microtubule motor. Biochim. Biophys. Acta., *1496*: 60-75, 2000.
14. Bowman, A. B., Patel-King, R. S., Benashski, S. E., McCaffery, J. M., Goldstein, L. S., and King, S. M. Drosophila roadblock and Chlamydomonas LC7: a conserved family of dynein-associated proteins involved in axonal transport, flagellar motility, and mitosis. J. Cell. Biol., *146*:165-180, 1999.
15. Ye, Y., Zangenehpour, S., and Chaudhuri, A. Light-induced down-regulation of the rat class 1 dynein-associated protein robl/LC7-like gene in visual cortex. J Biol Chem., *275*: 27172-27176, 2000.
16. Jiang, J., Yu, L., Huang, X., Chen, X., Li, D., Zhang, Y., Tang, L., and Zhao, S. Identification of two novel human dynein light chain genes, DNLC2A and DNLC2B, and their expression changes in hepatocellular carcinoma tissues from 68 Chinese patients. Gene, *281*: 103-113, 2001.
17. Goldsworthy, S. M., Stockton, P. S., Trempus, C. S., Foley, J. F., Maronpot, R. R. Effects of fixation on RNA extraction and amplification from laser capture microdissected tissue. Mol. Carcinog., *25*: 86-91, 1999.
18. Kreegipuu, A., Blom, N., and Brunak, S. PhosphoBase, a database of phosphorylation

sites: release 2.0. Nucleic Acids Res., *27*: 237-239, 1999.

19. Cuff, J. A., and Barton, G. J. Application of enhanced multiple sequence alignment profiles to improve protein secondary structure prediction. Proteins, *40*: 502-511, 1999.

20. Chen, X., Rubock, M. J., and Whitman, M. A transcriptional partner for MAD proteins in TGF-β signalling. Nature. *383*: 691-696, 1996.

21. Zeinoun, Z., Teugels, E., De Bleser, P. J., Neyns, B., Geerts, A., and De Greve, J. Insufficient TGF-beta 1 production inactivates the autocrine growth suppressive circuit in human ovarian cancer cell lines. Anticancer Res., *19*: 413-420, 1999.

22. Jozan, S., Guerrin, M., Mazars, P., Dutaur, M., Monsarrat, B., Cheutin, F., Bugat, R., Martel, P., and Valette, A. Transforming growth factor β_1 (TGF-β_1) inhibits growth of a human ovarian carcinoma cell line (OVCCR1) and is expressed in human ovarian tumors. Int. J. Cancer., *52*: 766-770, 1992.

23. Vale, R. D. The molecular motor toolbox for intracellular transport. Cell. 112: 467-480, 2003.

24. Hamamoto, T., Beppu, H., Okada, H., Kawabata, M., Kitamura, T., Miyazono, K., and Kato, M. Compound disruption of Smad2 accelerates malignant progression of intestinal tumors in Apc knockout mice. Cancer Res., *62*: 5955-5961, 2002.

LEGENDS

Fig. 1. A: Agarose gel analysis of a truncated form of km23 in two out of six human ovarian cancer cell lines. The bands corresponding to the relevant portions of the wt km23 (424 base pairs) and the truncated form of km23 (254 base pairs) in SK-OV-3 and IGROV-1 cells are indicated by arrows. **B: Detection of the truncated form of km23 in two out of nineteen ovarian carcinoma tissues.** Agarose electrophoresis (2%) of nested RT-PCR products. Case 3 (Lane 4) and case 8 (Lane 5) express the truncated form of km23, which is not present in the other 17 tumor samples or in 15 tumor-free tissues. **C: Amino acid sequence alignment of the truncated form of km23 with the wild-type form, indicating exon and amino acid sequence numbers.**

Fig. 2. km23 alterations disrupt binding to the DIC. A: The truncated form of km23 displays a diminished interaction with DIC. Sepharose-bound, bacterially expressed GST alone (lane 1), GST-truncated km23 (lane 2), and GST-km23 (lane 3) were incubated for 2 h with MDCK cell lysates. The interacting proteins were analyzed with SDS-PAGE (12%) and immunoblotted with anti-DIC (top panel). The purified proteins were verified by SDS-PAGE/Coomassie blue staining (bottom panel). **B: The association with DIC is disrupted by the elongated form of km23.** Sepharose-bound, bacterially expressed GST alone (lane 1), GST-km23 (lane 2), and GST-elongated km23 (lane 3) were incubated for 2 h with MDCK cell lysates. The pull-down proteins were analyzed with SDS-PAGE (12%) and immunoblotted with anti-DIC (top panel). The purified proteins were verified by SDS-PAGE/Coomassie blue staining (bottom panel).

Fig. 3. The elongated form of km23 dose-dependently inhibits Smad2-dependent transactivation in TGFβ/activin reporter assays. Mv1Lu cells were transfected with increasing amount of either wt km23 or elongated km23 DNA (125ng, 250ng, and 500ng) along with 200ng ARE-luc and 200ng FAST1. To normalize transfection efficiencies, 200ng renilla was co-transfected as an internal control. 24 h after transfection, the medium was replaced with serum-free medium for 1 h, and the cells were incubated in the absence (open bars) or presence (black bars) of TGF-β_3 (2.5ng/ml) for an additional 18 h. All reporter assays were performed in triplicate. Results are representative of two experiments.

Fig. 4. Human km23 sequence depicting expected phosphorylation sites and secondary structure for km23. Potential **phosphorylation** sites for protein kinase A (PKA), protein kinase C (PKC), and/or casein kinase II (CKII) were predicted using PhosphoBase v. 2.0 and NetPhos 2.0 (18). For these sites, prediction scores for serine and threonine were all over 0.91. Four serine residues that are conserved among the mammalian km23 forms are boxed. The secondary structure prediction was performed using the Jnet method (19). The black bars under the protein sequence represent α-helical regions, while the gray bars depict β-strands. There are two α-helices and six β-strands in km23. Among these, the second α-helix and four β-strands are located in exon 3.

Table 1 Clinical characteristics of 8 ovarian carcinomas with km23 alterations from 19 patients

Case No.	Age (yrs.)	Histology[a]	Stage/Grade [b]	Mutations
1	58	serous	IIIA/2	S55G, I89V
3	51	serous	IIB/2	exon 3 missing
4	48	serous	IIIA/2	elongated km23 107aa
7	49	serous	IC/2	T56S
8	72	serous	IIIC/2-3	exon 3 missing
14	57	endometrioid	IV/3	elongated km23 107aa
15	47	endometrioid	IIA/2	T38I
18	57	metastatic ov ca	IV/-	V90A

[a] Serous=serous cystadenocarcinoma; endometrioid=endometrioid adenocarcinoma.

[b] Stage and grade classified according to the criteria standardized by the International Federation of Gynecology and Obstetrics (FIGO). "-" not available.

Table 2 Comparison of km23 alteration rate between ovarian carcinoma and normal ovarian tissues

	Normal ovarian tissues	Ovarian carcinoma tissues
Alteration	0	8
No Alteration	15	11
Total	15	19
Alteration rate	0%	42.1%[a]

[a] Statistical calculation using Fisher's exact test demonstrated a significant difference in the km23 alteration rate between ovarian carcinoma and normal ovarian tissues, $p<0.005$.

Fig. 1A

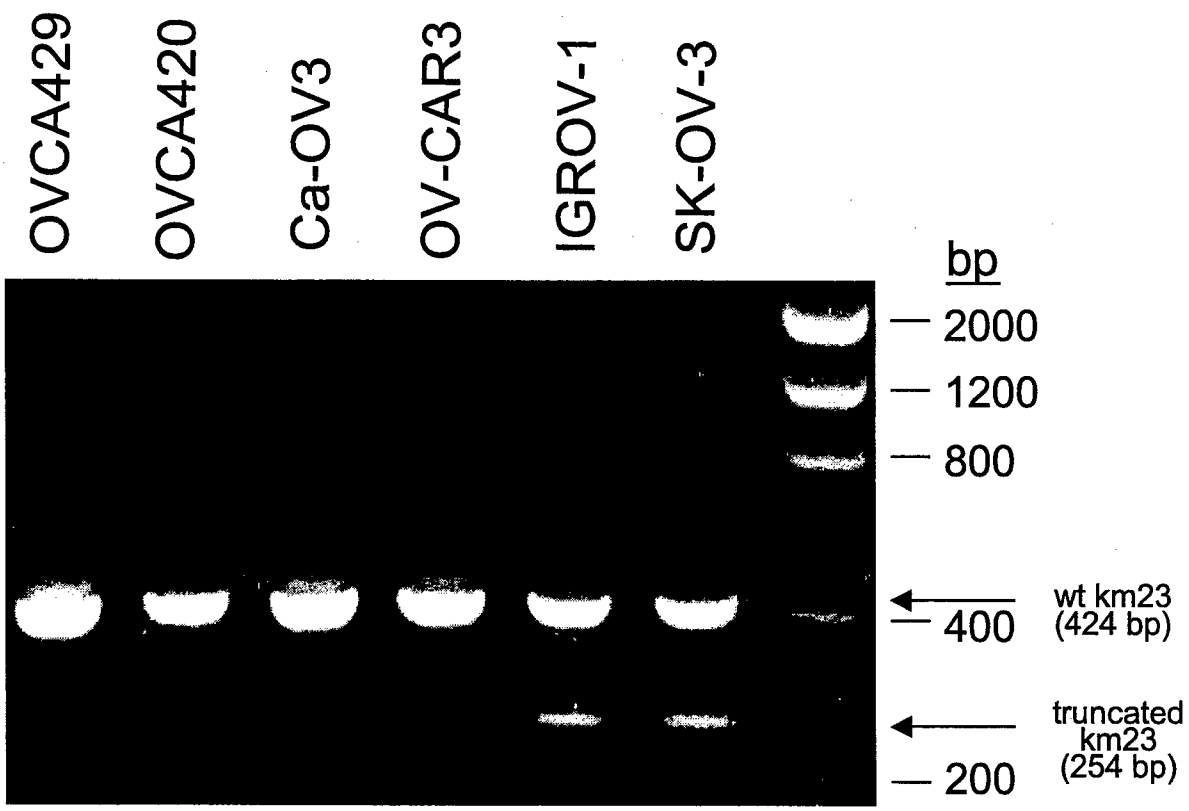
OVCA429
OVCA420
Ca-OV3
OV-CAR3
IGROV-1
SK-OV-3
bp
2000
1200
800
400
200
wt km23
(424 bp)
truncated
km23
(254 bp)

Fig. 1B

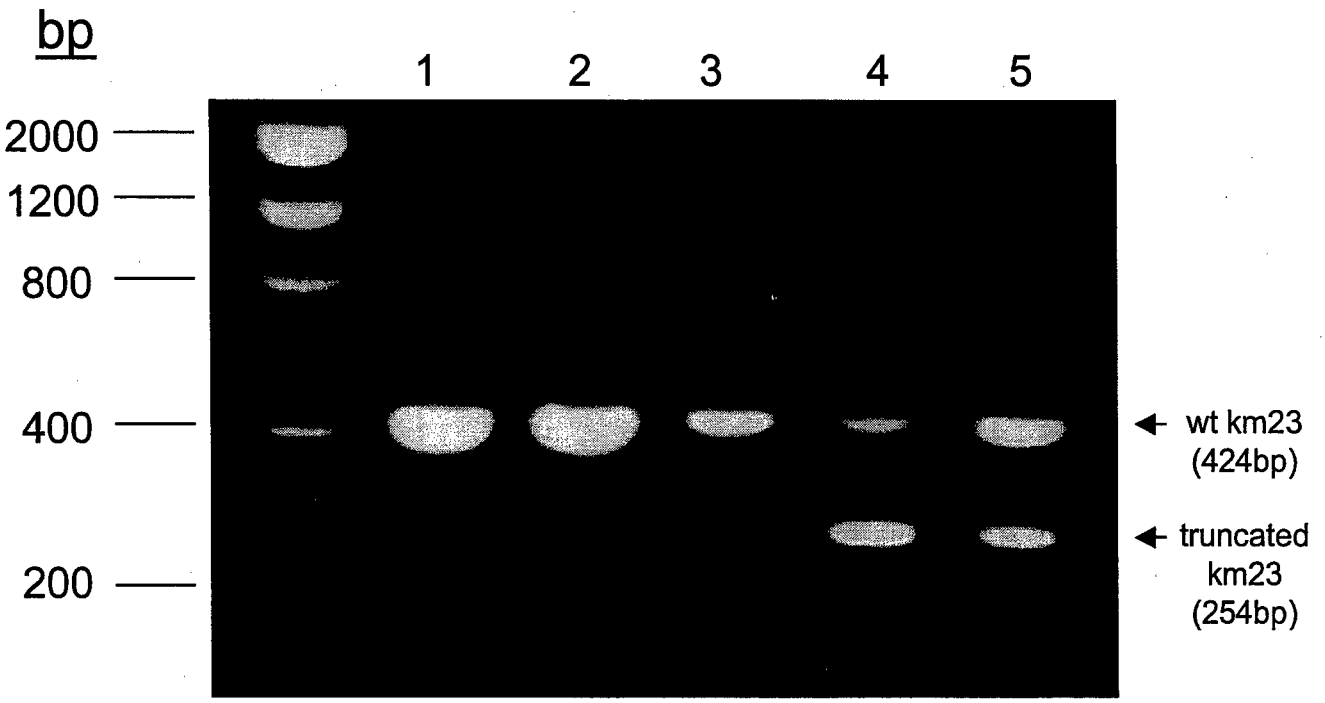
bp
1
2
3
4
5
2000
1200
800
400
200
wt km23
(424bp)
truncated
km23
(254bp)

Fig. 1C

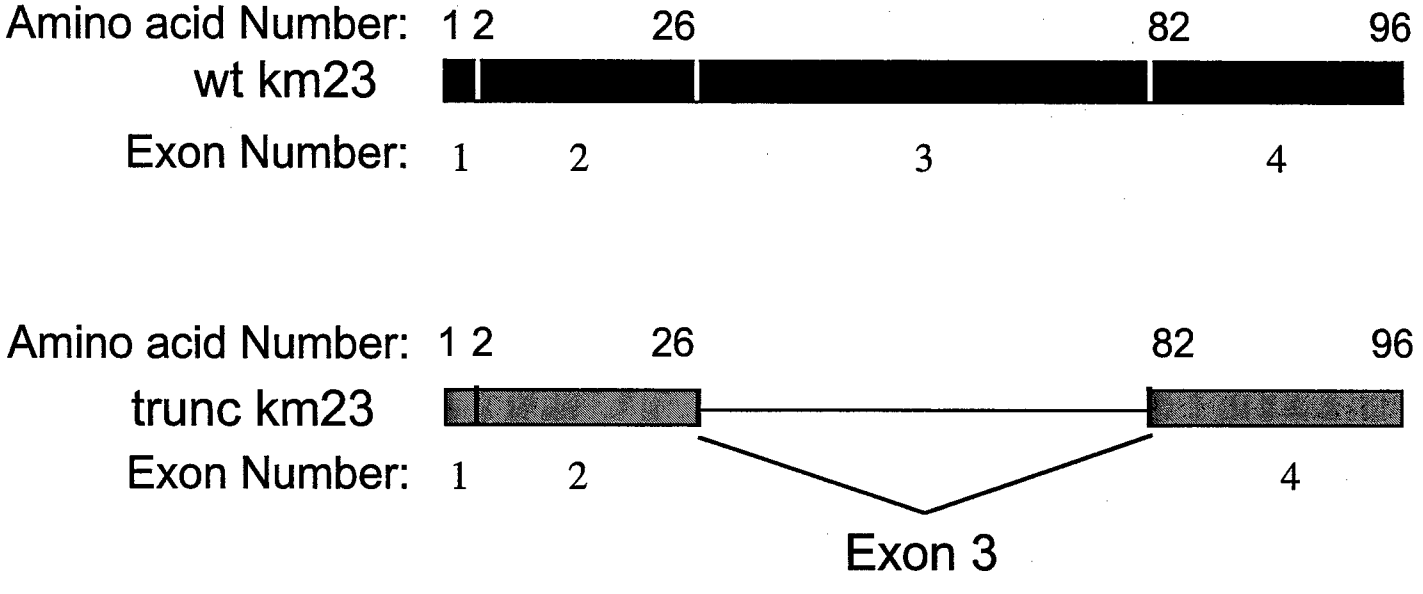
Amino acid Number:
1 2
26
82
96
wt km23
Exon Number:
1
2
3
4
Amino acid Number:
1 2
26
82
96
trunc km23
Exon Number:
1
2
4
Exon 3

Fig. 2 A

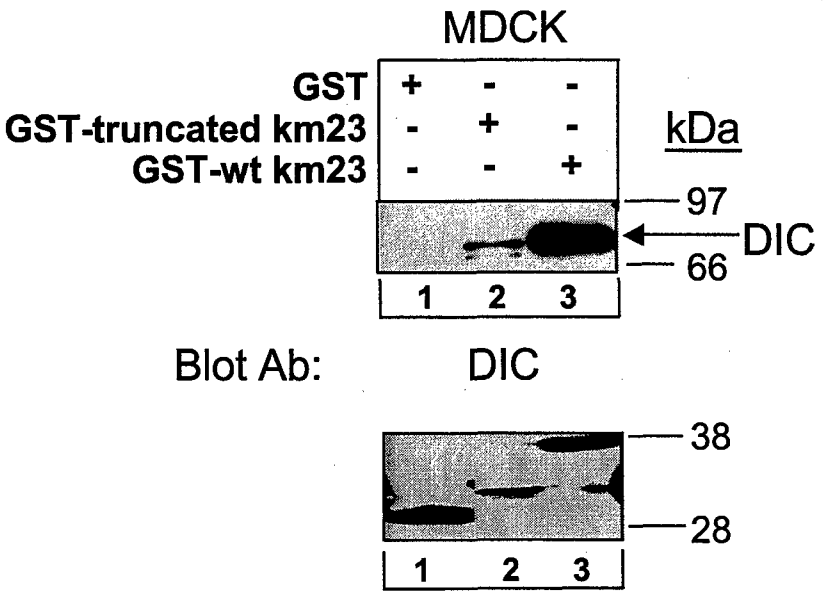
MDCK
GST + - -
GST-truncated km23 - + -
GST-wt km23 - - +
kDa
97
DIC
66
1 2 3
Blot Ab: DIC
38
28
1 2 3

Fig. 2 B

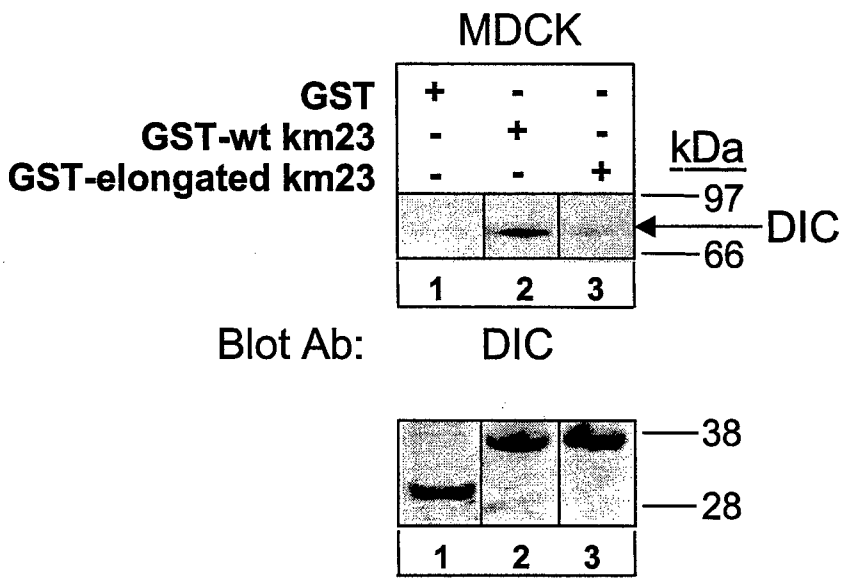
MDCK
GST
GST-wt km23
GST-elongated km23
+ - -
- + -
- - +
kDa
97
66
DIC
1 2 3
Blot Ab:
DIC
38
28
1 2 3

Fig. 3

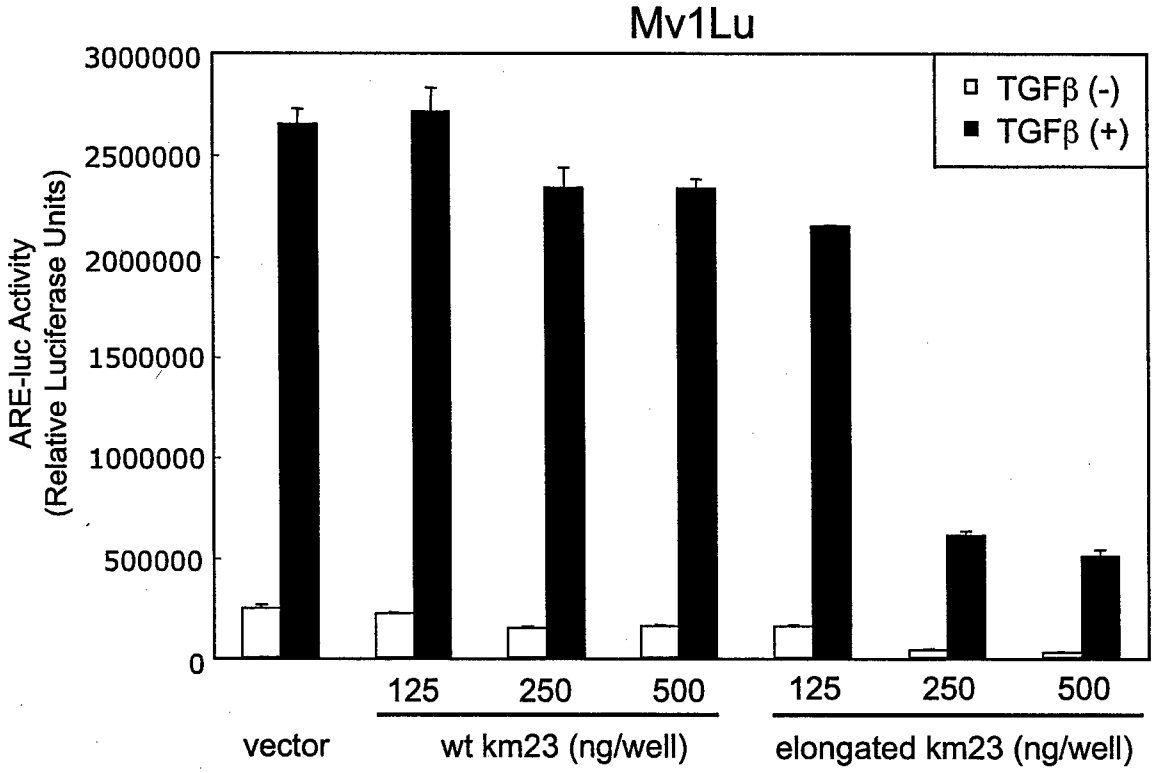
Mv1Lu
TGFβ (-)
TGFβ (+)
ARE-luc Activity
(Relative Luciferase Units)
3000000
2500000
2000000
1500000
1000000
500000
0
125
250
500
125
250
500
vector
wt km23 (ng/well)
elongated km23 (ng/well)

Fig. 4

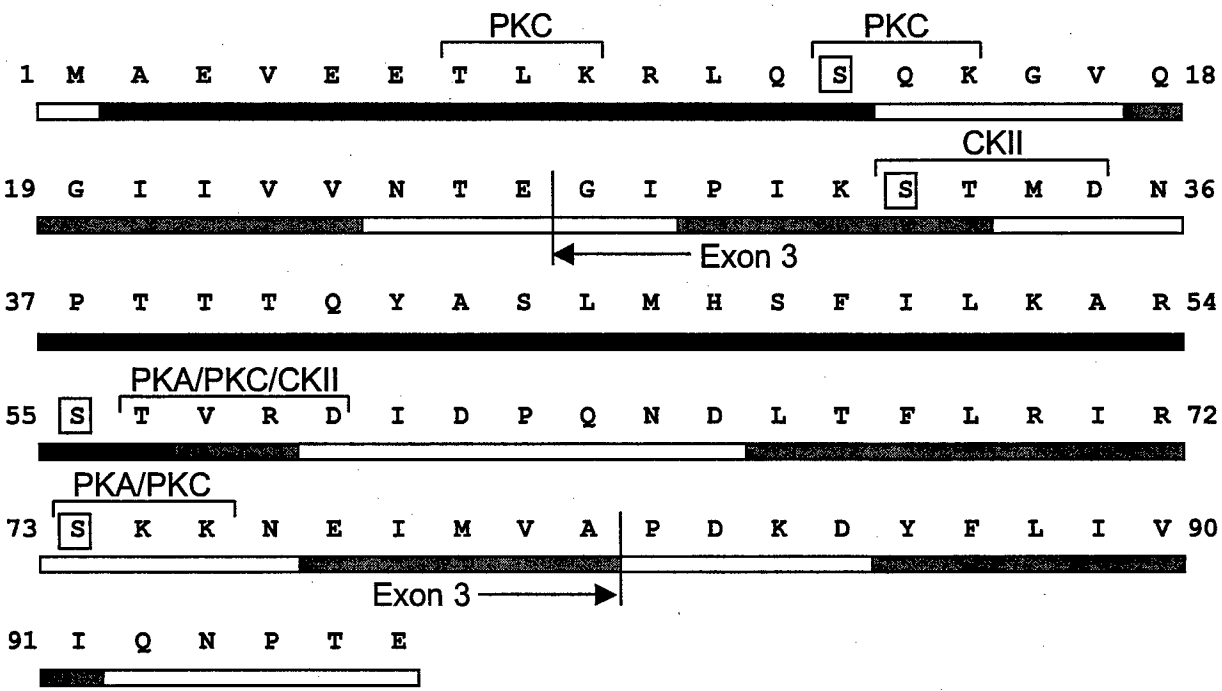
PKC
PKC
1 M A E V E E T L K R L Q S Q K G V Q 18
CKII
19 G I I V V N T E G I P I K S T M D N 36
Exon 3
37 P T T T Q Y A S L M H S F I L K A R 54
PKA/PKC/CKII
55 S T V R D I D P Q N D L T F L R I R 72
PKA/PKC
73 S K K N E I M V A P D K D Y F L I V 90
Exon 3
91 I Q N P T E